FUTURE CLIMATE RESILIENCE OF ENERGY-EFFICIENT RETROFIT PROJECTS IN CENTRAL EUROPE

Julija Sivolova, Jonas Gremmelspacher

Master thesis in Energy-efficient and Environmental Buildings
Faculty of Engineering | Lund University

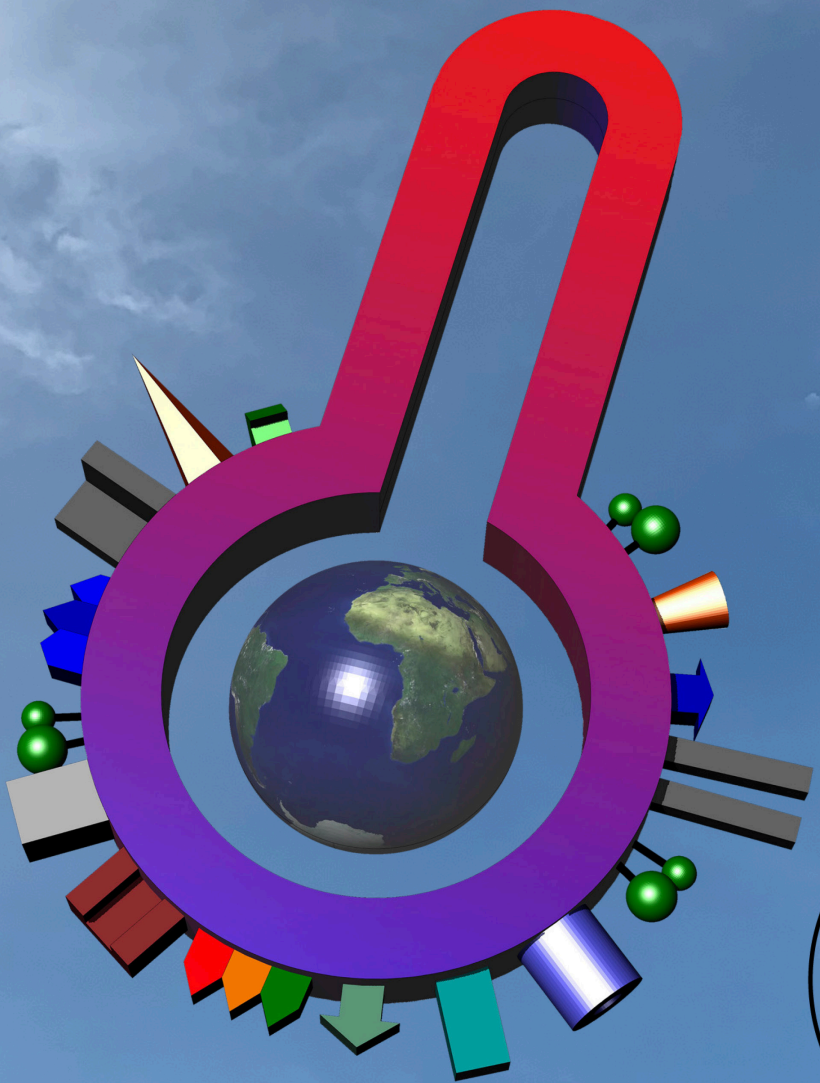

Lund University

Lund University, with eight faculties and a number of research centres and specialized institutes, is the largest establishment for research and higher education in Scandinavia. The main part of the University is situated in the small city of Lund, which has about 112 000 inhabitants. A number of departments for research and education are, however, located in Malmö. Lund University was founded in 1666 and has today a total staff of 6 000 employees and 47 000 students attending 280 degree programmes and 2 300 subject courses offered by 63 departments.

Master Programme in Energy-efficient and Environmental Building Design

This international programme provides knowledge, skills and competencies within the area of energy-efficient and environmental building design in cold climates. The goal is to train highly skilled professionals, who will significantly contribute to and influence the design, building or renovation of energy-efficient buildings, taking into consideration the architecture and environment, the inhabitants' behaviour and needs, their health and comfort as well as the overall economy.

The degree project is the final part of the master programme leading to a Master of Science (120 credits) in Energy-efficient and Environmental Buildings.

Examiner: Petter Wallentén (Division of Building Physics)

Supervisor: Vahid M. Nik (Division of Building Physics)

Co-Supervisor: Emanuele Naboni (KADK, Institute of Architecture and Technology)

Keywords: Climate change, Future climate, Climate action, Building Performance Simulations, Hygrothermal Simulations, Moisture, Heating demand, Retrofit, Renovation, Building stock, Residential, Dwellings, Thermal envelope, Heating peak loads, Thermal comfort, Indoor environmental quality, Actual case studies, Big data, Denmark, Germany, Iterative workflow, Weather files.

Thesis: EEBD - # / 19

Abstract

The following study assesses the performance of buildings affected by climate change under future climate predictions for three time-periods until the end of the 21st century. Objects studied are residential multi-storey buildings, originally built before 1970 and retrofitted during the last decade. A total of four actual retrofit projects, as they were performed, in Denmark and Germany were assessed in their initial and retrofitted stage. The investigation assessed indoor thermal comfort, heating energy demand, heating peak loads by means of building performance simulations. Further, hygrothermal simulations were used to test the performance of constructions in the thermal building envelope. Climate data sets employed composed of a set of nine weather files per location, accounting for non-extreme and extreme cold and warm conditions divided into 30-year periods.

The results show for all retrofitting measures a decrease of energy consumed for space heating. Due to the improved building airtightness and thermal conductivity of the building envelope constructions, sizing of heating systems and terminal devices was minimised accordingly. Similar paradigms show for periods closer to the end of the century, as the annual heating energy demand decreases gradually.

An increase in summer thermal discomfort towards the end of the century was observed in all study objects, especially during extreme hot summer-periods thermal discomfort is ubiquitous. The German case studies showed that passive measures to decrease local discomfort are insufficient during extreme periods with increasing thermal discomfort towards the end of the century. The realisation of highly insulated thermal envelopes yielded immense overheating issues for the German future climate predictions.

The majority of initial thermal envelope constructions showed vulnerabilities for moisture related issues within future climate scenarios. Most retrofitted elements are predicted to withstand climate change without high risk for mould growth. This mainly bases on the material selection which is crucial along with a thorough hygrothermal assessment for ensuring a resilient building design under the uncertainties of future climate.

Acknowledgments

We would like to express great gratitude to our supervisor Vahid M. Nik, who supported and gave us valuable advice during the whole process of this study. Not only has he been a great source of knowledge but has also supplied future climate weather data sets for three case study locations based on his method for statistical downscaling of RCM weather data models. Even during busy periods, he was responding quickly to all queries that came up along the way.

Four case studies were assessed based on actual data provided by companies, building owners and freely available academic studies. Various drawings, details, construction descriptions along with energy and thermal simulation models were provided, making a real case study possible. We would like to say thank you for your time and participation in this collaboration process, as well as making this research possible. Among the companies who do not want to be disclosed in this report, we want to express our gratefulness to Claus Fischer and the Bau- und WohnungsVerein Stuttgart e.V. for supplying us with the two German case study objects. In addition, we would like to thank Zeynel Palamutcu from Engineering consultancy 'DOMINIA A/S' for supplying us the necessary material for the second Danish case study.

Performing the simulations for energy use and thermal comfort would not have been possible without the work of Mostapha Sadeghipour Roudsari and Chris Mackey and many other contributors to the Plug-in collection Ladybug Tools, we thank you for the great job you are doing and especially for providing the software freely and open-source. We also thank the Fraunhofer IBP and the team of WUFI, for providing the Software for the hygrothermal analysis, as well as for the support provided to Jonas during the WUFI seminar in Holzkirchen.

We also want to express our appreciation to all lecturers, coordinators and other staff at Lund University who supported us during our master education. We thank all of you for making it possible for us to study at LTH and for being there for us.

Thank you to Emanuele Naboni for providing Jonas with the opportunity of experiencing the life as a research assistant at the Royal Danish Academy of Architecture, Design and Conservation, as well as for his inputs on academic writing. Jonas expresses his gratitude to KADK and everybody at IBT for providing a fruitful study environment and the necessary equipment during the time of this study.

Nomenclature

ACER	Energy performance in Buildings, Energy efficiency, Renewable energy, Governance, Electricity Regulation, Electricity Directive, Risk Preparedness and Agency for the Cooperation of Energy Regulators
ACH	Air changes per hour
AHU	Air handling unit
BPS	Building performance simulations
BR	Building regulations
CAD	Computer Aided Design
D-DRY	Danish Design Reference Year
DGNB	German sustainable building council
DIN	Deutsches Institut für Normung (German Institute for Standardisation)
DSY	Design summer year
ECY	extremely cold year
EnEV	Energy Conservation Ordinance
EPBD	European performance in buildings directive
EPS	Expanded polystyrene
EU	European Union
EWY	Extremely warm year
FS	Finkelstein-Schafer statistic method
GCM	Global climate model
HVAC	Heating, ventilation and air conditioning
IAQ	Indoor air quality
IPCC	Intergovernmental Panel on Climate Change
IWEC	International Weather for Energy Calculations
LED	Light-emitting diode
Level(s)	Voluntary framework to improve the sustainability of building
MFH	Multifamily houses
nZEB	Net zero energy buildings
PV	Photovoltaic
PVC	Polyvinyl chloride
RCA	Rossby Centre regional atmospheric model
RCP	Representative concentration pathway
RCM	Regional climate model
RH	Relative humidity [%]
SDG	Sustainable Development Goals
SEL	Specific electricity consumption for air transport [kJ/m^3]
SFH	Single-family houses
TDY	Typical downscaled year
TMY	Typical metrological year
TRY	Typical reference year
UN	United Nations
WAC	WUFI ASCII Climate
WWR	Window-to-wall ratio [%]

Notation

°	Degrees
ρ	Density [kg/m^3]
λ	Thermal conductivity [W/m K]
Ψ	Linear thermal transmittance [W/m K]
ΔT	Temperature difference [K]
ΔU	Difference in thermal conductance [W/m^2 K]
°C	Degrees Celsius
C_p	Specific heat capacity, at constant pressure [J/kg K]
f_f	Frame to glazing ratio [%]
g-value	Solar energy transmittance [%]
K	Degree Kelvin
kWh/ m^2	Kilowatt-hour per square meter
L	Length [m]
R-value	Thermal Resistance [m^2 K/W]
sd	Vapour diffusion equivalent thickness [m]
T_{vis}	Visible transmittance [%]
U-value	Thermal conductance [W/m^2 K]
W/ m^2	Watt per square meter

Table of content

1 Introduction

Decrease of carbon emissions, primary energy use and depletion of resources are some of the main challenges that the society of the 21st century has to cope with. Following the UN Sustainable Development Goals (SDG), the built environment and the building stock are key factors for achieving the ambitious goals by 2030 [1]. Especially the goal 13 (Climate Action) which calls for action against climate change and action to cope with the effects of climate change [2], [3]. Retrofit projects play a crucial role in fulfilling the ambitious energy and climate targets set by the European Union. The renovation of existing building stock holds a great potential for the overall energy savings, predicted to account for 5 to 6% of the total EU's energy use [4]. Indicating, this could result in a 5% decrease of CO_2 emissions [4].

As a large number of Europeans (42%) live in apartment blocks [5], it is natural that these type of dwellings receives a great share of attention. In order to fulfil the ambitious climate change policies, set by the EU for 2050, more and more of the existing dwellings are to be retrofitted. Sustainable development of cities and communities is fostered by the SDG number 11. It reflects the necessity to take threats that future climate holds into account in the planning stage of projects within the built environment [6]. Unfortunately, in practice attitude and knowledge towards renovation are lagging behind. Well-known renovation techniques that provide the large energy savings in current climatic conditions, currently applied by the industry, need to be investigated with exposure to changing climatic conditions. Only with a thorough investigation, it can be assured that the retrofitted buildings are habitable for the next decades.

Indoor well-being and health are greatly influenced by daylight, thermal comfort and ventilation. All of these should be considered in a renovation project [7]. Glazed windows and doors contribute to a large share of energy loss through the thermal building envelope. Additionally, they are a cause for solar gains that can have both positive and negative impact considering 'free heating' and space overheating respectively. Furthermore, it is important to take into account, that natural daylight stimulates productivity, mental alertness, health and psychological well-being of the individual occupant. It is therefore important to evaluate all benefits and downsides that glazed elements in the thermal envelope may inflict. This is in order to design buildings with a window to wall ratio that balances heating and cooling energy demand and indoor environmental quality through daylighting [8]. Good health and well-being is also the subject of the SDG number 3 and is therefore fostered in the challenge 2030 which poses important missions for the built environment to cope with [3], [9].

This study assessed the impacts of climate change on the energy and hygrothermal performance of four real case studies which have undergone energy efficiency retrofits. Cases are located in the EU countries Denmark and Germany. The two Danish case studies are situated in Aarhus and in Copenhagen, whereas both German projects are located in Stuttgart, seen in Figure 1. A comparison between the applied retrofit measures and the initial building construction was carried out. It was examined if the undertaken retrofitting measures result in the desirable performance of buildings for future climate conditions, considering moisture safety, energy efficiency and indoor thermal comfort. Therefore, building performance simulations as well as hygrothermal simulations were carried out with

the usage of location specific weather files. Those files represented climate predictions in three timeframes until the end of the 21st century. The approach for synthesizing future climate predictions into typical downscaled year (TDY), extreme cold year (ECY) and extreme warm year (EWY) by Nik [10] was employed and resulted in a total of nine climate files per location.

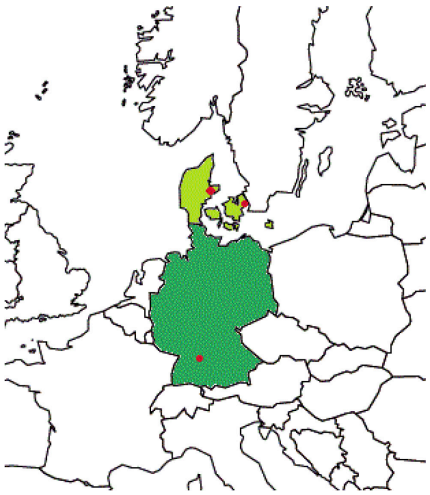

Figure 1: Geographical locations of the case study objects

1.1 Objectives

The main objective of this study was to assess climate change resilience and adaptation of the considered retrofitting projects. Real-life retrofitting measures were compared with initial conditions for three climate scenarios in three time periods towards the end of the 21st century. It was investigated how retrofitted buildings perform in future climatic conditions. The long-term evaluation was conducted assessing indoor thermal comfort, building energy demand and hygrothermal conditions in thermal envelope constructions, such as roofs and external walls.

The second objective was to create a workflow that allows for testing the resilience of buildings under future climate scenarios. The developed scripts for building performance simulations should provide a tool for the estimation of energy demand and indoor thermal comfort in current and future weather scenarios. By embedding such an analysis for building performance under future climate scenarios in the early design stage, a simple methodology to ensure resilience with the applied measures and systems can be employed. In order to allow for running simulations seamlessly, it was intended to create an iterative workflow that runs multiple weather files and captures the relevant data.

The carried-out simulations allowed conclusions to be drawn for overall building performance before and after the executed retrofits. Furthermore, the impact of design decisions within the building retrofit were evaluated.

1.2 Research Questions

The intention is to answer the following research questions with the results from the conducted study:

- Are the currently employed retrofitting measures effective for decreasing the building energy demand in future climate conditions?
- Will the indoor thermal comfort be affected in the future? How large will the effect of extreme climatic conditions be?
- How do design choices like increasing glazing ratios to increase daylight penetration affect indoor thermal comfort of the occupied spaces?
- Are exterior thermal envelope constructions moisture safe under future climate scenarios? Will moisture movement related issues increase or decrease in retrofitted buildings?
- Are the applied insulative and airtightness measures compatible with the building service systems and the terminal devices in future climate scenarios?
- How can passive and active measures be employed to improve and maintain good indoor thermal comfort in future climate?

1.3 Scope

The workflow in the present study was as illustrated in Figure 2 as a flat project process. The starting point of the study was a comprehensive literature review to examine the status quo of energy-efficient retrofits, the challenges imposed by climate change and the current governance to cope with these issues, followed by data collection from retrofitting projects executed in the past decade. The case studies are set in Aarhus within warm humid continental climate zone as well as Copenhagen and Stuttgart within oceanic climate zone. Predominant climatic conditions in all three cities are, however, warm climate, fully humid and warm summers according to the Köppen-Geiger Climate Classifictaion [11].

The studied buildings were modelled in Rhinoceros, representing the design as it was applied in practice. The created 3D models were used for numerical modelling by the means of EnergyPlus simulations through Grasshopper visual scripting to assess indoor thermal comfort and heating energy demands. In addition to the building performance simulations, general moisture related risks were assessed through WUFI and mould growth risks were evaluated according to the Viitanen model. Retrofitted and initial buildings were assessed under future climate scenarios while investigating the performance and safety of the applied measures. This was done using three time-periods as well as one non-extreme, one extreme cold and one extreme warm scenario. The weather file data sets were considered in building performance simulations and moisture assessment. Finally, a comparison between the applied measures and the initial building was carried out. It was examined if the undertaken refurbishment creates safe conditions for the climatic conditions in the future.

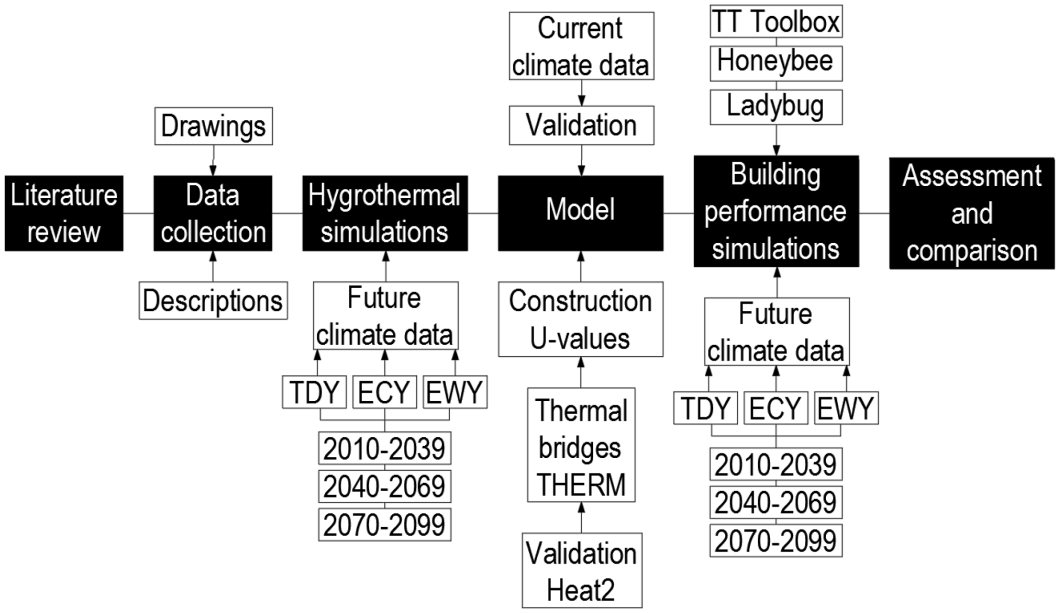

Figure 2:Graphical abstract of project process

1.4 Limitations

The study is investigating four building retrofits as they were applied in practice. All conclusions drawn in this report are based on the findings of the case studies. The building performance as well as energy consumption of the case studies were validated based on of the data provided by the companies, building owners and supplementary data from academic studies. Conclusions may not be applicable for other cities and buildings with different applications as the study was performed for residential projects located in three cities in warm humid continental and oceanic climate zones. In addition, simulations were executed with weather data generated by regional climate models (RCMs), where synthesising of future climate scenarios was done based on the dry-bulb temperature as the only weather parameter as described in more detail in Nik's publication [10].

The assessment is based on heating energy consumption, as neither non-retrofitted nor retrofitted buildings included active cooling systems, apart from small capacity cooling coil within air handling units. The energy use intensity of equipment, lighting, domestic hot water and auxiliary energy for HVAC systems are not assessed in this study. Window to wall ratio (WWR) were modelled parametrically with even distribution over the building envelope, thus local indoor thermal comfort can show slight discrepancies to actual conditions. Thermal bridges were simplified to an overall U-value, as described in section 3.1.1. Only the exterior thermal envelope constructions were studied for possible moisture damages and mould growth. Hygrothermal conditions were assessed with WUFI Pro for one dimensional moisture movement. The Viitanen VTT model [12] was used for estimating mould index and fungi growth for all materials as the primary method of investigation. Positive mould growth results assessed with WUFI simulations within organic materials in the initial building constructions were reviewed based on reported moisture damages and mould growth symptoms observed in on-site investigations.

2 Problem Motivation

Global warming and its effects are widely debated by politicians, the media and society [13]. Over the last century the average surface temperature on the planet has risen by approximately one degree Celsius [14]–[16]. Climate change is accelerated by a substantial contribution of human-caused emissions into the atmosphere [13], such as the burning of fossil fuels like coal and oil [17]. Emissions must be mitigated in order to ensure a healthy and sustainable environment for future generations. In addition, the fragile environment on the planet must be nurtured by humankind in order to sustain all forms of life present on Earth and in the Oceans [18]. Moreover, there is a common aim to limit human activities that contribute to the production of heat-trapping gases in the atmosphere which cause extreme events, such as: heat waves, storms, floods, wildfire, droughts, see level rise, ice-cap melting and others [17], [19]. As a result, policy makers around the world are focusing on reducing carbon dioxide (CO_2) emissions, as this gas along with methane (CH_4) contributes to approximately 81% of long-lived greenhouse gases released into the atmosphere [20]. Global emissions and worldwide energy consumption are inseparable. The increase of living comfort, which can be perceived on a global level, results in a rise of energy use. This, however, is a difficult challenge on its own, as technological benefits along with current living standards of the population are expected to be maintained while avoiding economic stagnation [20].

Buildings within the European Union (EU) consume around 40% of the overall energy use, contribute to 36% of CO_2 emissions, while 75% of the building stock is energy inefficient [21]. Due to these facts, the building sector is placed under observation, for EU directives to shape energy-efficiency goals. Along with the reduction of energy consumption, there is a great need for climate-friendly, renewable and affordable energy sources [22].

2.1 Climate Goals

As the atmosphere temperature is continuously warming and greenhouse gases in the atmosphere are increasing, it becomes very important to take action and preserve human health, freshwater supplies and ecosystems [17]. Half of the EU's energy use is being traced back to heating and cooling purposes in industry and households. In addition, only 16% of this energy is produced by renewable sources, meanwhile 84% of the overall energy consumption is being generated from fossil fuels [23]. As a conservation measure, the EU has launched a heating and cooling strategy in 2016, which aims to reach nearly zero emissions from buildings by 2050. It proposed to cut energy consumption by means of choosing high-performance insulation materials for renovation works, installing intelligent thermostats, upgrading outdated technical equipment such as: boilers, refrigerators, air conditioners and similar [24], [25]. The assessment on energy-efficiency progress was executed as a part of implementing the Energy Efficiency Directive 2012/27/EU [26] within the member states of the EU. The results showed that energy consumption decreased gradually throughout 2007-2014. However, in 2015-2016 it increased. This was assumed to be partially interconnected with the cheaper fuel prices and colder winters [23], [27], [28].

The European union has undergone a revision of its energy policies that marks a transition to the 21st century through energy legislative framework called 'Clean energy for all Europeans'. It is planned that the completed package will contain a total of 8 directives:

Energy performance in Buildings, Energy efficiency, Renewable energy, Governance, Electricity Regulation, Electricity Directive, Risk Preparedness and Agency for the Cooperation of Energy Regulators (ACER). The first four directives are already adopted by the EU, while the last four are currently pending as European commission proposals from 30th November 2016 [29]. The new policy framework emphasizes combating climate change with energy-efficiency, renewable energies and cost competitiveness through cross-border market. In other words, one of the aims of this package is to maintain leadership in a future of global clean energy markets, thus, secure access to sustainable and affordable energy supplies [30], [31]. As a part of the ambitious commitment to climate goals, former directives 2010/31/EU on the energy performance of buildings and 2012/27/EU on energy-efficiency have been amended with the directive 2018/844/EU on Energy Performance of Building Directive that officially entered into force on the 9th of July 2018 [32], [33]. This document aims to expedite cost-effective retrofit projects, facilitate transformation of existing building stock into a nearly zero energy building by 2050 along with the mobilization of investments. Smart technologies, health and well-being of building users shall be promoted through requirements for technical installations, control systems and automation [32], [34]. In addition, electromobility in infrastructure shall be boosted. It will be required that all non-residential buildings, that are new or undergo a major renovation, will be equipped with at least 20% charging stations for all the parking lots containing more than 10 parking spaces [35]. The revised directive 2012/27/EU on energy efficiency is now amended by the 2018/2002/EU version [36]. Reduction in final and/ or primary energy consumption is set to a minimum of 32.5% for 2030, with a review clause by 2023. In addition, rules for individual metering along with separate bills were strengthened. This policy enables the population to become more aware and handle their hot water, heating and cooling consumption with care. This issue is perhaps most applicable to multi-apartment dwellings where outdated collective technical installation systems are still in use [22], [36]. The revised Renewable Energy directive 2018/2001/EU came into force on the 24th December 2018 [37], where a binding renewable energy target is set to a minimum of 32% for 2030, with a review clause by 2023. Amongst others this act is drawing a clear path for the support of design and stability for renewable energy sources [22], [37].

New Governance of the Energy Union and Climate Action Regulation 2018/1999/EU entered into force the 24th December 2018 [38]. This act ensures collaboration between the EU member states in order to fulfil the targets set for 2030, thus it provides consistency with international commitments made under the Paris agreement [39]. The objective is set to maintain the increase of the global average temperature to a maximum of 2 °C above pre-industrial levels. Moreover, additional efforts should be made seeking to maintain the global average temperature of 1.5 °C above pre-industrial levels [38]. Governance requires EU member states to prepare a long-term plan for climate and national energy for a period of 2021 – 2030. The alignment on reporting obligations and frequency strengthen transparency, while minimizing administrative work was reached by the EU commission, the Member States including other EU institutions [22], [38]. The four directives that are still pending aim to create a modern and flexible electricity market within the European Union, that offers great possibilities to integrate renewables [22].

Targets set by the ‘Clean Energy for all Europeans’ package are binding for all EU Member States as a whole. Therefore, individual countries have a great flexibility and retain the right to reduce greenhouse gas emissions in the way that suits its energy mix along with a variety of renewables in the most cost-effective way [35]. In order to fulfil the ambitious energy and

climate targets set by the EU, energy consumption must be reduced drastically. In addition, price-competitive and clean, renewable energy sources must be established [23]. Initiatives and support schemes are available in order to stimulate energy efficiency investments [23], [40] along with additional EU funds for overall growth potential within research and innovation [41], [42].

2.2 Energy-efficient Retrofitting of Apartment Houses

Having the goal of decreasing carbon emissions globally, pushed governments to drastically intervene in building codes and regulations. This was necessary in order to mitigate transmission losses through the building envelope and extensive use of primary energy. Achieving so is done by setting benchmark values for maximum transmission losses through the building envelope and reducing the amount of primary energy use in the building code for newly constructed buildings, which was concisely followed by the EU member states since the 1990´s. For the building stock, composing of 86 % apartments in Germany built before 1990, most regulations regarding energy-efficiency were adopted in the 1990´s [43]. To address a large share of apartments with a high potential of savings, this study concentrates on apartment buildings, declared as multifamily houses (MFH) [44] which were built before 1990 and undertook an energy-efficiency retrofit in recent years.

The phrasing energy-efficient retrofit, stands for the concept of retrofitting buildings to conserve operational energy by firstly decreasing transmission losses and secondly by applying systems with high effectiveness [45]. To set incentives for building owners and operators to perform retrofits, the EU directive and local governments have taken a threefold approach: All buildings had to be ranked in an energy labelling system, which describes a buildings energy-efficiency in comparison to its potential performance [46]. Additionally, legislation prescribed property owners to establish a renovation roadmap to set the milestones towards increased energy-efficiency [47]. The biggest incentive was created by EU member states through providing subsidies or low-interest loans for the investment in energy-efficiency measures [47]. Today, the application of energy-efficiency retrofits is common throughout the EU countries. Measures that are applied in buildings can be divided into two categories. Firstly, measures to decrease the conductivity properties of the building envelope. These include the change of windows, adding of insulation to the building envelope to prevent conduction and radiation losses, as well as increasing the air- and wind-tightness of the exterior construction to cut losses through convection and infiltration. Secondly, the application of active building systems that supply heating, ventilation and air conditioning (HVAC). Herein, the heating and cooling energy production plays a central role, where highly efficient systems with a great use of renewable energy sources yield in decreasing the primary energy consumption.

2.3 Climate Change and Future Climate

Several studies indicate that human activities contribute to the predominant amount of greenhouse gas emissions in the mid-20th century [48]. Warming of the Earth's atmosphere can be observed through environmental consequences such as: rising sea levels, storms, flooding's, melting icecaps [48] and bleached coral reefs [49]. In accordance to the Paris Agreement, the response to a global Climate Change must be strengthened. Humankind

must maintain global average temperature to way below 2 °C above pre-industrial levels and peruse efforts to decrease it to 1.5 °C above pre-industrial levels. It is predicted that complying with these targets would mitigate the risk and impacts of global warming [39] [50]. Climate change is predicted to accelerate as stated by the Fifth Assessment Report of the Intergovernmental Panel on Climate Change (IPCC) [48]. Observational temperature data, measured over a period of the past 500 years, has been exceeded in the period between 2003-2010 throughout about 50% of Europe. The authors of the regional multi model study forecasted that the probability of mega-heatwaves in summer periods will increase by 5-10 % by 2050 [51]. Conclusions of other analyses have been very similar; heat waves are expected to last longer and become more frequent as projected by Fischer and Schär [52]. Unfortunately, human understanding of such extreme events is still partially limited and results in imperfect climate models [53]. Many Northern European countries like Sweden, Denmark, Norway, Ireland and the Netherlands have already experienced very warm and record-breaking temperatures during the summer of 2018 [54]. These high temperature anomalies were the main cause of droughts that led to devastating crop loss for farmers [55]. On the other hand, further natural extremes like heavy precipitation events can pose risks for construction materials and healthy indoor environment [56].

It is a common practice worldwide to design and simulate buildings using weather files containing a typical meteorological year (TMY), based on historical weather measurements. This is done without consideration of future climate scenarios embracing the extreme event probability [57], [58]. In order to avoid expensive renovations in the future, the thin balance between economically feasible investments and estimation of climate change must be thoroughly assessed for each individual building case [59].

2.4 Indoor Thermal Comfort and Air Quality

Architects and engineers are facing a difficult challenge when it comes to designing energy efficient dwellings while ensuring satisfying indoor air quality (IAQ). This conflict was already predicted in 1996 in the report ‘Indoor air quality and its impact on man’, where it was concluded that energy savings are leading to decreased air exchange rates. At that time it was suggested to develop appropriate control tools and maintenance procedures [60]. As people are spending roughly 90% of their time inside buildings it becomes crucial to provide healthy IAQ along with suitable thermal comfort to ensure wellbeing of occupants [61], [62]. It is extremely difficult to understand the correlation between human health and indoor comfort. Thermal, chemical, acoustical and visual factors can all be traced back to the well-being of humans [63].

Studies have indicated that poor IAQ can reduce one´s concentration levels and will have a negative effect in work performance and productivity [64]. In addition, bad IAQ can be the main cause of sore throat, acing nose/sinuses, headaches, lead to asthma, cardiovascular diseases and cause obesity [65]. Apte et al. suggest that improvements on the ventilation effectiveness or increased ventilation rates should result in a decrease of illness symptoms by up to 70-85% [66].

Indoor thermal comfort is closely interconnected with energy use of buildings. Depending on gender, age, race, geographical location and climate, individuals can experience thermal adaptation in different ways. Unlike IAQ, thermal comfort is being distinguished instantly.

At the same moment when occupants begin to feel cold or warm, skin receptors are being triggered and a warning signal is sent to the human brain. As soon as discomfort feeling is registered, heating and cooling systems are being tweaked to non-optimum levels which leads to higher energy consumption [63], [67]. In order to fulfil energy-efficiency targets set by the EU, existing buildings are being transformed into well insulated and airtight buildings during refurbishing projects. These upgrades very often lead to insufficient air exchange rates, as a result of minimised infiltration. Therefore, with an increase of building envelope tightness sufficient fresh air supply through ventilation and infiltration have to be ensured. [68]. Private investors who own apartment blocks often choose to neglect improvements in indoor air quality, like the implementation of mechanical ventilation, due to limited budgets or profit-oriented structures. On the other hand, there are various support schemes for major housing retrofitting projects, like the Danish operating aid 'Driftsstøtte' that is handled by the national building fund 'Landsbyggefonden'. A list of requirements must be met in order to prequalify for this support. Retrofits executed in cooperation with the national building fund tend to display sophisticated energy efficient solutions, reduced energy consumption, improved indoor climate and general barrier-free accessibility [69]. To interconnect IAQ requirements with energy-efficiency measures, designers have to concisely follow building codes and regulations. It is expected that new technologies within heating, ventilation and air conditioning (HVAC) along with smart monitoring and controls of the indoor environment will become the measure of the future, where sensors will detect compounds, supply an appropriate amount of fresh air and maintain comfortable thermal conditions. New technologies and building materials should be designed in balance with impact on human health [68], [70].

2.5 Moisture Safety

Moisture problems in buildings have been occurring over centuries, however, the appearance of these issues has changed over time. Some decades ago, building occupants had to deal with water intruding their indoor spaces, by wind-driven rain through gaps or openings in the exterior construction. Nowadays, the occurring problems are twofold, not least due to the more airtight way of construction. Firstly, moisture gets trapped indoors or between different construction layers. Especially in moisture production rooms such as bathrooms, the relative humidity (RH) levels can reach high values if insufficient or no ventilation or natural ventilation is provided. The exterior constructions, e.g. walls and windows, including the connection between them, are constructed in a more airtight manner, so no air exchange between indoors and outdoors can take place. Additionally, the improved thermal conductivity of building envelope constructions results in lower exterior surface temperature, which holds an increased vulnerability to moisture related issues. Also, state-of-the-art construction is using membranes, foils and felts, that prevent wind and wind-driven rain from intruding into the building envelope constructions. The vulnerability of these materials to be damaged, installed falsely and aged over time is very high, so the materials in the building envelope construction can be penetrated [71].

The issues that moisture in construction elements cause are manifold, extending from creating vulnerable mould growth conditions, over moisture accumulation that causes worse thermal properties for building materials and providing likely conditions for rotting to occur, to freeze thaw and corrosion in construction elements. Rotting, freeze thaw and corrosion can be a threat to the structural safety of a building [72], whereas mould can create serious

health issues [71], [73]. High or low indoor humidities can affect the well-being of occupants [73]. The conditions favourable for mould growth, are different between various kinds of material and also dependant on their placement in the construction [74]. However, as a precondition for mould growth, mould spores have to be present and since mould spores are available in outdoor air, it is inevitable to have them in building materials as well. Organic building materials show higher vulnerability to mould growth than non-organic materials such as expanded polystyrene (EPS) insulation [71]. For building materials, like wood and gypsum board, the vulnerable mould growth reaches from 75-85 % at room temperature, whereas at 10 °C the thresholds reach from 85-95 % [74]. Thus, likely conditions for mould growth are warm temperatures and relative humidities above 75 %. Reaching temperatures below 0 °C or above 50 °C, mould growth is interrupted and mould spores die if these conditions prevail. Additionally, RH values above 95 % hold higher probabilities for rot than mould growth. Generally, mould takes time to grow, therefore, the vulnerable conditions have to be predominant over a period of hours, weeks or months, depending on the respective material [71], [74].

2.6 Building Energy Use

The energy use of buildings in the EU is with 40 % of the total energy use within the EU one of the largest contributors [21]. For new buildings being constructed, the legislation among with incentives such as subsidies leads towards only net zero energy buildings (nZEB) being constructed. Diminishing the energy use of existing buildings is therefore the task being put in the focus of EU instruments, such as the EPBD [75]. The Energy Use of buildings within the EU is varying between different countries, which can be linked to multiple factors. The biggest difference in building energy use are the climate conditions the buildings are exposed to, therefore buildings in southern Europe having less heating energy use than buildings in central and northern Europe. Denmark is a country with a share of more than 70 % of Single-Family Houses (SFH), in Germany the number is between 60-70 % in relation to floor area of residential houses. In comparison, southern European countries like Spain and Italy reach shares as low as 33 % and 30 % respectively. The major difference between SFH and MFH are, that SFH tend to have a higher ratio of building envelope area per liveable floor area, increasing thermal losses and making building retrofits more expensive. Additionally, the thermal performance of buildings, hence the average building envelope properties vary widely between different countries. Amongst the four previously mentioned countries, Denmark reaches the lowest average U-values for building envelope constructions, Germany is not far behind Denmark, whereas the gap to Italy and Spain is extensive [44].

3 Methodology

The following chapter gives an overview over the methodology that was developed in order to tackle the study. The chapter is divided in three subchapters, starting with Building Performance Simulations, where the software that was used and the workflow is explained. Also, important input parameters are disclosed in this chapter. Secondly, the chapter Hygrothermal simulations provides an explanation on the methods and simulation software employed. In the third chapter, the weather files used in this study are explained and evaluated.

3.1 Building Performance Simulations

The assessed building geometries were modelled in the 3D-CAD modeler Rhinoceros 5 & 6 [76]. The processing of the geometry was done through the visual-scripting interface Grasshopper, which is an embedded plug-in for Rhinoceros [77]. The post-processing of the geometry and assigning inputs for the Building Performance Simulations (BPS), was carried out, using the legacy plug-ins Ladybug 0.0.67 and Honeybee 0.0.64, provided by Ladybug Tools [78]. The creation of iterative workflows as well as data capturing was completed with the TT Toolbox and Bumblebee plug-ins [79], [80]. The physics engine modelling platform OpenStudio and the simulation engine EneryPlus were used to carry out the BPS [81], [82]. The general modelling of geometry was done as solids, following measurement standards of the interior building envelope construction. For simplification, small interior zones were combined, resulting in saved simulation time. Geometry and construction, as well as material properties were assigned in the Honeybee workflow. The windows were assigned parametrically using the window to wall ratio (WWR) of each orientation, hence, each wall surface facing the exterior is assigned one or multiple windows that are evenly distributed over the façade area. The parametrically modelled surfaces were in the second step modelled as surfaces in the 3D-model and reassessed according to original constructions. WWR was calculated as the ratio of all windows and glazed doors in respect to the building model and its external wall area. As interior measurements were used for the building parameter, and OpenStudio and EnergyPlus assign material properties only as numerical values and not in extruded constructions, window reveals to the outside were extruded and modelled as shading elements. This methodology attempts to lower the overestimation of solar heat gains through non-opaque elements. The constructions of thermal envelope, interior elements and partitions as well as basement building elements were done modelling the employed materials separately and setting up the constructions out of those. The constructions were assigned to the respective surfaces in the model. Surface boundary conditions were set according to their function, exterior elements were set to ‘Outdoors’, resulting in surface heat transfer with the external environment exposed to sun and wind. Underground constructions were modelled with the boundary condition ‘Ground’, for heat transfer with the ground, which was modelled with transient monthly temperatures specified in the weather files. All interior zones were modelled as adjacent, resulting in interzone heat exchange. For simplicity, construction thicknesses for interior constructions were assumed to be unitary throughout the zones within the thermal envelope. Therefore, representative thicknesses and conductivities were chosen. Exterior constructions were handled analogically, where representative thicknesses and material conductivities for the building envelope were assigned to the surfaces with similar properties. Nevertheless, significant differences, such as large differences in thermal mass or conductivity in exterior

constructions were taken into account and different construction setups were assigned in these cases. Project specific constructions were as explained in chapter 4 (Model).

The assigned building loads and schedules were partially based on ASHRAE standard 90.1-2004, using values for equipment loads as well as schedules for occupancy, occupancy activity, lighting, equipment and ventilation. Lighting density for internal heat gains was specified as 7 W/m² in all apartments, using the schedule according to ASHRAE 90.1-2004. People density was specified to be one person per 25 m² lettable area, using the schedule subscribed in ASHRAE 90.1-2004. The ventilation and infiltration rates were specified differently in each project according to the specifications and on-site measurements. Similarly, heating setpoints were determined individually. Window ventilation was set in order to account for user-behaviour. As outlined by Andersen et al. [83], window ventilation leads to increased heating demand, but also helps in decreasing overheating. Thirty percent of the glazing area was specified as operable area, and windows being opened when the air temperature indoors reaches 24 °C or warmer, conditional to the outdoor air laying between 21 °C and 26 °C. As none of the buildings was equipped with an active cooling system, the function for cooling was disabled. For cases with a ventilation system, the respective ventilation rate was specified, and heat recovery was added in case it was in place. Only constant air volume systems were employed in the studies. For further processing, the results retrieved from the EnergyPlus simulations were processed and normalized according to the building specific circumstances. Capturing of the data sets in XLSX files allowed for running climate files iteratively and extracting the relevant measures for further investigation. Various measures ranging from peak heating loads, indoor comfort measures, overheating hours and zone energy demands were captured and analysed in the study.

The assessment of indoor thermal comfort is based on the adaptive comfort model, comfort band category II, as described in EN 15 251. The comfort band II describes a temperature range of 6 °C dependent on the daily average outdoor temperature, which lies in category II between 20 °C and 26 °C, which is corrected upwards when the day average outdoor temperature exceeds a value of 12.6 °C. Category II of the comfort model is advised to be used for buildings with normal levels of expectations and bases on occupant clothing levels of 1.0 for winter comfort as well as 0.5 for summer comfort respectively. Metabolic rates are expected to be sedentary with a value of 1.2 met, when assessing living spaces of residential buildings. Operative temperatures are calculated by taking both the zone air temperature, as well as the mean radiant temperature of the room surfaces into account, as visualised in Figure 3. The measurement does not include the evaluation of metabolic rates or clothing levels of space occupants. Commonly, measurements of the operative temperature require a temperature sensor to measure the dry-bulb air temperature, further a black globe thermometer is used to measure the mean radiant temperature of the surrounding surfaces. In the employed method, a globe thermometer is placed in the middle of the room, as seen in Figure 3. This was done, as in EnergyPlus simulations, the node, at which mean radiant temperature and air temperature is sensed, is placed in the middle of the room.

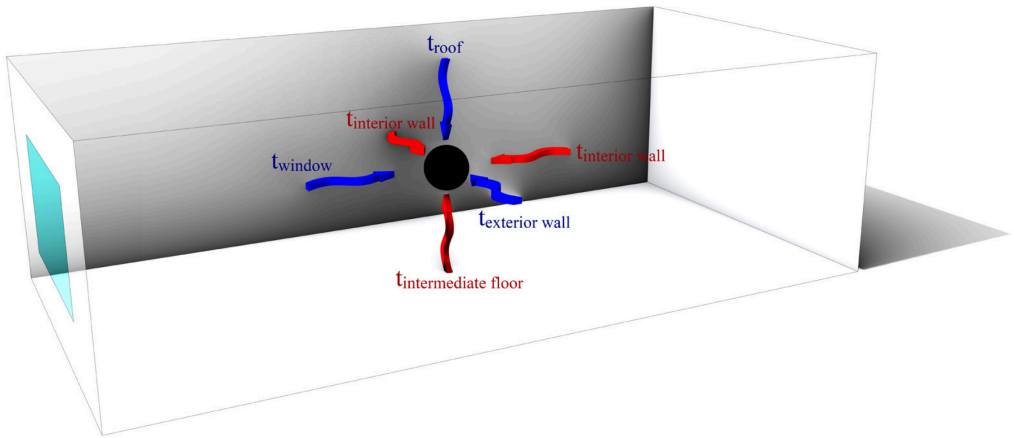

Figure 3: The concept of mean radiant temperature according to EN 15 251

3.1.1 Thermal bridges

A comprehensive case study performed by Berggren and Wall [84] showed that thermal bridges account for approximately 11 % to 20 % of the overall envelope transmission. It is, therefore, important to consider these losses when performing BPS assessing energy-performance and taking indoor thermal comfort into account. In this study, thermal bridges were accounted for by integration of thermal bridge impacts in the overall transmission losses. Thermal bridges were considered within the exterior building envelope, simplified into modified wall, roof and ground floor U-values accounting for thermal bridges. The respective calculations were executed using the software-engine THERM 7.6, operated through the visual scripting interface grasshopper using Honeybee. THERM is an engine programmed for one-, two- and three-dimensional conduction analysis of heat transfer [85], the present study only employed methods for 2D thermal bridge evaluation. The two-dimensional geometries with precise construction assemblies, heights and thicknesses were drawn in Rhinoceros 5 and 6 [76] as displayed in the exemplary diagram in Figure 4.

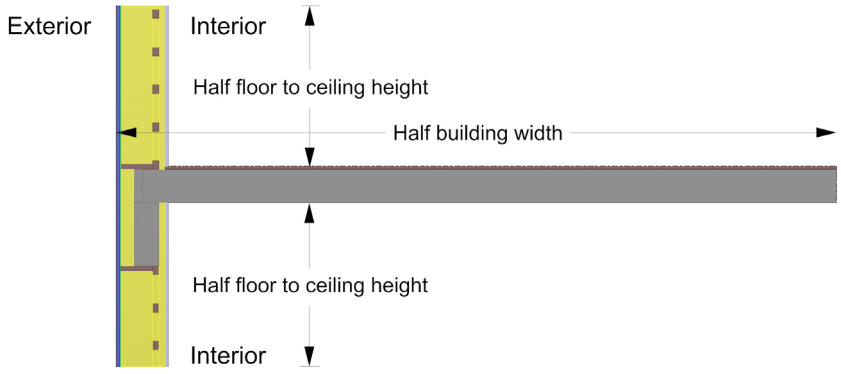

Figure 4: Example of thermally bridged intermediate floor junction

The polygon surfaces were referenced to grasshopper, where individual THERM polygons were created and specific thermal properties of materials in the respective projects were assigned. Simulations for case studies located in Denmark were executed with 21 °C interior and -9.6 °C exterior, whereas 22.0 °C interior and -11.9 °C exterior were used for buildings located in Germany. Unoccupied attic and basement spaces were set to 12.0 °C.

Firstly, the U-factors of 'ideal' external walls, excluding penetrations were determined. Secondly, all individual building elements were studied for inhomogeneous penetrations of insulation materials, such as wooden beams and rafters in plan and section cuts, modelled two dimensional. Moreover, junctions such as the intermediate floor were investigated, modelling exterior walls half a floor height above and below the intermediate floor as well as the floor construction for half the storey depth. Thus, a model for the steady state heat transfer calculation, as seen in Figure 4, was created. Exterior wall corners were neglected in the study as the impact on the U-value over the entire external wall area was proven to be marginal. The pre-study indicated that the modelled junction between exterior wall and intermediate floor throughout the four case studies were representative for a minimum of 75 % up to 93 % of the gross exterior wall area. These junctions were proven to yield a larger thermal loss than exterior wall connections to roof and ground slab. Thus, it was decided to apply the thermal bridges caused by the intermediate floor to represent the entire exterior wall thermal losses, simplifying the process by avoiding the separation of roof and ground slab junction linear losses. Equation 1displays the calculation of U-values including thermal bridges. U_{ideal} represents the U-value of an ideal cross-section without penetrations, $\Delta U_{section}$ and $\Delta U_{intermediate\ floor}$ are the difference between U_{ideal} and the U-value obtained in the respective thermal bridge simulations. The method of modelling 2D plan and section views was employed in order to account for 3D thermal bridges in a simplified manner. As the U-value measurement is normalised by the area, and the assessed sections of the external envelope constructions were representative for the entire building envelope, no additional weighting was required.

$$U_{new} = U_{ideal} + \Delta U_{section} + \Delta U_{intermediate\ floor} \left[\frac{W}{m^2 \cdot K}\right] \quad \text{(Equation 1)}$$

The procedure and simplification through integrated U-factor THERM results was chosen over other engines to enhance the benefits in easy and precise geometry modelling along with a simplistic way of adjusting thermal material properties matching the specified values in the respective projects. The validation of thermal bridge calculations was done utilising HEAT2 version 10 [86]. Keeping the exterior and interior temperatures as in the THERM workflow and the same material properties were used for HEAT2 simulations. Linear thermal loss calculation using HEAT2 and the overall U-value result validation of THERM output was executed for multiple sections of wall constructions, exemplary displayed for a retrofitted exterior wall with wooden studs visible in Figure 5. The method was deemed to be adequately validated, due to successful result comparison described closer in section 10.1. Further calculations were therefore executed using THERM software.

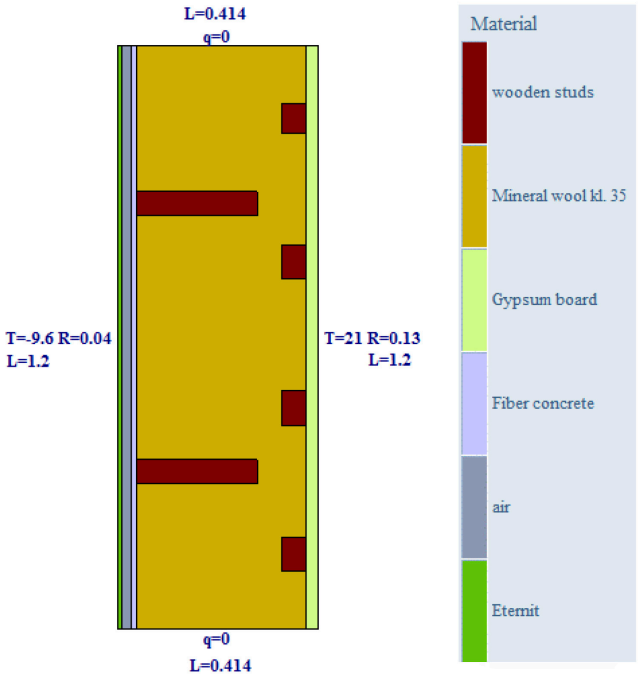

Figure 5: Retrofitted external wall section seen from top.

Thermal losses due to rafters in the roof construction and load-bearing beams in the floor partition between ground floor and basement were accounted for, employing the same method as described before. The thermal losses were accounted for in the respective construction U-values.

3.2 Hygrothermal Simulations

The assessments of moisture safety for exterior wall and roof constructions were carried out in WUFI Pro [87]. WUFI Pro is a software used to analyse the hygrothermal performance of building elements based on a one-dimensional transient calculation. The simulation engine analyses moisture movement through cross-sections of constructions, taking interior moisture loads, wind-driven rain, capillary movement and inbuilt moisture into account. The construction assembly was based on the available materials and constructions from the WUFI Database [88]. Non available materials in the WUFI Database were replaced by materials with similar properties, such as exterior façade cladding from natural slates were replaced by 'Eternit Cedral Struktur'. Ventilated air cavities of external walls and ventilated roofs were set to 30 ACH that is considered to be the optimal assumption providing reliable results [89]–[93]. Adhering fraction of rain was set to depend on the inclination of the component. Thermal insulation systems of exterior wall constructions were modelled with 1 % fraction of driving rain penetration behind the external insulation according to DIN 4108-3. Interior and exterior surface sd-values were selected according to actual finishing materials applied in the respective construction. Short-wave radiation absorptivity of the exterior surface was specified according to material color of the layer. Explicit radiation balance along with long-wave radiation emissivity was used for roof constructions. Outdoor temperatures and relative humidities were represented through the used weather files. Hygrothermal simulations were run for a 10-year period in order to see if moisture content

would stabilise during the provided timeframe. Failure in stabilizing within 10-years would represent inappropriate construction design in regard to moisture safety. Orientation for wall constructions was determined by comparing the exposure towards the least solar radiation receiving external walls and exposure towards the direction receiving the most wind-driven rain. The worse performing orientation was modeled in WUFI simulations. Actual case studies with different gable and façade constructions were evaluated separately. Roof inclinations were specified according to actual slopes of the respective building. Constructions facing interior boundary conditions such as intermediate floor construction towards basement and attic were excluded from the hygrothermal study. For buildings lower than 10 meters, driving rain coefficients of short buildings with height up to 10 meters were chosen. Driving rain coefficients for the buildings higher than 10 meters were assessed and worst-case conditions corresponding to the highest level of external walls and respective rain loads selected. Indoor climate conditions were modelled following EN 15 026 standard. Case studies without and with balanced mechanical ventilation were set to RH class Medium Moisture Load +5% and Medium Moisture Load respectively, according to WTA (Wissenschaftlich-Technische Arbeitsgemeinschaft) Merkblatt 6-2-01/D publication. Relative humidity values displayed in section 10.2 were integrated from three different time periods including three climate data sets for monitors positioned in the outermost exterior and interior sides of individual construction layers representing the most vulnerable conditions for moisture damages. Exterior cladding outside the wind-tight construction was excluded from this study. Monitors representing RH larger than 75% were further investigated with mould index created for the 10^{th} year of the simulations from three different time periods of TDY, marked with numbers within black dots in construction figures. Visible mould growth was further investigated with boxplot of mould growth rate for TDY and extreme weather conditions (ECY and EWY) including a 'triple' representing a combination of these three climate data sets for three individual time periods (2010-2039, 2040-2069, 2070-2099).

Hourly Temperature and RH values at studied depths in the construction were imported from the transient simulation and processed in MATLAB [94]. The Viitanen VTT model [12] for mould fungi growth was used to calculate the mould index as well as the mould growth rate. The VTT model represents a mathematical model to predict the mould growth index on a scale from 0 to 6, displayed in Table 1, as well as the mould growth rate [12]. Even though, the VTT model was developed and validated for wooden materials, it has been used in several scientific publications for the predictions of mould growth in various materials [12], [74], [95].

Table 1: Mould Index Integer Values [12]

Mould Index Integer	Scale
0	no growth
1	some growth detected only with microscopy
2	moderate growth detected with microscopy (coverage more than 10%)
3	some growth detected visually
4	visually detected coverage more than 10%
5	visually detected coverage more than 50%
6	visually detected coverage 100%

Boxplot diagrams were chosen for graphical presentation of the probability distribution based on the hygrothermal simulation results, such as 8670 hourly values a year of RH and mould growth rate, as seen in the explementary Figure 6. This type of diagram is a widespread tool for statistical analysis, with the main core strength imbedded within displaying the distribution of large amount of numerical data in a single diagram. Furthermore, it emphasises the occurrence of the greatest amount of data in the specific set. Four equal sets, each comprising of a quarter data values are formed when dividing the data into three quartiles, called Q1, Q2 and Q3. The median or Q2 is representing the value lying at the midpoint in the data set, meanwhile the part forming a box between Q1 and Q3, or otherwise called 'Interquartile range' is indicating the middle 50 % of values. Whiskers are the lines extending up to a maximum of 1.5 times the minimum and the maximum interquartile ranges (IQR). Outliers outside the minimum and maximum IQR represent the numerical values that appear to differ significantly from the original source of data it occurs in [96].

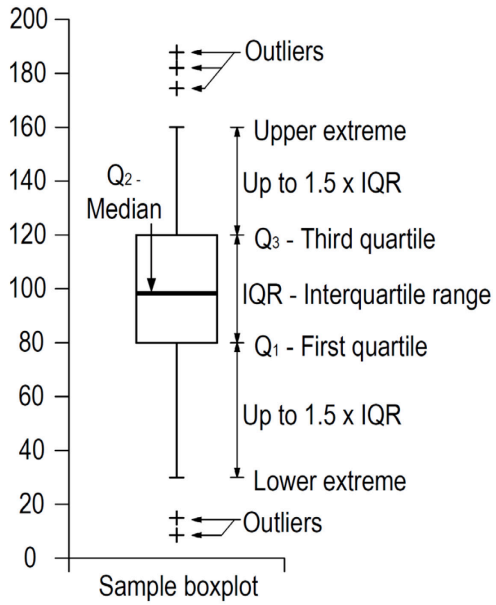

Figure 6: Example of a boxplot (Illustration by the author).

3.3 Weather Data

A typical weather file used for building energy simulations is generated from actual historical data for a period of 20-30 years. This sort of file typically includes hourly dry bulb temperature, dew point, diffuse solar radiation, global horizontal radiation, wind direction and wind speed. The type of weather file can be defined from specific weighting and the number of included meteorological variables. For example, the typical metrological year (TMY) includes mean, maximum and minimum values of dry bulb temperature, dew point, maximum and minimum wind speed. As Fischer and Schär [39] elaborated, data sets of TMY are derived for a period between the 1960's and 1990's and are based on the Finkelstein-Schafer (FS) statistic method [53] that selects a typical month for each of 12 calendar months from the whole database [39]. Typical reference year (TRY) is also based on the FS method for the datasets derived for the years 1961-1990. Nevertheless, TRY includes less variables compared to TMY, as normal and global radiations are not included [97]. There are, however, differences in TRY files depending on the institution that creates it. For example, the specific Danish Design Reference Year (D-DRY), includes sunshine hours per day derived from computed five-minute values of direct normal irradiance. Thus, the representative months are selected by comparing the standard deviations with the long-term mean of relevant parameters [98]. The downside of TMY and TRY is the underestimation of extreme weather conditions that are traced back to the averaging process induced by typical data generation [54]. Kershaw et al. found that the design summer year (DSY) lasting between April and September repeatedly underestimates overheating risk and the levels of human discomfort [99]. Using historical weather data is representing building performance in the past and not in the future. Moreover, weather files patched from a selection of typical months, provide an unlikely time series, even though a file created from recent 20-30 years of measured data is believed to be representative for the next decade [57].

In order to design a sustainable and comfortable dwelling, the building industry should use robust and credible weather files that not only take into consideration typical conditions with one-hour resolution and precise geographical location but include extreme conditions as well as possible future climate scenarios [39]. 'The resilience and adaptation' in regard to climate change is one of the key areas in a voluntary framework to improve the sustainability of buildings named 'Level(s)' that is currently undergoing its testing phase. This publication by the European Commission includes the full life cycle of the buildings and amongst others, it sets requirements for building performance tests against future climate conditions. Level(s) is an attempt to stress Paris Agreement goals to tackle issues like sustainable development, climate change, health and well-being [100].

Extreme weather files derived from observed data are not looking into long enough periods to identify extreme events with singular frequencies per century. Synthetic weather generators, on the other hand, can produce extreme weather conditions that have not yet been observed for a specific location. Even statistical representation along with the ability to mimic extreme weather behaviour is ensured. Future climate projections are created by employing computer-based algorithms that derive long-term or even different time scale weather variables comparable to measured historical data. Weather generators can be categorised as parametric, non-parametric and semi-parametric. Parametric generators include assumptions for the distribution functions of the inputs and statistical properties,

meanwhile non-parametric ones are run solely by the input data. Both options are used in semi-parametric weather generator category [57].

Weather data is fed into simulation software in multiple file types, this study employed weather files as WAC (WUFI ASCII Climate) for hygrothermal simulations in WUFI as well as EPW (EnergyPlus Weather) for BPS with EnergyPlus. Common and open-source platforms for weather files are established by IWEC (International Weather for Energy Calculations) and OneBuilding.

3.3.1 Future Weather Data

In this section a short description of the method employed for the generation of the future weather data is provided. For the detailed description of synthesized typical and extreme weather data sets, refer to Nik´s methodology [10], [101]. Future climate weather files applied in energy simulations are also thoroughly described in Nik´s publications [10], [102]. The hygrothermal simulations were executed using TDY, ECY, EWY data sets created employing Nik´s methodology [59], [103]. As concluded by Moazami et al. [104], there is a great need for weather files representing extreme conditions to account for the uncertainties that future climate holds. The beforementioned work also provides a comparison of the TDY method with other available weather data sets.

Energy and thermal comfort simulations were executed using climate data for Copenhagen and Aarhus cities representing the actual geographical location of studied buildings in Denmark, whereas weather files from Munich were used for simulations for the two German case studies situated in Stuttgart.
Three different climate data sets, including Typical Downscaled Year (TDY), Extreme Cold Year (ECY) and Extremely Warm Year (EWY) were used in this study. These climate data sets were produced from Regional Climate Models (RCMs). RCMs employed in this study for the generation of future climate scenarios were developed by the Rossby Centre and are therefore, referred to as Rossby Centre Regional Atmospheric Model (RCA4). Three Representative Concentration Pathways (RCP's) 2.6, 4.5 and 8.5 have been considered during the generation of representative future weather files. RCP's are projection sets widely used in research and climate modelling, describing possible future climate scenarios depending on the intensity of radiative forcing/ greenhouse gas emissions.
The outdoor dry-bulb air temperature was used to downscale and synthesize climate data sets implemented further in energy and hygrothermal simulations. Therefore, the total climate data of thirty years is assessed by calculating monthly quantiles of individual years and comparing them to the quantiles of all 30-year data together. Representative months for the TDY data sets are selected to represent the most typical temperature throughout the 30 years. For ECY data sets, the months with maximal difference to the 30-year quantiles were selected and the ones with the least difference for the EWY data sets. Employing this method, one-year weather files representing the respective extremes or typical weather conditions were used in hygrothermal simulations as well as BPS. Resulting in sets of nine weather files for each location, composing the three scenarios for the near-term (2010-2039), medium-term (2040-2069) and long-term (2070-2099) periods.

The two extremes and TDY weather scenarios for all three time-periods in between 2010 and 2099 are visualised for Aarhus (Figure 7), Copenhagen (Figure 8) and Munich (Figure 9). TDY represents the typical metrological year and lays therefore in the middle of ECY and EWY in all three cities. Yearly average temperatures are increasing with each time period from near-term, over medium-term towards long-term periods from 2010 towards the end of the century (2099).

Yearly average temperatures in TDY scenarios for Aarhus vary between 8.1 °C and 9.5 °C for the investigated three time periods, whereas ECY vary between 3.0 °C and 4.2 °C, and EWY vary between 12.3 °C and 14.6 °C. Even though the yearly average temperatures between TDY 2010 – 2039 climate scenario of Aarhus city and the historical weather data is matching within one decimal, the historical/ current weather data displays lower temperatures in winter season compared to the TDY future climate scenarios. This signals a global temperature increase due to climate change. The same increasing trends are noticed for both Copenhagen and Munich/ Stuttgart. Yearly average temperatures of Copenhagen are always within 0.7 °C difference compared to the ones of Aarhus, where TDY scenarios vary between 8.7 °C and 10.1 °C, ECY vary between 3.5 °C and 4.7 °C, and EWY vary between 13.0 °C and 15.2 °C for the investigated time-periods. Yearly average temperatures of Munich for TDY scenarios vary between 10.9 °C and 12.4 °C, for ECY between 5.7 °C and 6.5 °C, and EWY between 16.4 °C and 19.3 °C for different time-periods.

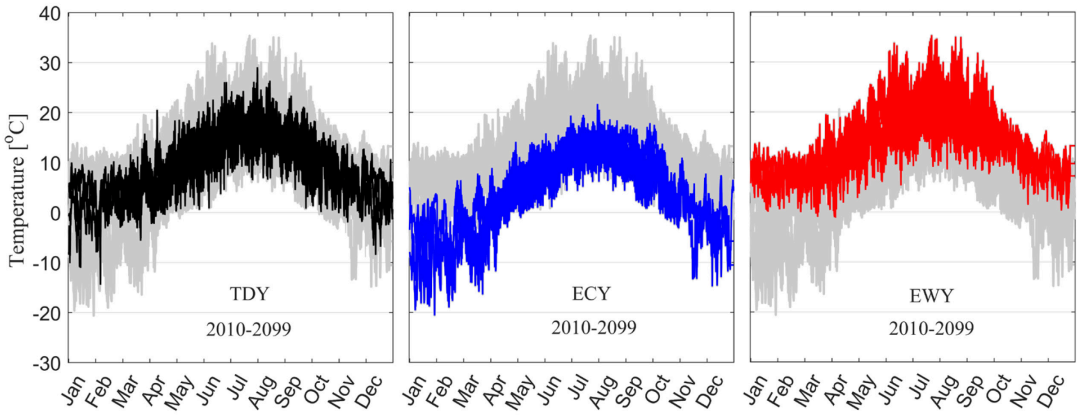

Figure 7: Temperature variations in TDY and two extreme climate scenarios between 2010 and 2099 of Aarhus. TDY – black, ECY-blue, EWY – red, Triple for combined TDY, ECY and EWY – grey.

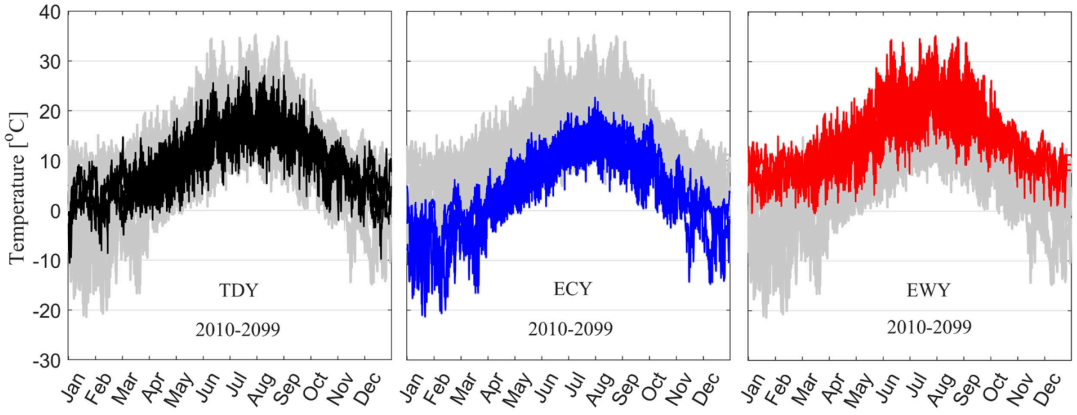

Figure 8: Temperature variations in TDY and two extreme climate scenarios between 2010 and 2099 of Copenhagen. TDY – black, ECY-blue, EWY – red, Triple for combined TDY, ECY and EWY – grey.

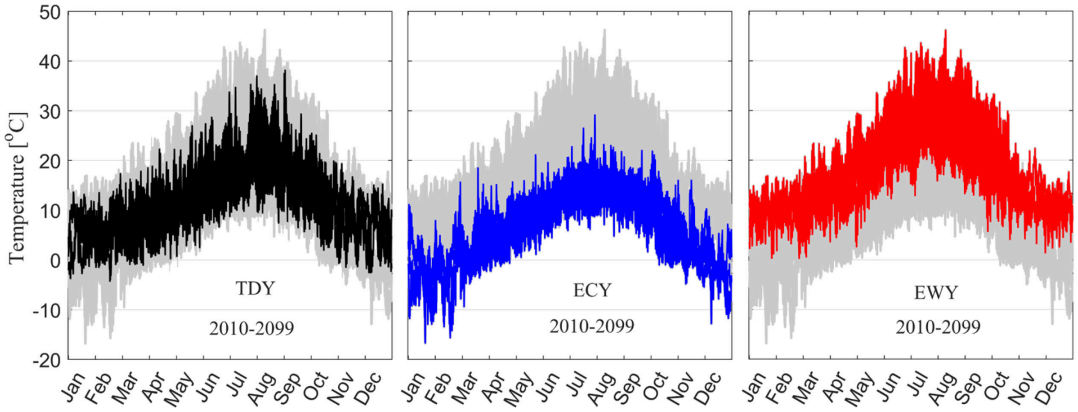

Figure 9: Temperature variations in TDY and two extreme climate scenarios between 2010 and 2099 of Munich TDY – black, ECY-blue, EWY – red, Triple for combined TDY, ECY and EWY – grey.

Figure 10 and Table 2 show exemplary a comparison of the outdoor dry-bulb temperatures for the three TDY future periods obtained from the RCM for Munich with the historical weather data from the IWEC [105]. It can be observed, that average temperatures between the historical data and the future predictions differ by about 1.8 °C from the TMY to the TDY 2010-2039. Minimal temperatures differ by 6.5 °C, in both cases the TDY being warmer than the TMY. For the maximum temperature, the TMY is 1.1 °C warmer than the TDY, which can be explained by the geographical location. In general, the TMY for Munich for the same time period and the same source shows lower average, minimum and maximum temperatures than the Stuttgart file. What is remarkable are the large differences in the average temperatures in the winter months between the TMY and TDY data seen in Table 2. December, January and February as the coldest months of the year show differences of 3.2 °C to 5.3 °C. Figure 10 additionally represents, that all three TDY periods show no extensive cold periods.

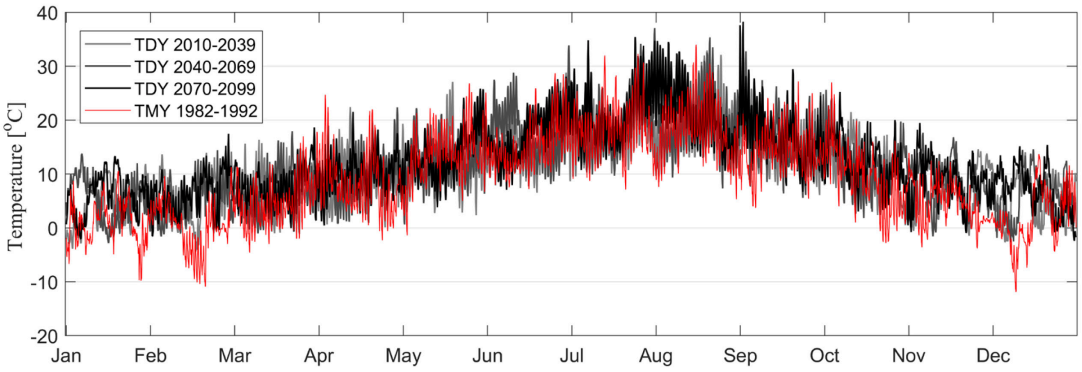

Figure 10: Temperature comparison between TDY scenarios for Munich and historical/current TMY weather file of Stuttgart.

Table 2: Monthly average, annual average and annual minimal and maximal dry-bulb temperatures for TDY 2010-2039, 2040-2069 and 2070-2099 and historical TMY file for Stuttgart 1982-1992.

[°C]	Jan	Feb	Mar	Apr	May	Jun	Jul	Aug	Sep	Oct	Nov	Dec	Annual average	Min. Temperature	Max. Temperature
TDY 10-39	4.4	5.1	6.6	8.9	12.2	15.8	18.4	19.0	15.7	11.1	7.3	5.2	10.9	-4.4	32.9
TDY 40-69	5.3	5.6	7.1	9.4	12.7	16.7	19.4	19.9	16.8	12.1	8.3	5.9	11.6	-2.8	37.1
TDY 70-99	5.9	6.3	7.8	10.1	13.4	17.2	20.8	21.4	17.7	12.5	8.7	6.8	12.4	-2.4	38.3
STR 82-92	1.0	-0.2	4.5	8.3	13.2	15.1	18.6	17.9	14.1	9.3	4.6	2.0	9.1	-11.9	34.0

4 Model

This chapter presents the case study objects examined in this work. Separated by the countries Denmark and Germany in the two main chapters, building properties of each project of the initial and retrofitted state are described. Settings and parameters used in the BPS and hygrothermal simulations are presented, as well as assumptions and simplifications concerning the respective project.

4.1 Denmark

Danish apartment buildings erected between 1850 and 2000 can be divided into 5 main types in terms of architecture, plan layout and engineering solutions. Understanding their key differences in material choices and construction solutions are vital for a well-designed and properly implemented renovation project [106].

The first and the oldest Danish apartment type can be traced back to the beginning of the 18th century. It was considered as a superior dwelling type all the way up to the 1890's. The exterior envelope was made of thick solid-brick walls, while interior partitions were constructed as lightweight walls. Floor partitions were made from wooden joists; thus, wood was also used for staircases. Pitched roofs were typically built by means of wooden rafters and included dormers. Foundations were constructed from bricks or made from stone. As a lot of load carrying parts were constructed from organic materials e.g. timber framing, it is common nowadays to notice fungus and other moisture caused damage in the interior spaces. Most of these houses are a part of cultural heritage. Therefore, the preferable thermal renovation from the exterior is not a valid design option [106].

The second type is very similar to the first one in terms of architecture, layout and construction, it remained popular up until 1930's. As from 1889 walls around staircases along with load carrying internal walls were built from bricks. This was an attempt to decrease the number of deaths in case of fire. Use of in-situ concrete began to be a common practice for foundations. Smaller size reinforced concrete elements were introduced as lintels for bay windows, cantilever overhangs, moisture and fire protection towards the basement [106].

The signature design element of the third type became the use of reinforced concrete which was used for main staircases. Buildings now included cast in place reinforced concrete balconies. The resulting thermal bridge issue is difficult to minimize when performing a major renovation and insulating the exterior building envelope. Basement walls and foundations were cast from reinforced concrete. Unlike the first two types, these dwellings did not include a rear staircase. The use of concrete based tiles along with asphalt paper allowed smaller roof inclinations to be constructed. Roof beams and partitions were still made of wood. Even though this type of apartment buildings was quite common in the 1930's, it was phased out in the 1950's when new legislation came into force regarding fire-resistant roof slabs [106].

Type four was very similar to type three. However, the noticeable difference could be seen in concrete floor partitions. It was commonly used around the 1950's [106]. The majority of construction parts like exterior and interior stabilizing walls, staircases, floors and roof

partitions in the fifth type were made from prefabricated elements. Only the interior separation between rooms were built as light weight constructions [106].

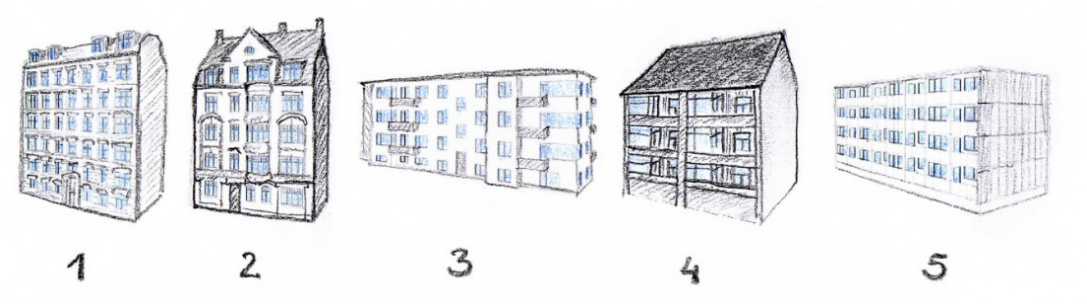

Figure 11: Five common types of apartment buildings in Denmark [106] (Drawing by the author)

It was a common practice to demolish old and outdated apartment buildings that faced health hazard conditions up until the 1970's. In the 19th century public attitude towards cultural and architectural heritage began to change, landlords began to retrofit and modernise spaces in regard to urban renewal and sanitation laws. Households were equipped with central heating, hot water supply, ventilation, new kitchens and bathrooms. Even though thermal insulation was added to roof construction and gables facing outside, it was avoided on facades due to preservation of original external look along with mounting difficulties caused by story partitions and space loss of the interior areas. Existing windows were replaced with 2 pane glass or by applying additional pane on the inside [106].

In the old days it was a common practise to ventilate a dwelling through its windows by means of natural ventilation. Therefore, in order to ensure a fresh air supply building laws required openable windows that were meant to be used as a rescue opening in case of fire [107]. With time, fresh air intake began to be designed through air valves. Mechanical extract ventilation was introduced as a new alternative to natural ventilation in Building Regulations 1961 (BR61) [107]. Newly constructed multi-storey dwellings must be designed with balanced mechanical ventilation systems that supply multiple apartments with heat recovery efficiency of at least 73 % [108] following EU regulations 1253/2014 for ventilation units [109]. Fresh air must be provided to living rooms, bedrooms and extracted from 'contaminated' spaces like kitchens and toilets. A minimum air flow of 0.30 l/s per square meter heated floor area or an air exchange rate of 0.5 h^{-1} must be supplied to the dwelling [109]. Retrofitting projects might be exempted from the installation of mechanical ventilation when such renovation work cannot be carried out without major changes in the building [109].

The Danish building stock has encountered many building laws and building code publications through its history [110]. New requirements in regard to administrative provisions, design and layout, structures, fire safety, indoor climate, technical services, energy consumption and others were implemented along the way, while older ones kept on being improved. Buildings constructed after 1979 and falling under Building Regulations 1979 (BR1979) needed to meet tightened thermal insulation requirements. These were assumed to be extremely strict at the time. Individual building parts along with windows and doors towards the outside needed to meet a minimum thermal performance expressed through U-value. Thermal bridges were only allowed to some extent [111]. This was the first substantial step towards mitigation of thermal losses through the exterior envelope.

With a release of Building Regulations 1995 (BR95) [112] the action plan for sustainable development 'ENERGI 2000' from 1990's [113] was implemented through tightening thermal insulation requirements that were estimated to meet 25 % reduction in energy consumption. Required insulations thickness were approximately the double compared to the ones from 1961 (BR61). Moreover, 'ENERGI 2000' aimed to reduce CO_2 emissions by 20 % in comparison to 1988 levels [113]. In addition, an overall heat loss frame calculation was introduced in BR95 [112].

'A visionary Danish energy policy' (En visionær dansk energipolitik) was presented back in 2007 that described energy targets for 2025. The government amongst others aimed to reduce the use of fossil fuels by 15 %, increase renewable energy sources to a minimum of 30 % with a vision of exploiting wind power potential, continue economic growth without increasing energy consumption and additionally reducing it by 1.25 % yearly [114], [115]. In order to meet energy mitigation targets, building codes were continuously tightening building energy requirements and increasing minimum values for thermal insulation for both new and retrofitting projects. This process can be easily observed when comparing Building Regulations 2008 (BR08) [116] with 2010 (BR10) [117], followed by 2015 (BR15) [118] and finishing with current Building Regulation 2018 (BR18) [109]. The Danish Government sees a need for strengthening European energy policy by long-term and well-prepared initiatives across Member States. As a result, politicians are eager to collaborate, discuss and implement newest climate goals present in latest EU directives [114], [115].

4.1.1 Project 1

A residential apartment block of three stories constructed in the 1970's on the mainland of Denmark 'South Jutland'. It contained a total of 22 differently sized apartments, four households of 1-room, four of 3-rooms, nine of 4-rooms and three of 5-rooms. Oblong facades were facing east and west, respectively the gables were facing north and south, as displayed in Figure 12. The building was designed with 3 separate entrances with 90° turn staircases. On the west façade, apartments based on the ground floor were equipped with a terrace, meanwhile first and second floor apartments with balconies. The dwelling was constructed as a construction-time typical prefabricated sandwich concrete element block with natural ventilation. For space heating and domestic hot water, the building was connected to a district heating system. Setpoint temperature for all occupied spaces were established as 21 °C, meanwhile unoccupied spaces such as basement and staircases were set to 15 °C. The building undergone a major renovation in the beginning of the 2010´s. Measures to mitigate the energy use along with thermal bridges were carried out. The retrofit resulted in a more airtight building envelope that was reflected in minimised infiltration rates. All old windows and doors were replaced. Outdated technical installations, like inefficient hot water tanks, were exchanged with new fixtures. Heating and hot water pipes were insulated. The extract ventilation system in the initial building with a ventilation rate of 0.3 l/(s·m^2), was replaced by a balanced mechanical ventilation with heat recovery of up to 82 % and SEL- value of 1.2 kJ/m^3. A minimum air flow of 0.3 l/(s·m^2), corresponding to about 0.5 air changes per hour (ACH) was introduced in each apartment. The infiltration rate was lowered from 0.23 l/(s·m^2) in the initial building stage to 0.13 l/(s·m^2) at normal pressure after the retrofit. Kitchens and bathrooms were redesigned in accordance with disabled accessibility requirements. New energy-efficient white goods replaced older ones. Approximately 230 m^2 of PV-panels were integrated in the roof, corresponding to roughly

36 kW_p of installed output, in order to be used for lighting in common areas and running the central ventilation unit. In addition, the production of a 57 m^2 solar thermal system was used as an additional resource for heating of domestic hot water.

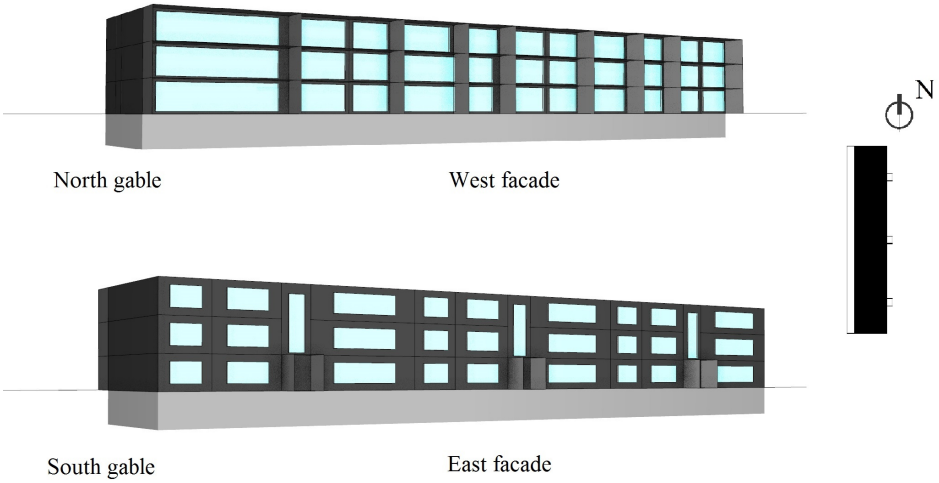

Figure 12: Geometry used in energy and thermal comfort simulations. Visualisations taken from North-West and South-East rotations. Building orientation shown from the top displayed on the right side of the figure. Building Properties Original and Retrofitted

4.1.1.1 Building Properties Original and Retrofitted

External walls were constructed from prefabricated sandwich elements containing inner and outer concrete leafs and 100 mm mineral wool insulation as shown and described in Figure 13 and Table 3.

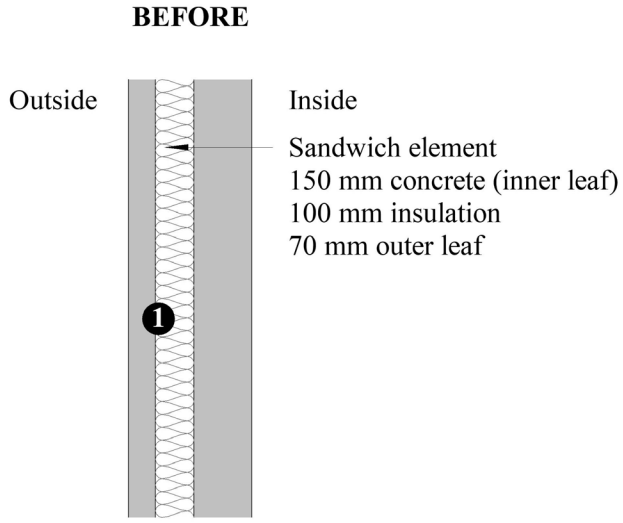

Figure 13: Plan section, external wall construction, initial state.

Table 3: Construction assemblies and thermal properties of walls, initial state.

Location	Material layers (Exterior to interior)	Thickness [m]	Bulk Density $\left[\frac{kg}{m^3}\right]$	Specific Heat $\left[\frac{J}{kg\,K}\right]$	Thermal Conductivity $\left[\frac{W}{m\,K}\right]$
Initial gables and facades	Reinforced concrete	0.070	2200	850	1.600
	Mineral wool insulation	0.100	60	850	0.040
	Reinforced concrete	0.150	2200	850	1.600

During the renovation, exterior walls were divided into 2 separate constructions. The load bearing and stiffening gable walls maintained their original structure and additional exterior thermal insulation was added. The remaining facades were demolished and replaced with new prefabricated light-weight elements (see Figure 14 and Table 4).

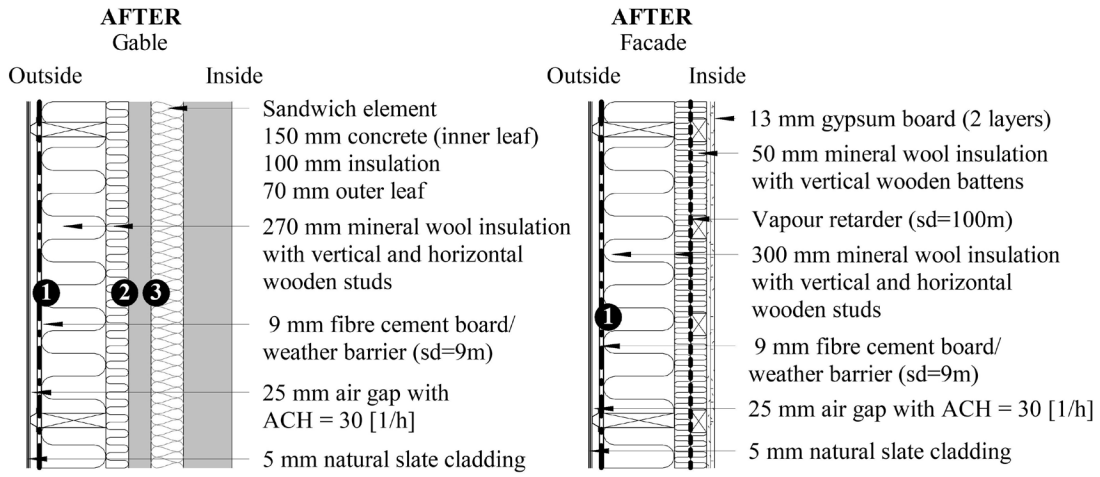

Figure 14: Plan section, gable and façade construction, retrofitted state. Black dots indicate monitor positions in wufi.

Table 4: Construction assemblies and thermal properties of gable walls, retrofitted state.

Location	Material layers (Exterior to interior)	Thickness [m]	Bulk Density $\left[\frac{kg}{m^3}\right]$	Specific Heat $\left[\frac{J}{kg\,K}\right]$	Thermal Conductivity $\left[\frac{W}{m\,K}\right]$
Gables retrofitted	Eternit Cedral Struktur	0.005	1347	850	0.210
	Ventilation gap	0.025	1.3	1000	
	Fibre cement sheathing board	0.009	1380	840	0.245
	Mineral wool insulation*	0.270	25.2	1000	0.035
	Reinforced concrete	0.070	2200	850	1.600
	Mineral wool insulation	0.100	60	850	0.040
	Reinforced concrete	0.150	2200	850	1.600
Facades retrofitted	Eternit Cedral Struktur	0.005	1347	850	0.210
	Ventilation gap	0.025	1.3	1000	
	Fibre cement sheathing board	0.009	1380	840	0.245
	Mineral wool insulation*	0.300	25.2	1000	0.035
	Vapour retarder; sd=100m	0.001	130	2300	2.300
	Mineral wool insulation*	0.050	25.2	1000	0.035
	Gypsum board (2 layers)	0.025	625	850	0.200

* Insulation layer with wooden studs. For thermal bridges see section 5.1.1.2.

The roof construction, which is characteristic for Danish construction during the 1970's, included wooden trusses mounted directly on the hollow core deck with 100 mm insulation placed in between. During the renovation, roof elements above the hollow core decks were removed and a highly insulated flat roof construction with bitumen felt was introduced (see Figure 15 and Table 5).

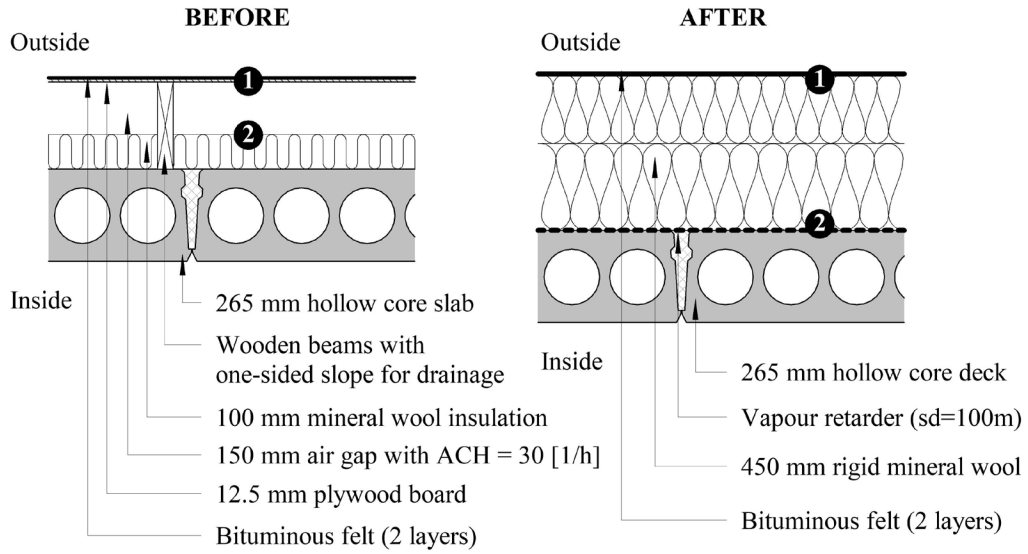

Figure 15: Cross-section view, roof construction, initial and retrofitted state.

Table 5: Construction assemblies and thermal properties of roof, initial and retrofitted state.

Location	Material layers (Exterior to interior)	Thickness [m]	Bulk Density $\left[\frac{kg}{m^3}\right]$	Specific Heat $\left[\frac{J}{kg\,K}\right]$	Thermal Conductivity $\left[\frac{W}{m\,K}\right]$
Roof before renovation	Bituminous felt	0.001	715	1500	2.300
	Plywood board	0.012	560	1500	0.130
	Ventilation cavity	0.150	1.3	1000	0.940
	Mineral wool insulation*	0.100	60	850	0.040
	Hollow core concrete deck	0.265	2200	850	1.600
Roof after renovation	Bituminous felt	0.001	715	1500	2.300
	Rigid mineral wool	0.450	176	850	0.036
	Vapour retarder; sd=100m	0.001	130	2300	2.300
	Hollow core concrete deck	0.265	2200	850	1.600

* Insulation layer with wooden rafters. For thermal bridges see section 5.1.1.2.

The building contained a basement which was mainly used for technical installations.
The initial floor construction facing the basement did not contain any thermal insulation. As a result, apartments based on the ground floor contributed to an unintentional heating of unoccupied spaces. During the renovation, 200 mm of mineral wool insulation was added underneath the ceiling construction in the basement (see Figure 16 and Table 6). This was done in order to maintain floor to ceiling height in occupied spaces. Concrete walls in the basement were insulated with 100 mm exterior EPS insulation.

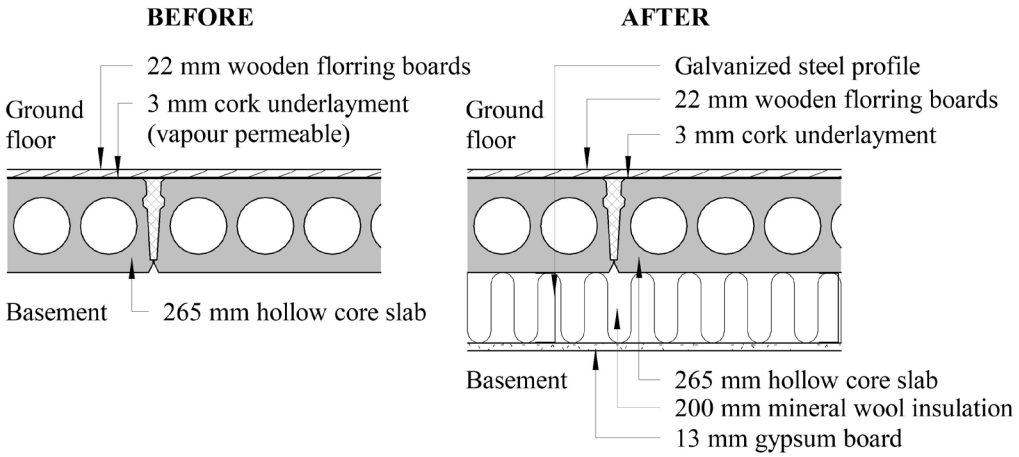

Figure 16: Cross-section view, floor construction towards basement, initial and retrofitted state.

Table 6: Construction assemblies and thermal properties of floor construction towards unheated basement, initial and retrofitted state.

Location	Material layers (Exterior to interior) Indoor condition; basement	Thickness [m]	Bulk Density $\left[\frac{kg}{m^3}\right]$	Specific Heat $\left[\frac{J}{kg\,K}\right]$	Thermal Conductivity $\left[\frac{W}{m\,K}\right]$
Intermediate floor before renovation	Hollow core concrete deck	0.265	2200	850	1.600
	Cork	0.003	140	1872	0.043
	Wood	0.022	560	1500	0.130
Intermediate floor after renovation	Gypsum board	0.013	625	850	0.200
	Mineral wool insulation*	0.200	60	1000	0.037
	Hollow core concrete deck	0.265	2200	850	1.600
	Cork	0.003	140	1872	0.043
	Wood	0.022	560	1500	0.130

*Indicates thermal bridges created by aluminium profiles (inhomogeneous layer). Thermal bridge is included in the overall U-value of the construction, as described in section 3.1.1. Other constructions marked with the same sign contain the same issue.

Energy use and thermal comfort simulations were executed with the window to wall ratios (WWR) as seen in Table 7. Windows installed in the initial building in 1967 were estimated to represent properties specified in Table 8. Specification of windows and glazed doors used in retrofitted project were as stated in Table 8. Solar energy transmittance of glazing is referred to as g-value in percent, the frame to glazing ratio is expressed as f_f and T_{vis} is describing visual transmittance of the glazing.

Table 7: WWR ratio of the initial and retrofitted projects.

	North	South	West	East
Initial	0 %	0 %	71 %	30 %
Retrofitted	5 %	5 %	71 %	35 %

Table 8: Window Specifications

Location	U-value incl. frame $\left[\frac{W}{m^2 K}\right]$	g-value [%]	f_f [%]	T_{vis} [%]
Initial				
All glazing	2.8	63	20	78
Retrofitted				
All glazing	1.1	50	20	75

4.1.1.2 Assumptions and Simplifications

Around 1990, the housing company attempted to reduce the energy consumption caused by thermal losses due to the poorly insulated building envelope. Therefore, 100 mm of granulate insulation was blown into cavities between the wooden studs in the roof construction. Exterior walls were retrofitted with the addition of a secondary skin façade incorporating 100mm of mineral wool insulation along with exterior cladding panels made from glass fibre and reinforced polymer composite. During the latest renovation these structures were torn down completely and replaced with new elements. As the target group of this study was existing buildings erected before 1990, it was chosen to exclude the mid-way retrofits and only explore the performance of the original structures. Due to missing initial façade drawings and lack of scaled technical drawings, WWR was calculated by means of site visits and partial estimations. The housing company exchanged windows in the bathrooms in 2006, updated thermal properties of these elements were ignored in the study and the original window properties were used instead. Openings were modelled as a window to wall ratio (WWR). In addition, interior thermal zones were simplified for individual apartments, as per east and west facing rooms along with hallway in the middle. Unheated spaces, such as staircases and basement were excluded from the indoor comfort study.

4.1.2 Project 2

The building consists of 15 habitable stories and a basement, as visualised in Figure 17. In total there are 9 different apartment types varying between one to six rooms. Smaller one room apartments are primarily located on the ground floor. The architect and engineer teams developed an overall retrofit plan, focusing on improving the energy performance of the building, and implementing disability friendly access. All elements of the initial exterior building envelope undergone thorough retrofitting process, resulting in minimised heat losses and infiltration rates. These were simulated with 0.20 l/s·m^2 for the initial case and 0.10 l/s·m^2 for the retrofitted building at normal pressure difference. The project plan was developed in a thorough process favouring the preferences of inhabitants. As a result, the balcony spaces were enlarged by 50%, and daylight penetration improved by larger openings. Also, bathrooms and kitchens were remodelled in all households. Furthermore, individual metering of water and heat was installed in order to promote energy awareness and create fair and equitable utility invoicing according to the actual consumption. Original radiators were replaced by the new ones with intelligent thermostats that provided automatic adjustment of the heating according to the actual room temperature. Heating pipes were

changed for a 2-pipe system with diameters according to the new flow rates. The original mechanical ventilation as extraction system with a ventilation rate of 0.4 l/(s·m^2), was replaced with a balanced ventilation system with heat recovery, while retaining the same ventilation rate. Due to traces of asbestos discovered in the existing ventilation ducts they were replaced by galvanised steel ducts. The new ventilation unit with an estimated heat recovery efficiency between 65 % and 85 % with a SEL-value of 1.8 kJ/m^3 was installed in the newly erected attic space. The slanted attic construction was also used for the installation of 300 m^2 photovoltaic (PV) panels facing South-West. The energy yield from this system was dedicated to being used for lighting common areas, supplying electricity for ventilation unit and laundry room equipped with both washing machines and dryers. The main heating system based on a natural gas boiler was exchanged for a connection to the district heating system. Setpoint temperature for all occupied and unoccupied spaces were specified as 21 °C, and 15 °C respectively. The old electricity wiring and cables were replaced in order to comply with official regulations for new structures and to mitigate the risk of fire. In addition, energy-efficient light fixtures with LEDs and occupancy-sensor lighting controls in the common spaces were implemented. All executed retrofitting measures were a part of a holistic sustainability approach, in which energy optimization, maintenance and occupant satisfaction were the driving factors for design decisions. The project was nominated for the anniversary renovation award 'RENOVER' issued by a non-profit business association 'Realdania' in 2017, additionally it was certified as DGNB (Deutsche Gesellschaft für Nachhaltiges Bauen) gold building.

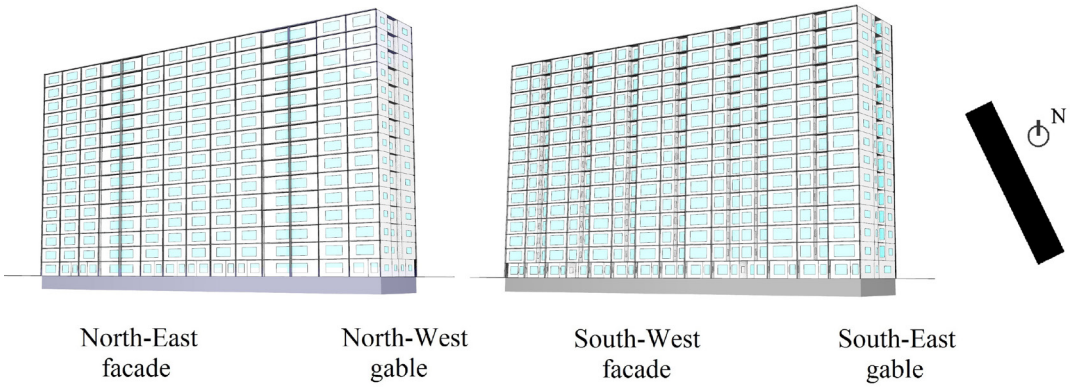

Figure 17: Geometry used in energy and thermal comfort simulations. Building orientation shown from the top displayed on the right side of the figure.

4.1.2.1 Building Properties Original and Retrofitted

The exterior light-weight walls facing South-West and North-East were originally constructed as prefabricated elements consisting a weather resistive barrier as the wind tight membrane, 100 mm of mineral wool insulation between wooden studs, an aluminium foil as vapour-proof membrane, interior Masonite boards and exterior cladding from aluminium sheets (see Figure 18). On-site investigation of initials conditions did not reveal any noticeable changes due to low airtightness of the initial aluminium foil. However, exterior wooden battens in the ventilation gap showed rot-damage, which indicated predominant high RH and wind-driven rain penetration. The water related damage in the existing construction was taken into account when designing the new façade elements. Specific architectural expression of the initial building was created by the protruding façade frames in the exterior envelope. These framings were originally built as concrete elements connected directly from floor slabs and internal partition walls with a simple thermal separation of 15 mm cork, but continuous starter bars. The chosen realisation created an extensive geometrical thermal bridge and posed a risk of mould due to condensation.
The improvement of thermal comfort, minimisation of thermal bridges, decrease of thermal losses through building envelope and upgrade of the vapour retarder was done by replacing the old façade construction with new prefabricated light weight elements as seen in Figure 18. The new façade elements along with the original concrete frames which were wrapped with insulation, formed the retrofitted wall construction. In order to maintain the original look of the building new light weight fibre concrete shell frames were indirectly connected to the exterior wall.

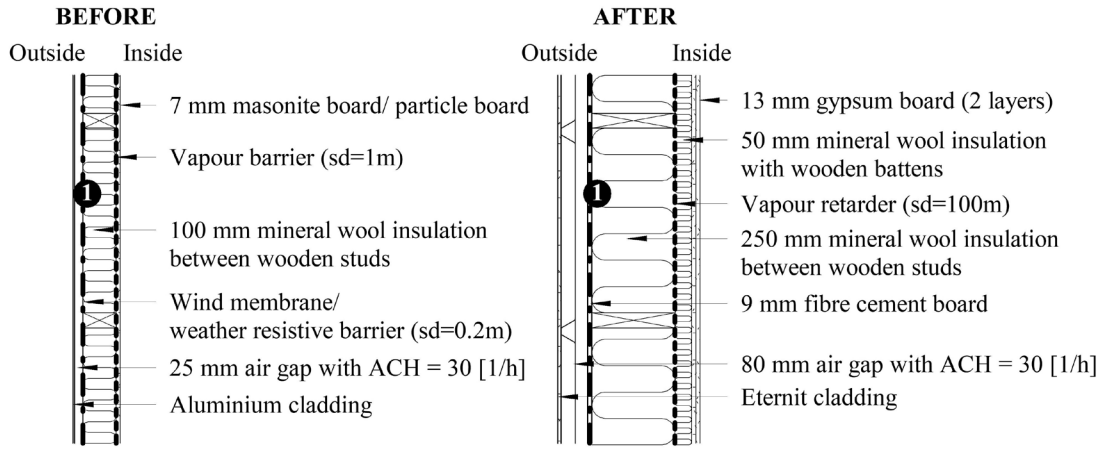

Figure 18: Plan section, façade construction, initial and retrofitted state.

Table 9: Construction assemblies and thermal properties of facade walls, initial and retrofitted state.

Location	Material layers (Exterior to interior)	Thickness [m]	Bulk Density $\left[\frac{kg}{m^3}\right]$	Specific Heat $\left[\frac{J}{kg\,K}\right]$	Thermal Conductivity $\left[\frac{W}{m\,K}\right]$
Facades initial	Aluminium cladding				
	Ventilation gap	0.025	1.3	1000	
	Weather resistive barrier; sd= 0.2 m	0.001	130	2300	2.300
	Mineral wool insulation*	0.100	60	850	0.040
	Vapour barrier; sd= 1m	0.001	130	2300	2.300
	Particle board (Masonite)	0.007	664	1400	0.120
Facades retrofitted	Eternit cladding	0.010	1220	850	0.210
	Ventilation gap	0.080	1.3	1000	
	Fibre cement sheathing board	0.009	1380	840	0.245
	Mineral wool insulation*	0.250	25.2	1000	0.035
	Vapour retarder; sd=100m	0.001	130	2300	2.300
	Mineral wool insulation	0.050	25.2	1000	0.035
	Gypsum board (2 layers)	0.025	625	850	0.200

* Insulation layer with wooden studs. For thermal bridges see section 5.1.2.2.

The gable walls were originally constructed with a load-bearing concrete inner leaf, a thin layer of pressure resistive insulation, exterior concrete tiles made from 150 mm of light weight concrete and 50 mm outer concrete tiles as visible façade elements as displayed in Figure 19. Reviewing the operational energy consumption of the building revealed that apartments interconnected with gable walls failed to provide comfortable indoor temperatures in winter periods. It was decided to demolish the whole concrete tile construction outside the load-bearing structure along with the old insulation material. A ventilated steel profile structure including 300 mm of mineral wool insulation and fibre concrete boards were attached onto the preserved concrete wall during the retrofit.

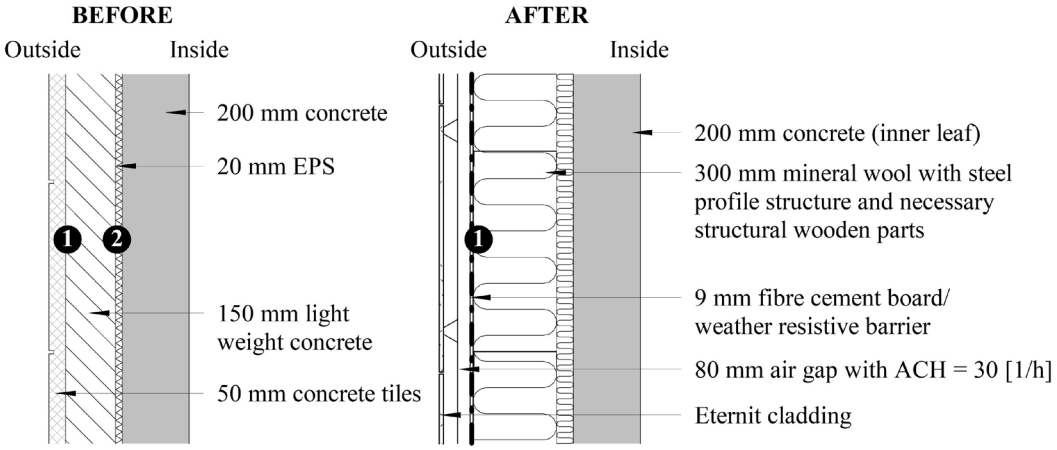

Figure 19: Plan section, gable construction, initial and retrofitted state.

Table 10: Construction assemblies and thermal properties of facade walls, initial and retrofitted state

Location	Material layers (Exterior to interior)	Thickness [m]	Bulk Density $\left[\frac{kg}{m^3}\right]$	Specific Heat $\left[\frac{J}{kg\,K}\right]$	Thermal Conductivity $\left[\frac{W}{m\,K}\right]$
Gables Initial	Concrete	0.050	2200	850	1.600
	Light weight concrete	0.150	599	850	0.066
	EPS	0.020	30	1500	0.040
	Concrete	0.200	2200	850	1.600
Gables Retrofitted	Eternit cladding	0.010	1220	850	0.210
	Ventilation gap	0.080	1.3	1000	0.460
	Fibre cement sheathing board	0.009	1380	840	0.245
	Mineral wool insulation*	0.300	25.2	1000	0.035
	Concrete	0.200	2200	850	1.600

* Insulation layer with wooden studs and metal profiles. For thermal bridges see section 5.1.2.2.

The internal load-bearing and stiffening walls were constructed from concrete elements, separating individual apartments and the common staircase. Internal partition walls within individual households were constructed as lightweight walls with pasteboard finishing. The original roof construction was assembled from wooden beams with wooden profiled boards and roofing felt on top, as seen in the details in Figure 20. Although the roof inspection showed that the existing wooden rafters were in a rather good shape, it was decided to replace it with a new insulated concrete slab construction, as shown in Figure 20, with increased fire resistance and better load-capacities as a base for the technical room accommodating the ventilation unit.

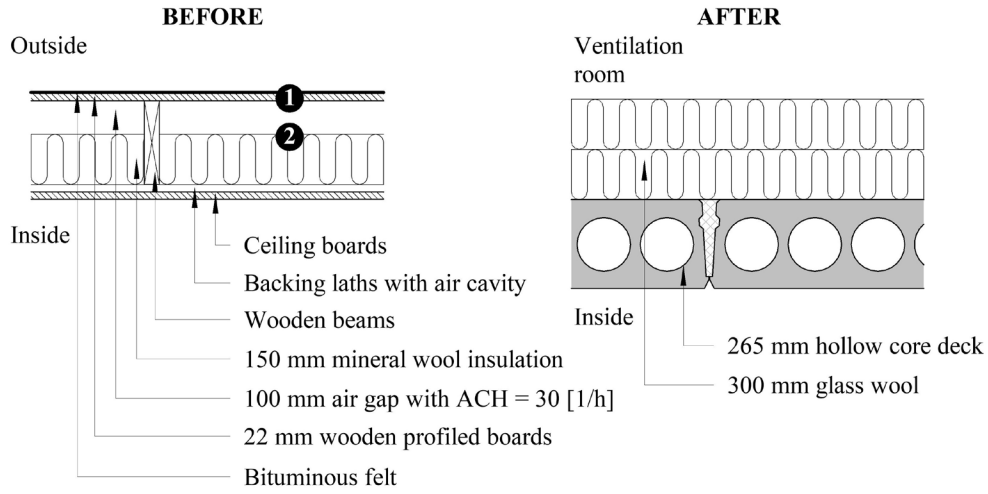

Figure 20: Cross-section view, roof construction, initial and retrofitted state.

Table 11: Construction assemblies and thermal properties of roof thermal envelope constructions, initial and retrofitted state.

Location	Material layers (Exterior to interior)	Thickness [m]	Bulk Density $\left[\frac{kg}{m^3}\right]$	Specific Heat $\left[\frac{J}{kg\,K}\right]$	Thermal Conductivity $\left[\frac{W}{m\,K}\right]$
Roof before renovation	Bituminous felt	0.001	715	1500	2.300
	Wooden profiled boards	0.022	400	1400	0.090
	Ventilation cavity	0.100	1.3	1000	0.940
	Mineral wool insulation*	0.150	60	850	0.040
	Air cavity and backing laths	0.021	1.3	1000	0.130
	Wooden ceiling boards	0.015	400	1400	0.090
	Indoor condition; ventilation room				
Roof after renovation	Glass wool	0.300	20	850	0.034
	Hollow core concrete deck	0.265	2200	850	1.600

* Indicates insulation layer with wooden rafters. For thermal bridges see section 5.1.2.2.

Existing uninsulated basement walls were retrofitted with 100 mm exterior EPS insulation. The intermediate floor between the basement and the ground floor was initially insulated with 60 mm insulation. The design proposed additional thermal insulation to mitigate heat losses towards the basement which was heated to 15 °C. The values specified in Table 12 were followed in this study and the respective constructions can be seen in Figure 21.

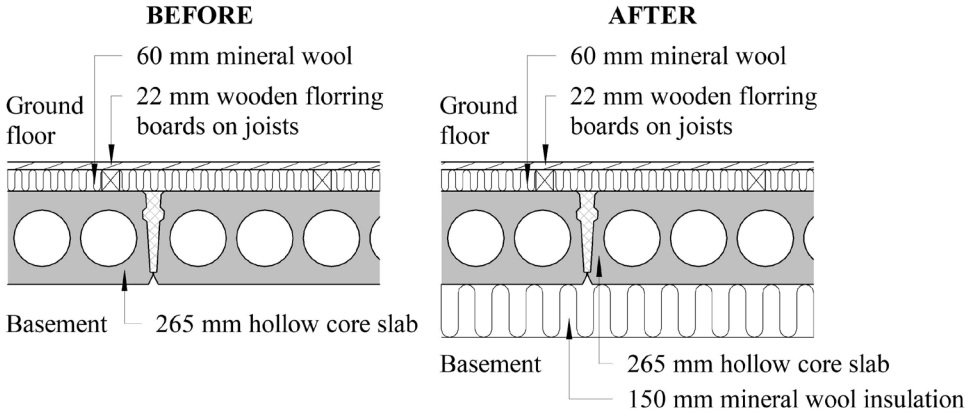

Figure 21: Cross-section view, floor construction towards basement, initial and retrofitted state.

Table 12: Construction assemblies and thermal properties of intermediate floor towards basement.

Location	Material layers (Exterior to interior) Indoor condition; basement	Thickness [m]	Bulk Density $\left[\frac{kg}{m^3}\right]$	Specific Heat $\left[\frac{J}{kg\ K}\right]$	Thermal Conductivity $\left[\frac{W}{m\ K}\right]$
Intermediate floor before renovation	Hollow core concrete deck	0.265	2200	850	1.600
	Mineral wool insulation*	0.060	60	850	0.040
	Wood	0.022	560	1500	0.130
Intermediate floor after renovation	Mineral wool insulation	0.150	60	1000	0.037
	Hollow core concrete deck	0.265	2200	850	1.600
	Mineral wool insulation*	0.060	60	850	0.040
	Wood	0.022	560	1500	0.130

* Overall U-values increased by thermal bridges that were caused by wooden elements can be seen in section 5.1.2.2.

The new retrofit design emphasised spacious and bright areas, formed with the help of increased window heights, which allowed for deeper daylight penetration within the individual apartments. The height of windows was generally increased from 1.2 m to 1.5 m. Size of the balconies were enlarged, leading to larger openings and execution of sliding doors. Furthermore, the common staircases were opened up by implementing glazed elements spanning from basement to the 14th floor, sharply increasing the overall WWR on the North-East facade. Barrier-free access along with glazed elevators were introduced in these common areas. BPS were done with the WWR as seen in Table 13.

Table 13: WWR ratio of the initial and retrofitted projects

		South-West	**North-East**	**South-East**	**North-West**
Initial	Ground floor	30 %	30 %	15 %	12 %
	1-14th floor	40 %			
Retrofitted	Ground floor	39 %	35 %	21 %	15 %
	1-14th floor	49 %	39 %		
	Staircases	90 %	92 %		

During the retrofit, existing windows and doors were replaced with new ones with better thermal properties as seen in the window specifications displayed in Table 14.

Table 14: Window Specifications

Location	U-value incl. frame $\left[\frac{W}{m^2 K}\right]$	g-value [%]	f_f [%]	T_{vis} [%]
Initial				
All glazing	2.0	63	20	78
Retrofitted				
Apartments	0.9	50	20	70
Staircase	1.5	63	10	78

4.1.2.2 Assumptions and Simplifications

The project contained many carefully designed, individual connection solutions, as around the balcony, initial concrete façade frame, newly installed ventilation supply ducts located in the exterior building walls as well as slight variation in insulation thicknesses of the prefabricated façade elements. Deviations like these were simplified to an average insulation thicknesses and standard construction details for hygrothermal simulations, thermal bridge study and BPS. Unheated spaces were excluded from the indoor comfort study. For this reason, none of the openings were modelled in the exterior basement walls.
New air handling units (AHU) were placed inside the newly erected and insulated attic, located on the top of the existing roof. Thus, the structure was excluded in BPS and simplified in hygrothermal simulations. Due to a lack of drawings of the initial facades, an estimation of WWR based on the descriptions and measurements provided in the master plan of the overall renovation work of the facades was taken into account.

4.2 Germany

Regarding the implementation of policies and subsidy structures for more energy-efficient construction and retrofitting, Germany is seen as one of the most progressive countries [119]. As one of the first EU member states, Germany implemented the ´Wärmeschutzverordung` (Thermal Protection Regulations) in 1977, setting construction rules in order to decrease the heat losses through the thermal envelope of buildings. Followed by amendments in 1982 and 1995, the ´Energie Einspar Verordnung` (EnEV – Energy Conservation Ordinance) was adopted in 2002 and annuls the previous regulation, amendments followed in 2009 and 2014 [120], [121]. The overall objective of German legislation was set in the Paris Agreement, followed by the Climate Action Plan 2050, that was adopted by the federal cabinet in 2016, aiming to mitigate the greenhouse gas (GHG) emissions by 80 % compared to the 1990 levels [122]. Galvin and Sunikka-Blank [123] suggest therefore, that the energy consumption for space heating and domestic hot water has to be lowered to 30-35 kWh/(m²·a) in both building stock and newly constructed dwellings.

Germany, among other countries, prescribes an up to standard energy-efficient retrofit if a major renovation is undertaken [124]. This accounts if e.g. the external façade is renovated by changing the plaster or adding cladding to the exterior. In that case, it is mandatory to execute an energy-efficiency retrofit for the entire façade [121]. However, the standard also composes a clause for the renovation and retrofitting measures to be economically viable, which means, that the savings on heating and cooling energy have to be lower than the expenses on the energy-efficiency measures [123], [125], [126]. In their 2013 paper, Galvin and Sunikka-Blank suggest that in order to reach the ambitious targets, the economic feasibility clause should be removed from the EnEV [123].

In another study, carried out by Weiss et al. [120], the authors proclaim, that the lack of involvement and long-term perspectives for homeowners as well as insufficient funding led to refurbishment rates that covered only half the predictions. However, the predictions anticipated the rate necessary to reach the ambitious targets for mitigating the GHG emissions for 2050 [120]. Further, the paper suggest to extend the incentives for homeowners to carry out renovations and retrofits, which lines up with the conclusions drawn by Galvin and Sunikka-Blank [120], [123]. The general number of energy-efficient retrofits in Germany, is predicted to grow within the 2020´s. It is also expected, that the incentives and regulations regarding this matter will change to enlarge the number of retrofits [127].

4.2.1 Project 3

The case study ´Project 3`, displayed in Figure 22, is situated in the East of Stuttgart, Germany, composing of two attached MFHs with an adjacent wall. Both parts of the house have separate entrances and are each equipped with a staircase. The building originally built in the 1950´s was object of a complete restauration in 2014. Within the restauration, a retrofit of the existing and newly added structures was carried out to decrease the heating demand drastically to an energy-efficient house complying to the standard ´KfW-Effizienzhaus 70`. The standard represents building retrofits with a primary-energy demand and transmission losses lower than 70 % and 85 % respectively as the reference building for new construction in Germany subscribed by EnEV 2009. According to the energy

classification, the building scored a 57 % primary-energy demand and 83 % transmission losses. To mitigate thermal losses through infiltration losses, measures to increase the airtightness were taken. Those resulted in a decrease of the infiltration from 5 ACH at 50 Pa in the initial building stage to slightly under 3 ACH at 50 Pa after the completion of the retrofit, tested with a blower door test.

Along with a retrofit of the existing external walls, new construction of the roof construction including the addition of dormers, extensions on the South facing side of the building were added to the building perimeter. The building gained about 300 m² lettable floor area, resulting in a total of 18 apartments rather than 16 in the initial stage, all equipped with a South-facing balcony. Apartment sizes from ground floor to 3rd floor are about 60 m² of lettable floor area, whereas the two apartments in the attic are about 100 m² lettable floor area. The retrofit did include the change of the heating system from a fossil fuel-based system to a connection to the district heating system powered by the nearby natural gas combined heat and power plant. Both heating as well as domestic hot water were connected to the district heating network, new installation of hydronic radiators and all sanitary pipes up to standard were realised in the retrofit. In bathrooms extractor fans without heat recovery, regulated by humidity were installed and windows were equipped with window rebate valves, ensuring a minimal fresh air supply, no additional mechanical ventilation system was installed. The building owner, a foundation owning about 5.000 apartments in the Region Stuttgart, has a high standard for soundproofing between separate apartments and thus, several measures to enhance the acoustic separation of apartments were carried out in the retrofit. With a construction time of over a year, the renovation and retrofit was carried out by a turn-key contractor delivering the apartments ready to use.

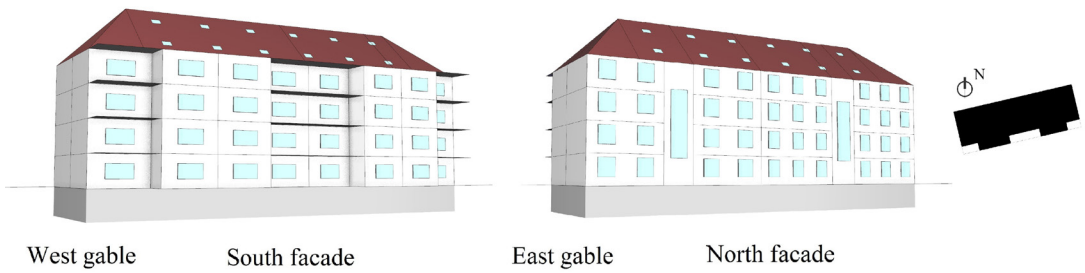

Figure 22: Geometry used in energy and thermal comfort simulations. Building orientation shown from the top displayed on the right side of the figure.

4.2.1.1 Building Properties Original and Retrofitted

The existing exterior walls composing of hollow pumice concrete blocks, gypsum plaster as the interior finishing and a render system as the exterior finishing were a common building type in multi-storey apartment houses in the 1950´s. During the retrofit, an external thermal insulation system was added on top of the old wall construction. The existing rendering system was kept, but paint and loose plaster elements were removed before mounting the 200 mm rigid EPS insulation boards. In order to mitigate the fire risk, horizontal stripes of rock wool insulation were mounted instead of EPS boards in the intermediate floor junction. This was in order to stop vertical fire spread over multiple stories. The finishing of the

facades was done in white with design elements in light grey on the North façade, nuances were set by window frames, entrance buffer zone as well as balcony railings in anthracite. On the South facing façade, the building extensions were highlighted with orange paint finishing. The used façade paint was equipped with fungicides and algaecides to prevent growth of fungi and algae on the façade. Construction sections of both initial and retrofitted walls are displayed in Figure 23, properties of the used materials were modelled as shown in Table 15.

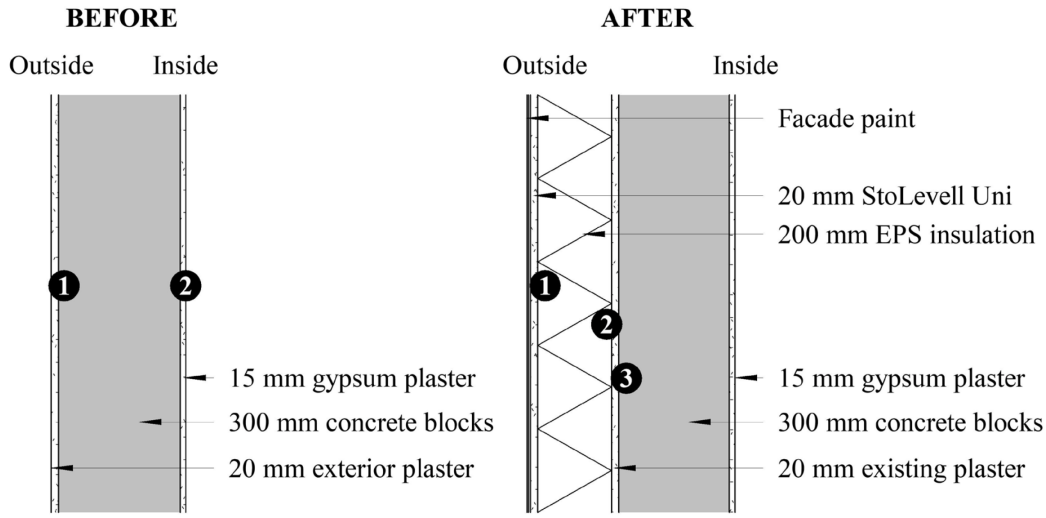

Figure 23: Plan section, exterior wall construction, initial and retrofitted state.

Table 15: Construction assemblies and thermal properties of external walls, initial and retrofitted state.

Location	Material layers (Exterior to interior)	Thickness [m]	Bulk Density $\left[\frac{kg}{m^3}\right]$	Specific Heat $\left[\frac{J}{kg\,K}\right]$	Thermal Conductivity $\left[\frac{W}{m\,K}\right]$
Initial walls	Exterior mineral plaster	0.020	1900	850	0.800
	Concrete blocks, pumice aggregate	0.300	664	850	0.860
	Interior gypsum plaster (sd = 0.1m)	0.015	1120	960	0.510
Retrofitted walls	StoColor Silco 2x	0.001	960	1000	0.700
	StoSilco K	0.003	1340	1000	0.700
	StoLevell Uni	0.020	1300	850	0.890
	EPS insulation	0.200	15	1500	0.040
	Exterior mineral plaster	0.020	1900	850	0.800
	Concrete blocks, pumice aggregate	0.300	664	850	0.860
	Interior gypsum plaster (sd = 0.1m)	0.015	1120	960	0.510

The previously uninsulated and unused attic was torn down completely and erected newly, to allow for the use as apartment spaces. To comply with the district's urban masterplan, all roofs have to be slanted and tiled with red or red-brown rooftiles, this was followed by realising red roof tiles. Spaces between the 160 mm high rafters were insulated with mineral wool insulation, followed by a vapour barrier to the inside. The installation layer with 50 mm of insulated insulation space between wooden planks and gypsum board was added as interior finishing. On top of the rafters to the outside, 80 mm of wood-fibre insulation boards were installed, to provide protection against summer overheating. The back side of roof tiles were ventilated, which was ensured by battens and counter battens on which the tiles were mounted. The attic in the initial building was used as storage space, therefore, the floor construction of the former attic is seen as the thermal envelope. The assemblies of the effective thermal envelope roof construction can be seen in Figure 24, Table 16 shows the respective material properties.

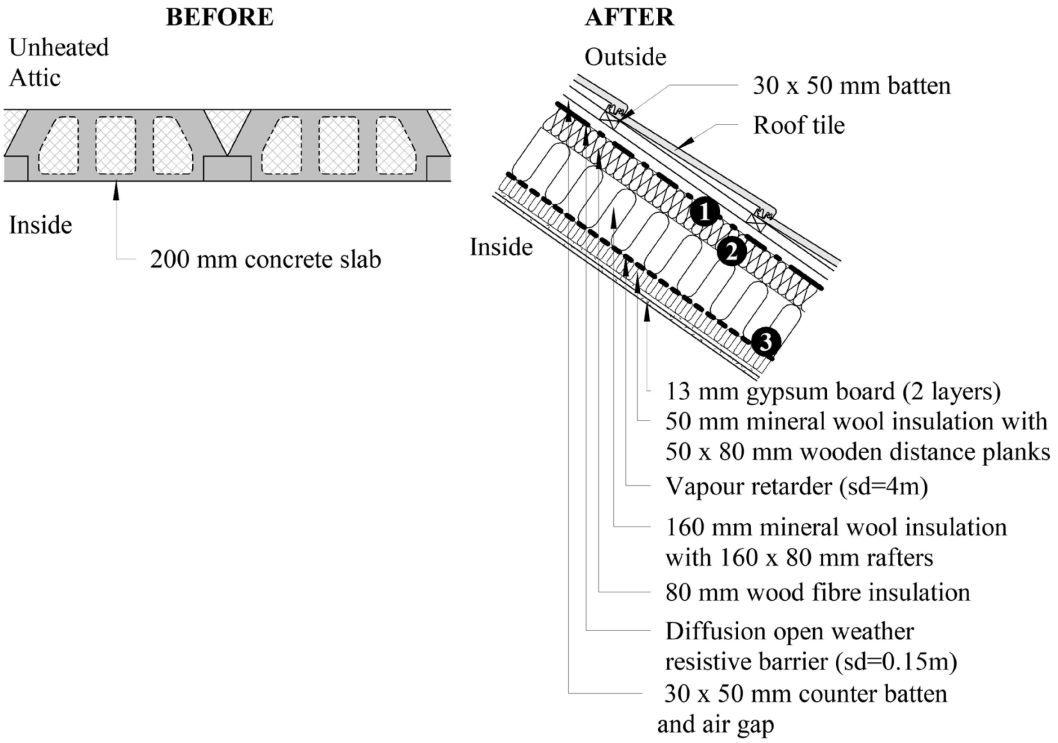

Figure 24: Cross-section view, roof construction, initial and retrofitted state.

Table 16: Construction assemblies and thermal properties of roof thermal envelope constructions, initial and retrofitted state.

Location	Material layers (Exterior to interior)	Thickness [m]	Bulk Density $\left[\frac{kg}{m^3}\right]$	Specific Heat $\left[\frac{J}{kg\,K}\right]$	Thermal Conductivity $\left[\frac{W}{m\,K}\right]$
Initial roof towards unheated attic	Reinforced concrete	0.200	2200	850	1.600
Retrofitted roof towards outside	Roof tiles	0.020	1890	880	0.800
	Air gap and roof battens	0.060	1.3	1000	0.337
	Weather resistive barrier (sd=0.15m)	0.001	229	2300	2.300
	Wood fibre insulation	0.080	140	1400	0.035
	Mineral wool insulation*	0.160	21	840	0.035
	Vapor retarder (sd=4m)	0.001	83	2300	2.300
	Mineral wool insulation**	0.050	21	840	0.035
	Gypsum board (2 layers)	0.025	850	850	0.200

Layer includes rafters* or wooden distance planks**.

To mitigate heat losses from ground floor towards the basement, the floor slab towards the basement was treated in a different way than the ones between the heated apartment stories. The main difference was presented by the addition of 100 mm of highly insulative phenol resin insulation boards, located on the cold side of the floor slab. The previously used poured asphalt screed including the mineral wool thermal break was also removed in the retrofit and replaced by 60 mm of EPS insulation and 50 mm of concrete screed. The section of the initial and retrofitted ceiling over the basement can be seen in Figure 25, building materials and their respective properties can be obtained from Table 17.

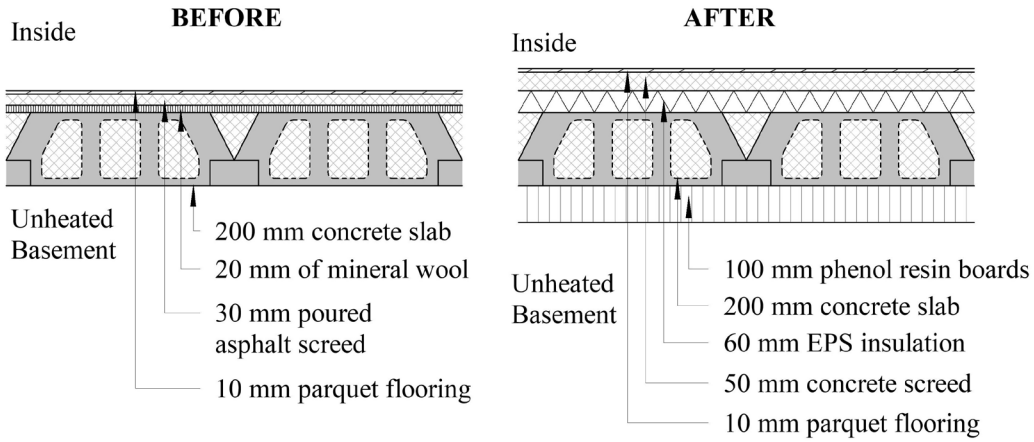

Figure 25: Cross-section view, ground floor slab towards basement, initial and retrofitted state.

Table 17: Construction assemblies and thermal properties of ground floor slab towards basement, initial and retrofitted state.

Location	Material layers (Exterior to interior) Indoor condition; unheated basement	Thickness [m]	Bulk Density $\left[\frac{kg}{m^3}\right]$	Specific Heat $\left[\frac{J}{kg\,K}\right]$	Thermal Conductivity $\left[\frac{W}{m\,K}\right]$
Intermediate floor before renovation	Reinforced concrete	0.200	2200	850	1.600
	Mineral wool	0.020	180	850	0.040
	Poured asphalt screed	0.030	2100	1700	1.200
	Parquet flooring	0.010	560	1500	0.130
Intermediate floor after renovation	Phenol resin boards	0.100	30	1590	0.022
	Reinforced concrete	0.200	2200	850	1.600
	EPS insulation	0.060	50	850	0.035
	Concrete screed	0.050	2000	1700	1.400
	Parquet flooring	0.010	560	1500	0.130

Table 18: WWR ratio of the initial and retrofitted projects

		South	**North**	**East/West**
Initial	0-4th floor	20 %	26 %	0 %
	Staircase	-	31 %	-
	Skylights	4 %	4 %	0 %
Retrofitted	0-4th floor	43 %	34 %	0 %
	Staircase	-	56 %	-
	Skylights	18 %	18 %	18 %

The 3D-model of the building was modelled with the WWR and skylight ratios as displayed in Table 18. During the retrofit, existing windows and doors were replaced with new ones with better thermal properties as seen in the window specifications displayed in Table 19. The new window elements were realised as PVC hollow-chamber profile windows, reaching the necessary U-value of 0.9 W/m²K to comply with the certifications. All windows were equipped with shutters as external shading elements, which are manually controlled. The respective schedule used in the BPS was applied to night closing when the outdoor temperatures were under 15 °C as well as day and night closing when outdoor temperature exceeded 24 °C or received a higher solar radiation incident than 400 W/m².

Table 19: Window Specifications

Location	U-value incl. frame $\left[\frac{W}{m^2 K}\right]$	g-value [%]	f_f [%]	T_{vis} [%]
Initial				
Windows and doors	2.7	63	30	78
Skylights	5.4	90	10	30
Retrofitted				
Windows and doors	0.9	50	30	60
Skylights	1.0	50	30	65

In addition to the already described constructions of the thermal envelope of the building, the basement walls were insulated with 11 cm of EPS insulation boards from the exterior to mitigate the thermal bridges between basement walls and ground floor slab.

4.2.1.2 Assumptions and Simplifications

The extensions on the southern façade were already included in the 3D-model for the initial case, the attic construction was modelled according to the actual conditions for both stages. The dormers in the retrofitted attic construction were neglected in the model, the window areas, however, were taken into account as skylights. Hygrothermal and simulations for energy and thermal comfort were done with weather file sets obtained from the RCM of Munich, as no data for Stuttgart was available.

4.2.2 Project 4

Closely located to project 3, is the multi-family house assessed in project 4, displayed in Figure 26. The rental object in the quarter ´Ostheim` in Stuttgart-East owned by a foundation, was case of a complete renovation and retrofit in 2012. The buildings in the quarter date back to the 19th century, whereas the study object in question was constructed around the turn of the century [128]. Even without being classified a heritage protected building, the façade and general appearance of the building was seen as worthy to preserve. The building owner thus decided against demolishing the building or realising a classical energy-efficient retrofit with the addition of external insulation to the existing façade. The appearance of the house is dominated by the red brick façade that shows the great level of attention to detail that was paid in the original construction in the early 20th century. The five-storey building is divided into three houses with separate access and staircases. Due to the unchanged façades, the 15 apartments retained their floor plans, only minor changes to allow for reasonably sized bathrooms were made in the retrofit.

A complete-new installation of water, drainage and hydronic-heating pipework as well as new sanitary objects was carried out during the renovation. The fossil fuel-based heating system was removed, the exhaust chimneys were demolished, and the building was connected to the district heating system powered by natural gas for space heating and domestic hot water. Apart from extract fans in the bathrooms controlled by humidity, no mechanical ventilation system was installed. The airtightness of this building was not tested, and the ventilation type was free ventilation. For those reasons, simulations were done with

an infiltration rate of 0.7 ACH at standard pressure. The same assumptions were made in the calculation carried out in order to obtain a building energy certification and are in accordance to DIN V 4108-6. In order to comply with the legislation EnEV 2009, the primary heating energy demand cannot exceed 140 % of the standard for new buildings. By designing a highly efficient system and the connection to the district heating power plant, the building passed the benchmark for the annual primary energy demand.

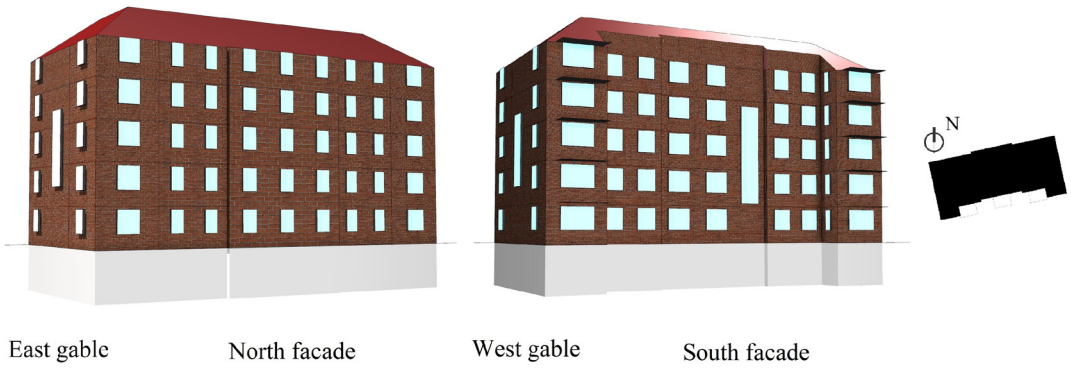

Figure 26: Geometry used in energy and thermal comfort simulations. Building orientation shown from the top displayed on the right side of the figure.

4.2.2.1 Building Properties Original and Retrofitted

The key element of the retrofit concept was the conservation of the brick façade. Therefore, a manufacturer of insulation systems made a comprehensive study over 4 years, taking measurements in the building in question, to prove the external wall construction to be moisture safe. Object of the test were insulation thicknesses, as well as temperature and relative humidity profiles in the constructions. The performance of interior perlite insulation boards with a thickness of 80 mm proved to be the most adequate one and was chosen as the way to insulate the existing walls consisting of 320 mm solid brick masonry and 20 mm mineral plaster. The insulation boards were mounted directly on the existing plaster, after removing layers of wallpaper and paint. Adhesives were used to mount the boards onto the existing wall construction, as well as a reinforced render layer to bridge the gaps of the insulation boards. Diffusion open interior plaster was used for the finishing, allowing to be painted with diffusion open paint. The construction setup for initial and retrofitted wall constructions are shown in Figure 27, the respective material properties are shown in Table 20.

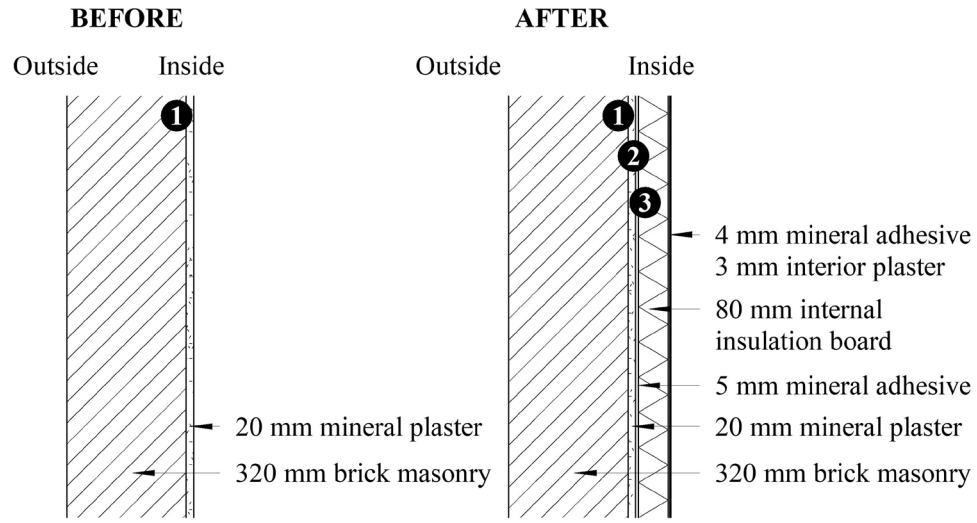

Figure 27: Plan section, external wall construction, initial and retrofitted state.

Table 20: Construction assemblies and thermal properties of external walls, initial and retrofitted state.

Location	Material layers (Exterior to interior)	Thickness [m]	Bulk Density $\left[\frac{kg}{m^3}\right]$	Specific Heat $\left[\frac{J}{kg\ K}\right]$	Thermal Conductivity $\left[\frac{W}{m\ K}\right]$
Initial walls	Solid brick masonry	0.320	1900	850	0.600
	Mineral plaster (sd=0.5 m)	0.020	1900	850	0.800
Retrofitted walls	Solid brick masonry	0.320	1900	850	0.600
	Mineral plaster	0.020	1900	850	0.800
	StoLevell in mineral	0.005	1330	850	0.870
	Sto Perlite Interior Insulation Board	0.080	100	850	0.042
	StoLevell in mineral	0.004	1330	850	0.870
	StoDecosil	0.003	1640	850	0.870

Dominated by an unheated attic with partially slanted red-tiled roof and partially flat roof with metal siding, the roof constructions facing outdoors were not the thermal envelope of the heated spaces. Thus, the ceiling over the 4th floor was seen as the thermal envelope construction, it was therefore insulated towards the unheated attic in the retrofit. The constructions in Figure 28 with the material properties stated in Table 21, show the enhanced thermal properties after the retrofit. A layer of 160 mm mineral wool between rafters was added to the slanted roof construction. Mineral wool of 50 mm thickness and 160 mm of EPS insulation was supplementary to the existing flat roof construction.

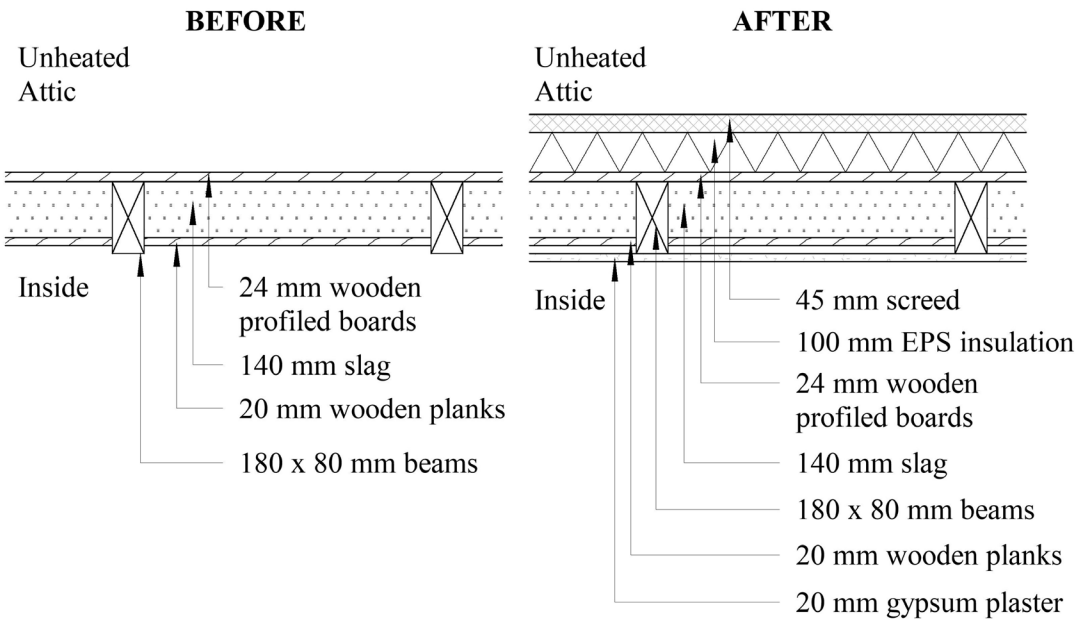

Figure 28: Cross-section view, roof construction, initial and retrofitted state.

Table 21: Construction assemblies and thermal properties of roof thermal envelope constructions, initial and retrofitted state.

Location	Material layers (Exterior to interior) Indoor condition; unheated attic	Thickness [m]	Bulk Density $\left[\frac{kg}{m^3}\right]$	Specific Heat $\left[\frac{J}{kg\ K}\right]$	Thermal Conductivity $\left[\frac{W}{m\ K}\right]$
Initial roof	Wooden profiled boards	0.024	600	1380	0.130
	Slag	0.140	1200	1680	1.000
	Wooden planks	0.020	600	1880	0.130
Retrofitted roof	Screed	0.045	2000	1700	1.400
	EPS insulation	0.100	30	850	0.035
	Wooden profiles boards	0.024	600	1380	0.130
	Slag	0.140	1200	1680	1.000
	Wooden planks	0.020	600	1880	0.130
	Gypsum plaster	0.020	1120	960	0.510

The ground floor construction towards the unheated basement built the thermal envelope in the bottom of the building. The floor construction with wooden beams filled with slag in the spaces between was also subject of thermal insulation being added to the unheated side. Boards of 80 mm EPS insulation were mounted onto the wooden beams. The wooden profiled boards as the floor construction in the initial stage of the building was covered by a 20 mm layer of mineral wool acting as thermal break and footfall sound insulation. On top, a 45 mm layer of concrete screed was placed, finished by 10 mm of parquet flooring. The constructions can be observed from Figure 29 with the material properties in Table 22.

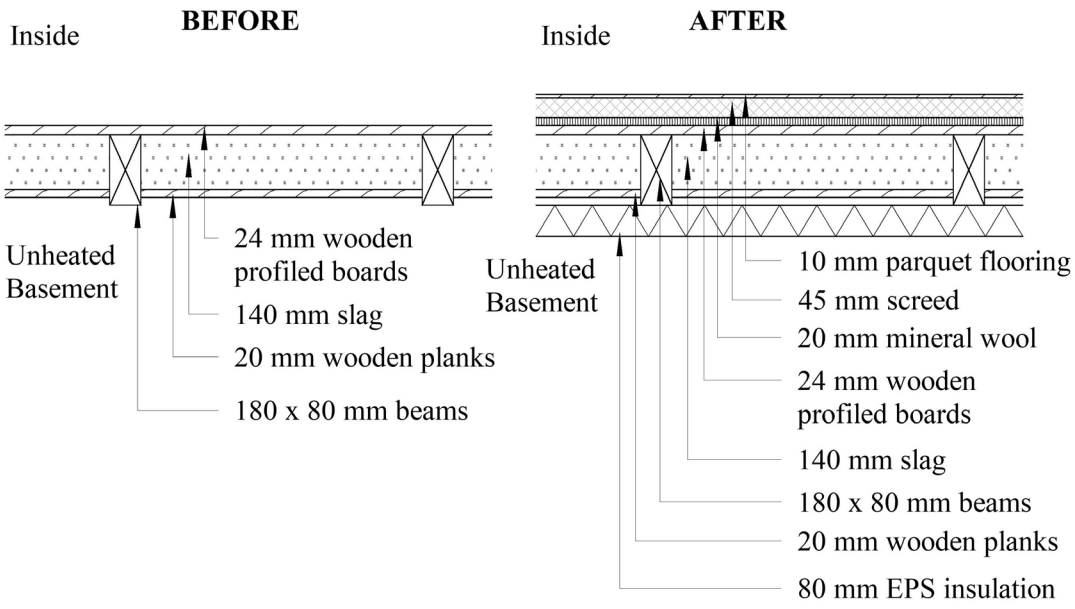

Figure 29: Cross-section view, ground floor slab towards basement, initial and retrofitted state.

Table 22: Construction assemblies and thermal properties of ground floor slab towards basement, initial and retrofitted state.

Location	Material layers (Exterior to interior) Indoor condition; unheated basement	Thickness [m]	Bulk Density $\left[\frac{kg}{m^3}\right]$	Specific Heat $\left[\frac{J}{kg\,K}\right]$	Thermal Conductivity $\left[\frac{W}{m\,K}\right]$
Intermediate floor before renovation	Wooden planks	0.020	600	1880	0.130
	Slag	0.140	1200	1680	1.000
	Wooden profiled boards	0.024	600	1380	0.130
Intermediate floor after renovation	EPS insulation	0.080	30	850	0.035
	Wooden planks	0.020	600	1880	0.130
	Slag	0.140	1200	1680	1.000
	Wooden profiled boards	0.024	600	1380	0.130
	Mineral wool insulation	0.020	30	850	0.035
	Screed	0.045	2000	1700	1.400
	Parquet flooring	0.010	560	1500	0.130

The windows of the building were originally double-pane windows with air filament. The slightly increased WWR in the retrofit, as seen in Table 23, were due to the addition of balconies on the Southern side of the building and the addition of balcony doors instead of normal windows. The windows used in the retrofit were double-glazed windows with enhanced thermal properties to the original windows, as displayed in Table 24. Shutters for shading and night darkening were installed in all windows and were simulated in the BPS as specified in 4.2.1.1.

Table 23: WWR ratio of the initial and retrofitted projects.

	North	South	West	East
Initial	20 %	31 %	15 %	15 %
Retrofitted	20 %	31 %	22 %	22 %

Table 24: Window Specifications

Location	U-value incl. frame $\left[\frac{W}{m^2 K}\right]$	g-value [%]	f_f [%]	T_{vis} [%]
Initial				
All glazing	2.7	63	30	78
Retrofitted				
All glazing	1.3	60	30	60

4.2.2.2 Assumptions and Simplifications

The external wall construction was modelled to uniform thickness, neglecting different thicknesses of the initial interior plaster and the brick façade. The attic construction was modelled without roof inclination, the materials and total volume were adjusted to the actual conditions. Both, hygrothermal and BPS simulations for energy and thermal comfort were carried out with weather file sets obtained from the RCM of Munich, due to a lack of data for Stuttgart.

5 Results and Discussion

In the following chapter, the results and discussion are presented. The project specific results are presented separated by the countries they are located in. Generally, an analysis of the indoor thermal comfort is presented for each individual project, followed by the analysis of the heating energy demand and heating peak loads. Indoor comfort is represented by scatter plots of building average percentages of discomfort according to EN 15 251 category II. Additionally, representative zones used for living rooms and bedrooms are displayed. The assessment of heating energy demands is carried out both parametrically, as well as statistically. Cumulative heating demand plots show the parametrical assessment of all nine future climate scenarios plus one TMY scenario, representing historical climate measurements. Similarly, a statistical analysis by means of boxplots for the hourly heating loads, composes the results for each three ECY, EWY and TDY periods as well as one for the historical TMY file. In the third part of each case study, the moisture safety assessment of building envelope constructions is given and analysed. In the last subchapter, 5.3 Common Results and Discussion, the obtained results of the different case study objects are compared and discussed.

5.1 Denmark

Both Danish projects, presented below, have shown detailed design solutions, aiming to mitigate the heating energy demand, but also providing better daylight conditions for space occupants. To achieve the latter objective, the window area was increased in both cases, the retrofit went along with a complete renovation of the interior.

5.1.1 Project 1

The results of BPS and hygrothermal simulations for the first case study are shown and discussed in the following. The design of the house was the archetype for the retrofit of similar buildings in the periphery. As the building was object in many studies, the results of this work are a new insight to the performance of the building in future climate conditions until the end of the 21st century. Validation of the model and script employed for BPS was done by means of the TMY weather file for Copenhagen in comparison to the available results of heating energy demands. The initial building had a predicted annual energy use of 143 kWh/m² including heating energy as well as electricity for lighting in common areas and energy for fans and auxiliary heating energy. Compared to the simulation results of the initial building with 112 kWh/m² annual heating energy demand, a deviation of 22 % shows. The simulated number does, however, not include electricity so that the actual deviation between the heating energy demand is lower. The validation process showed that accuracy of modelling constructions, as well as ventilation system inputs and infiltration rates were crucial to the simulation results.

5.1.1.1 Thermal Comfort

An assessment of the thermal comfort in the building case study in accordance to EN 15 251 was carried out. The results are as shown in Figure 30, the left diagram showing the percentage of thermal discomfort of the initial building and the right diagram of the building after the retrofit. The percentage of hours were displayed for the entire building as an average and for representative zones on the East and West side of the building. Chosen zones in the East represented rooms with a floor area of 26 m² and in the West with a floor area of 23 m². The building average shows, that in the initial case of the building, the least thermal discomfort was scored in the EWY 70-99 scenario. Throughout all three weather data sets (TDY, ECY and EWY), a downward trend of thermal discomfort towards the end of century is seen.

The winter comfort threshold of 20 °C operative temperature is only kept during sunshine hours, in overcast or night hours, the operative temperature falls often under the threshold. The heating setpoint being 21 °C which is maintained during all hours of the year is not equal to the operative temperature, which also accounts for the surface temperatures of the respective zones. The large glazed areas facing East and West, are seen as the cause for the mean radiant temperature to fall below the threshold in winter months. The overheating hours were recorded to be minimal in the initial case. However, zones yielded thermal discomfort during the cold seasons. Thus, with an increase in temperature and solar radiation given in the weather data sets towards the end of the century, the winter-discomfort decreased.

In the TDY scenarios of the retrofitted building, the trend reversed, increasing thermal discomfort from period to period. This reflects the trends in the overheating hours which increase towards the end of the century. Overheating and thermal discomfort levels observed over the three TDY periods indicates the need for measures to mitigate those. In order to decrease the overheating, a shading strategy should be implemented, external vertical shading would allow to block solar gains when they are undesirable, which leads to a decrease of both zone air temperature and the mean radiant temperature due to less heat emitted from the glazed surfaces. In the ECY scenario, an increase of thermal discomfort from the first to the second period can be observed, decreasing again in the third period, this can be due to a long-lasting cold period in the medium-term period. Here, the discomfort during the wintertime accounts for most discomfort in all three periods, decreasing towards the end of the century, but simultaneously increasing overheating hours. Within the EWY scenarios, a general downward trend can be observed, due to decreasing discomfort caused by low temperatures and only minimal increase of overheating hours. As the extreme conditions (ECY, EWY) are unlikely to occur for extensive periods, the observations for those are presenting indications, if thermal comfort rises or decreases in the event of an extreme weather incident.

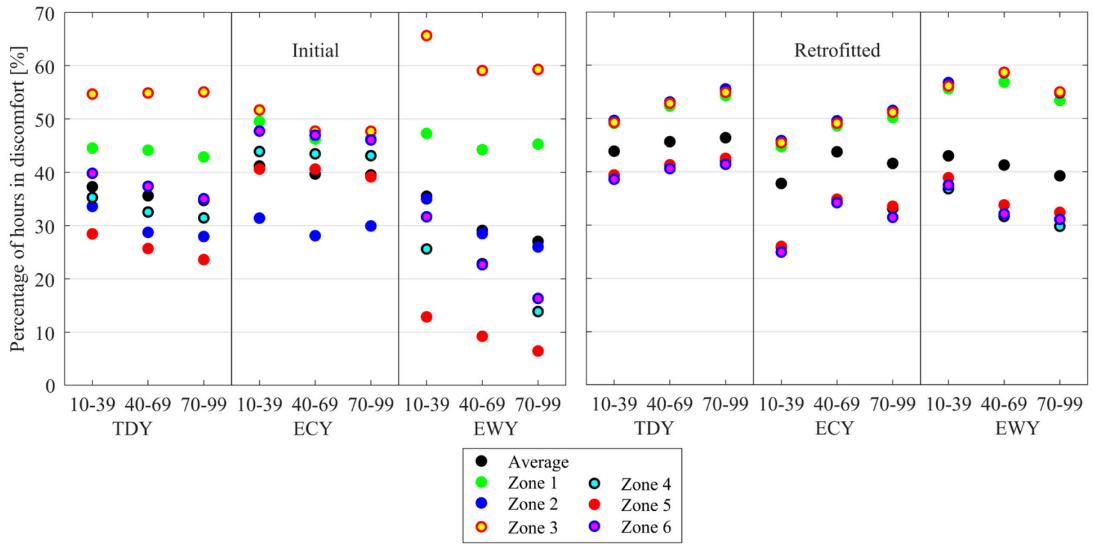

Figure 30: Percentage of time in discomfort: Building average, zone 1: Typical Zone East Ground Floor, zone 2: Typical Zone East Middle Floor, zone 3: Typical Zone East Top Floor, zone 4: Typical Zone West Ground Floor, zone 5: Typical Zone West Middle Floor, zone 6: Typical Zone West Top Floor.

5.1.1.2 Energy Use

Thermal bridges in the constructions of the thermal envelope of the building were evenly distributed over the U-value of the respective constructions for initial and retrofitted building, as seen in Table 25 and Table 26. A high negative impact on the construction of the retrofitted floor between ground floor and the basement due to steel-studs. Similarly, the exterior façade construction for East and West façades show a high impact on the thermal conductivity due to the junctions with the intermediate floor construction and concrete beams above the glazed partitions.

Table 25: Overall U-values including thermal bridges of initial building.

Construction	Heat loss projection	U-value $\left[\frac{W}{m^2 K}\right]$	$\Delta U_{thermal\_bridges}$ $\left[\frac{W}{m^2 K}\right]$	Overall U-value $\left[\frac{W}{m^2 K}\right]$
Exterior wall	'Ideal'	0.3621		
	'Wall-intermediate floor junction'	0.3872	0.0251	
				0.3872
Roof construction	'Ideal'	0.3284		
	'Section'	0.3471	0.0187	
				0.3471
Ground-Basement intermediate floor	Construction without penetrations	1.8994		**1.8994**

Table 26: Overall U-values including thermal bridges of retrofitted building.

Construction	Heat loss projection	U-value $\left[\frac{W}{m^2K}\right]$	$\Delta U_{thermal\_bridges}$ $\left[\frac{W}{m^2K}\right]$	Overall U-value $\left[\frac{W}{m^2K}\right]$
Exterior façade wall	'Ideal'	0.0966		
	'Plan section'	0.1096	0.013	
	'Wall-intermediate floor junction'	0.1656	0.069	
				0.1786
Exterior gable wall	'Ideal'	0.0945		
	'Plan section'	0.1012	0.0067	
	'Wall-intermediate floor junction'	0.1067	0.0122	
				0.1155
Roof construction	Construction without penetrations	0.0782		
				0.0782
Ground-Basement intermediate floor	'Ideal'	0.1668		
	'Section'	0.2632	0.0964	
				0.2632

Figure 31 shows the cumulative heating demand normalized by the heated floor area for both initial and retrofit of the building. The diagrams reveal the heating periods and heating intensities per month, but also the annual heating demand for each of the three time periods of the different weather scenarios. Initial and retrofitted heating energy demands demonstrate similar patterns, where the ECY scenarios show about double the heating demand compared to the TDY scenarios and EWYs about half of the TDY predictions. Retrofitted heating energy demands show about 15 % of the one simulated in the initial buildings, which indicates tremendous effectivity of the energy-efficient retrofit. The differences in heating energy demand between the time periods are within a 5 kWh/m² range for the retrofit, in the initial scenarios, the decrease from the near-term period to the long-term period are within a 15 kWh/m² for the three TDY periods. More significant are the differences comparing TDY, ECY and EWY scenarios, however, those scenarios are unlikely to happen in a continuous time-period as they represent worst-case extremes. The validation of the model which was done by means of the TMY file for Copenhagen, shows 30 % to 40 % higher cumulative heating demands than the near-term TDY period. Examining the statistical analysis, presented in Figure 32, the TMY scenarios yield lower peaks in hourly building heating loads. In order to statistically analyse the occurrence of typical and extreme conditions within the 30-year periods, Triple data sets were created, combining TDY, ECY and EWY data sets of the respective period. The frequency of hourly loads over 40 kW, however, is higher comparing to both TDY and Triple value distributions for the near-term period. The statistical distribution also shows, that in the retrofitted building more than 50 % of the year, no heating at all is required. Where the upper whisker for the Triple in the near-term period reaches a value close to 10 kWh, the mid-term shows around 7 kWh and the long-term period about 5 kWh. Outliers above the upper whisker show very few occasions with higher hourly heating demand values. The decrease in

frequency of high hourly heating loads towards the end of the century, demonstrates, that the number and endurance of cold periods decrease, so less heating intensity is required.

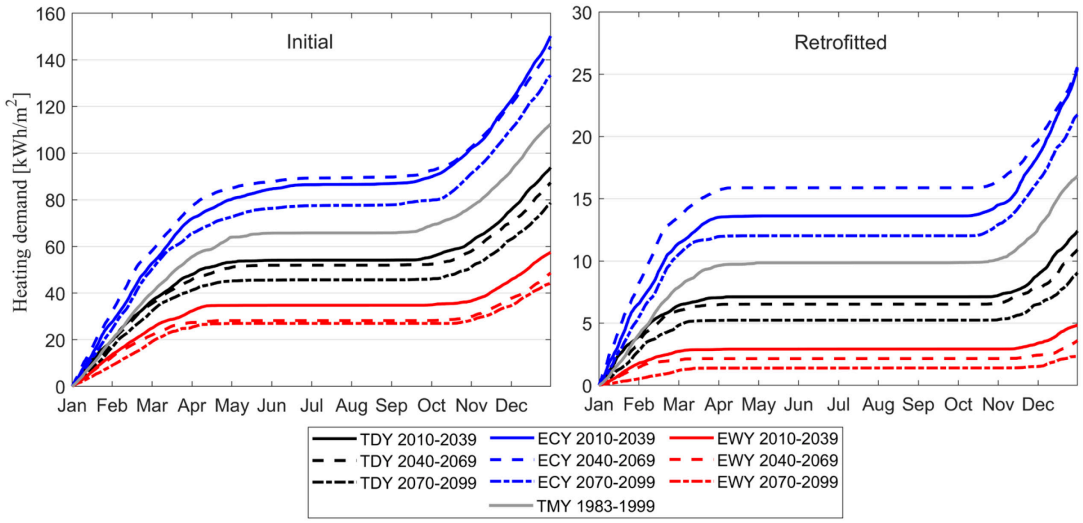

Figure 31: Cumulative heating demand. Initial building on the left, retrofitted building on the right.

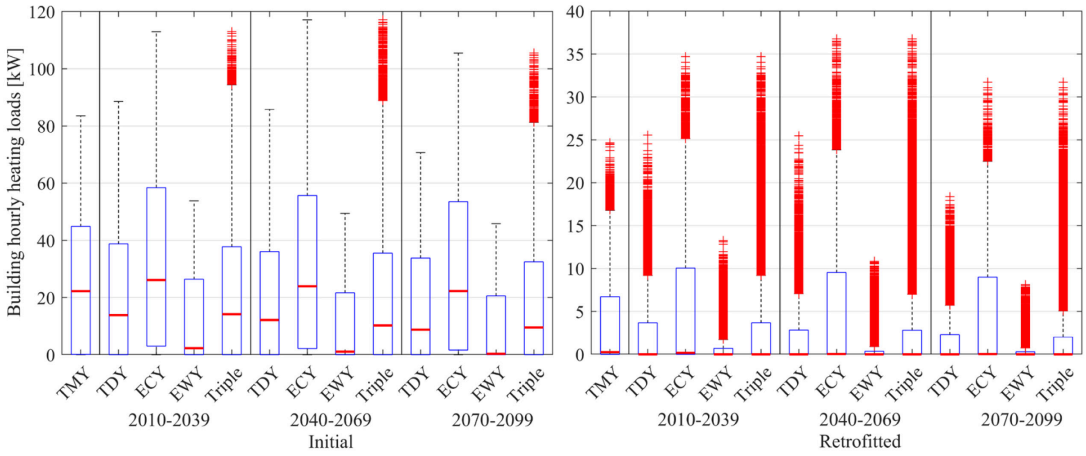

Figure 32: Statistical analysis of hourly building heating energy demands. Scale for initial on the left and retrofitted on the right adjusted for better visibility.

In Figure 33, heating peak loads for the 72 conditioned zones as well as a building average are shown. The peak loads for the individual zones are displayed as boxplots, whereas the building average is represented by a black square. Both zone and building average peak load values are plotted as W/m² normalized by the respective heated floor area. The lowest peak loads for the retrofitted building are reached for the EWY scenario during the period closest to the end of the century, highest occur in the medium-term period of the ECY scenario. Whereas peak loads during ECY and EWY periods are constant within a 1 W/m² margin, the peak loads decrease by over 5 W/m² during the TDY periods. The trends and relations between scenarios and time periods are similar for the initial building, before retrofit measures were taken. However, the peak load values are more than threefold compared to

the retrofitted building. Designing the heating system, as well as terminal devices according to the loads retrieved for the TDY periods would yield in underestimating the peak loads during extreme cold periods. Dimensioning of the building system should be according to the upper whisker range of the hourly load frequency in the Triple data set represented in Figure 32. When sizing the zone terminal devices, provision for extreme cold periods should be implemented. The dimensioning of heating systems, however, should be done taking economical aspects into account. Over-dimensioning the systems to account for once-in-a-century extreme weather events should be avoided.

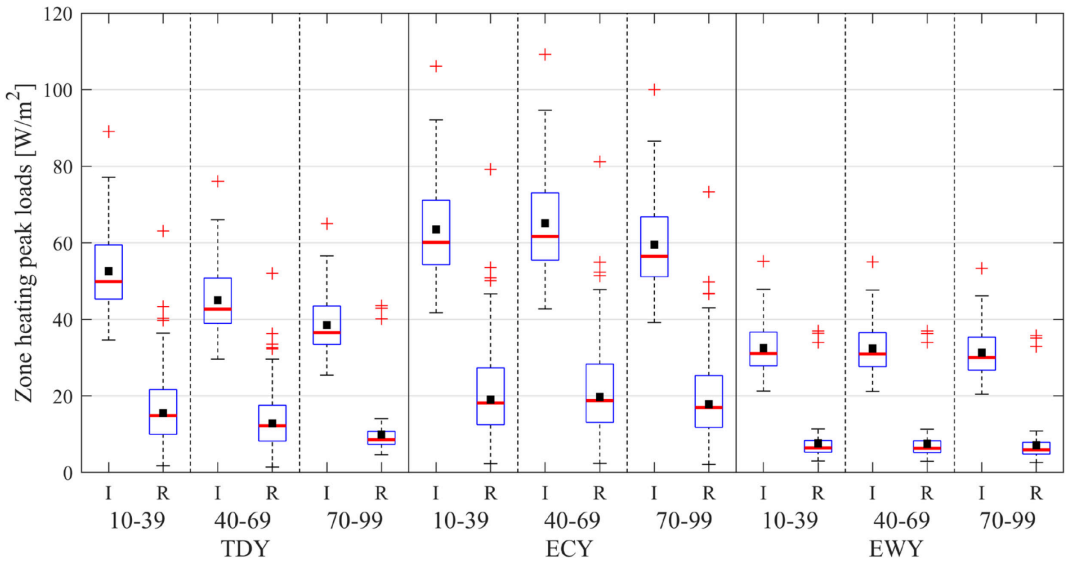

Figure 33: Zone heating peak loads represented through boxplots, building peak load shown as a black square.

5.1.1.3 Moisture Safety

Hygrothermal simulations for initial external walls and retrofitted façades were carried out for the most wind-driven rain exposed West orientation, as results showed that it performed worse than the least solar radiation receiving North orientation. North orientation was set for retrofitted gables, as it performed worse than the South facing gable wall. Driving rain coefficients in WUFI were set to low building with total height of up to 10 meters, which is applicable to the analysed building.

Exterior side of exterior insulation of the initial wall construction, shown as monitor one in Figure 13, displayed RH values above 75 % as seen in section 10.2.1. Other construction layers were not tested further, as they did not show any vulnerability to moisture issues by high number of hours exceeding the threshold of 75 % RH. The performed mould index study for the exterior insulation of the initial façade construction, as seen on the left side of Figure 34, indicates high mould growth risk all year around, corresponding to visually detected coverage up to 100 %. The positive mould growth rate, shown on the right side of Figure 34, demonstrates favourable conditions in which growth of mould spores are fostered. The respective wall construction however composes of mineral (stone) wool insulation that contains approximately 97 % of slag and inorganic rock along with three percent of thermosetting resin binder and oil combination [129]. Due to its unique

composition, there are almost no nutrient sources to promote mould growth [130]. Concrete is the second material within the assessed wall construction, which is considered to embody a medium resistance to mould growth [131]. Mould growth process could be initiated in the event of pollen, dust and other organic residue formation on the exterior surface, if it is not treated with protective compounds or/and cleaned regularly [132]. The total water content of the construction is decreasing and stabilizing within the examined 10-year period. Furthermore, no mould issues as such were reported during on-site inspections. As a result, the construction is therefore concluded to be safe, despite the mould index and mould growth rates predicting otherwise.

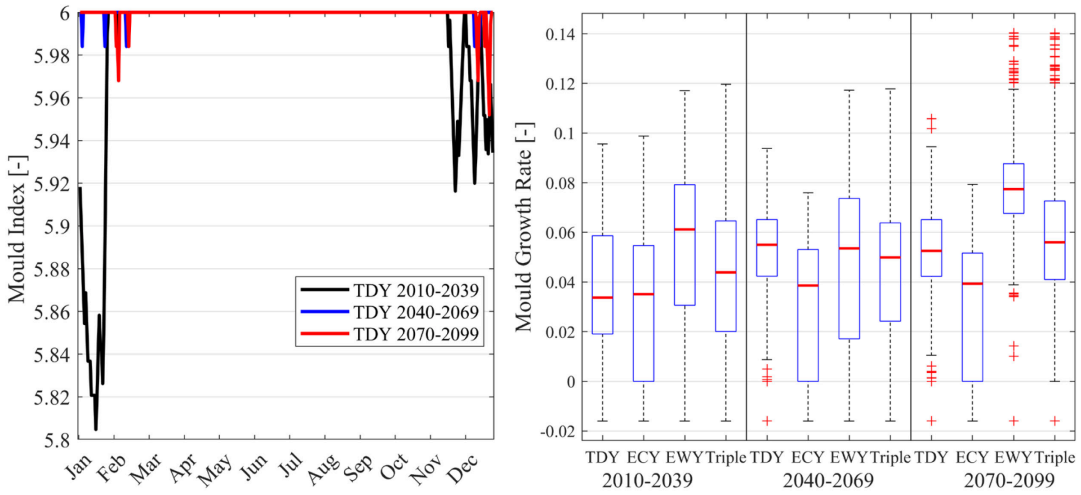

Figure 34: Mould index (on the left) and Mould growth rate (on the right) for exterior side of insulation of initial wall.

The assessment of retrofitted gables showed high RH values, as displayed in section 10.2.1, for three monitor positions visible on the left side of Figure 14. Mould index for monitors two and three showed no mould growth with a stable integer of zero, therefore, the constructions were seen as moisture safe. Mould index for the exterior side of the insulation (monitor one) showed mould growth detected only with microscopy for late spring and summer months for all three TDY periods, as seen on the left side of Figure 35. Mould growth rate for this monitor position presented negative mould growth values for most time periods, as well as a Triple data sets that combined hourly mould growth rate values of 10 year simulation period for TDY, ECY and EWY, displayed on the right side of Figure 35. This indicates that favourable conditions for mould growth are negative, relating to conditions in which mould spores die. Hence, the few occasions with a positive mould growth rate within whiskers and interquartile range do not result in favourable mould growth conditions as they are being followed by longer periods with negative mould growth rate, as confirmed by mould index.

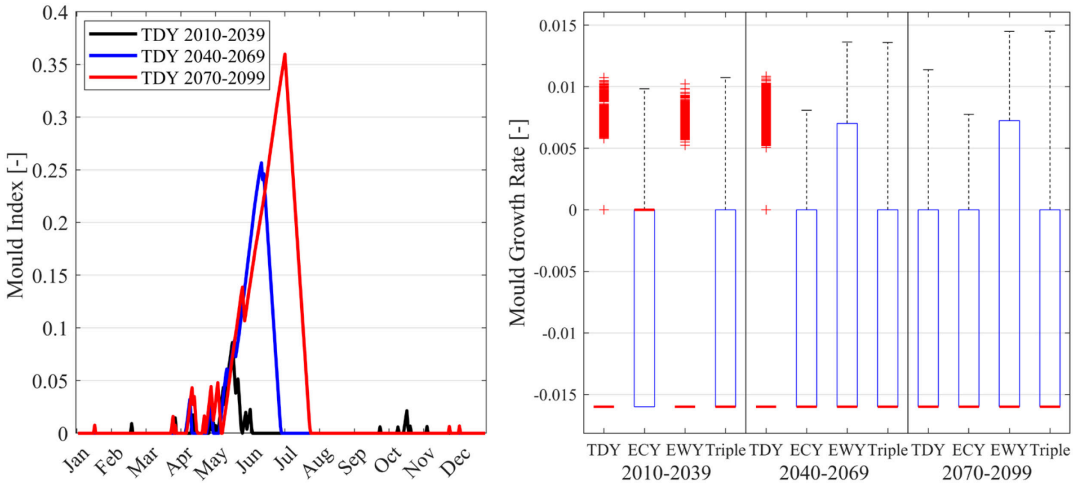

Figure 35: Mould index (on the left) and Mould growth rate (on the right) for exterior side of exterior insulation of retrofitted gable wall.

High RH values were present in the exterior side of exterior insulation of retrofitted façade, as displayed in section 10.2.1, marked with monitor position one on right side of Figure 14. Mould index indicated microscopic detectable growth for late spring and the first half of summer months for the three TDY periods, as seen on the left side of Figure 36. Mould growth rate for monitor one displayed negative mould growth for most events within the assessed dataset, as seen on the right side of Figure 36. The few occasions with a positive mould growth rate within whiskers and upper extreme range (upper half of interquartile range) in EWY weather data for periods between 2040 and 2099 do not result in favourable mould growth conditions as they are being followed by longer periods with negative mould growth rate. The same conclusions can be drawn from the mould index results. In addition, the triple combination within all three time-periods shows negative values for the largest share of the data set, which suggests a moisture safe construction.

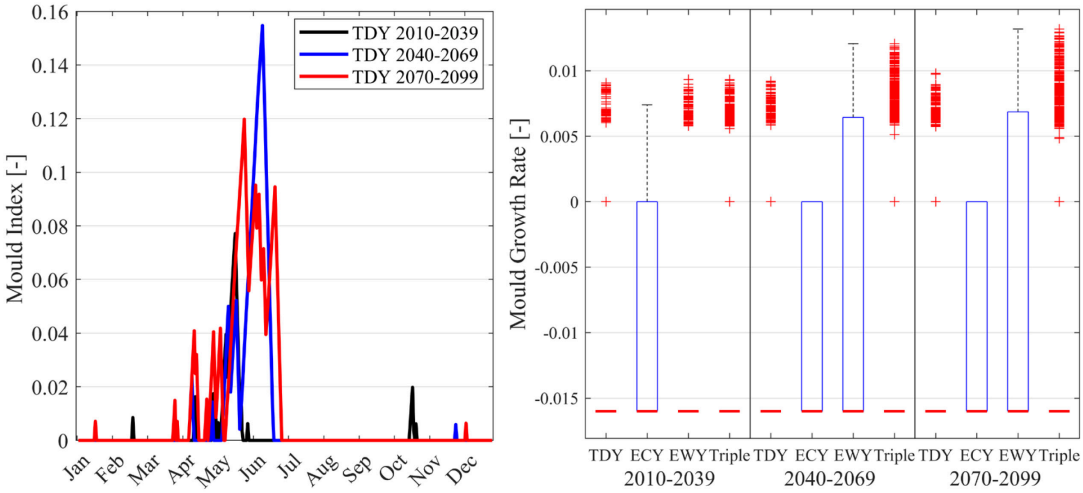

Figure 36: Mould index (on the left) and Mould growth rate (on the right) for exterior side of exterior insulation of retrofitted facade wall.

More than three thirds of all values throughout the datasets have a higher RH than 75 % within plywood boards (monitor one) and exterior side of insulation (monitor two), as displayed in section 10.2.1 and construction assembly shown in Figure 15. Mould index for both layers indicated mould growth ranging between none to some growth with larger coverage than 10 % visible with microscopy (see the left side of Figure 37 and Figure 38). Assessment of mould growth rate, displayed on the right side of Figure 37 and Figure 38 revealed that the construction is to some extent vulnerable for mould growth. This observation corresponds to on-site investigation, where minor mould growth was observed on some wood-based elements such as plywood boards and rafters. Construction is therefore evaluated to be moisture unsafe and it is advised to undergo properly designed retrofitting measures.

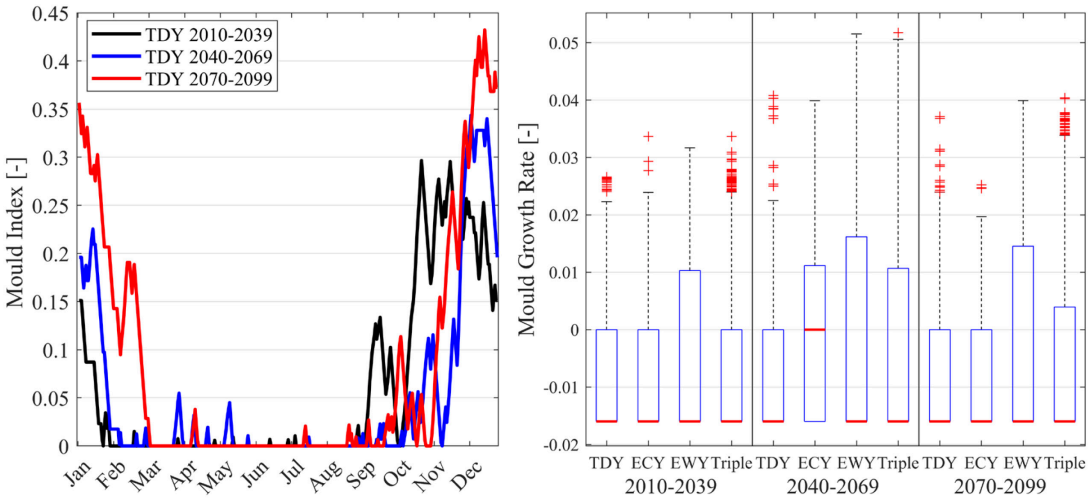

Figure 37: Mould index (on the left) and Mould growth rate (on the right) for exterior side of plywood boards of initial roof construction.

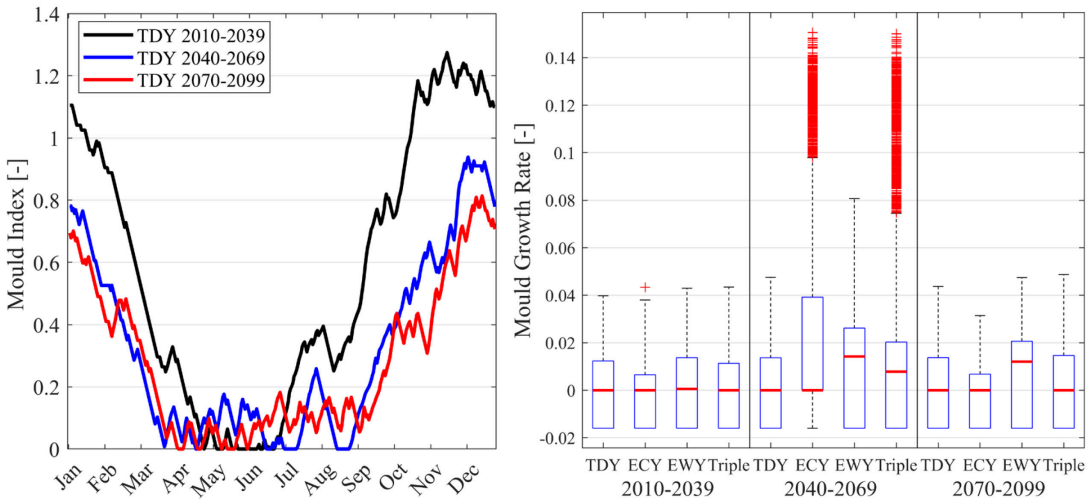

Figure 38: Mould index (on the left) and Mould growth rate (on the right) for exterior side of insulation of initial roof construction.

Monitor positions one and two (see right side of Figure 15), representing exterior and interior sides of insulation displayed heightened RH values, seen in section 10.2.1 and were therefore further assessed. Favourable conditions for mould growth within the interior side of insulation are not lasting long enough for mould spores to survive, as second quartile (the median) is displayed within negative range as seen in Figure 40. The conclusion is coherent with mould index plots. Mould index for exterior side of insulation, displayed in Figure 39, represents visible mould growth with coverage between 10 and 100 %, where smallest event probability is represented in ECY climate scenario and largest in EWY. As it is highly unlikely that extremes will take place in a continuous time-period, it should be referred to triple that displays a stable positive mould growth throughout all three time-periods. As the retrofitted roof construction does not include wooden-based or other mould sensitive organic materials [131] mould growth risk is unlikely, due to the absence of sufficient nutrient sources that promote mould growth.

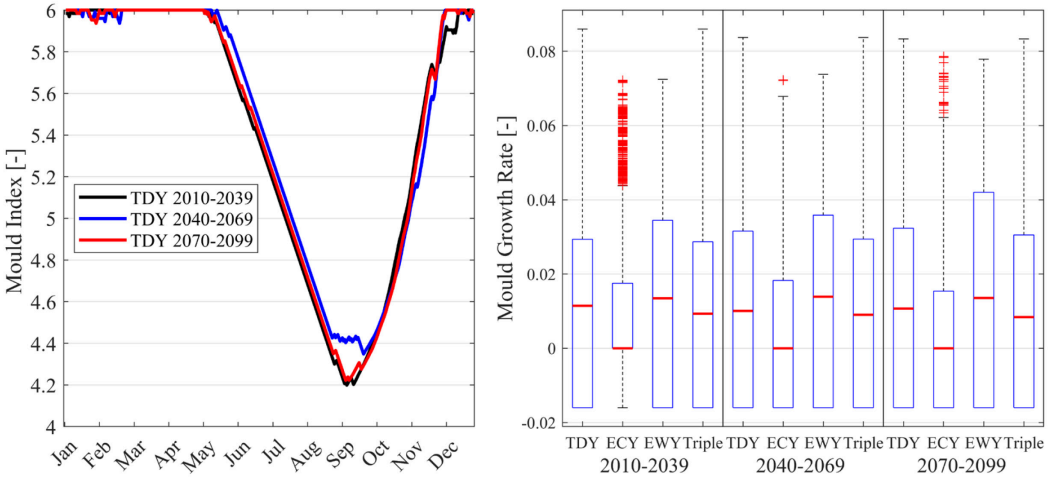

Figure 39: Mould index (on the left) and Mould growth rate (on the right) for exterior side of insulation of retrofitted roof construction.

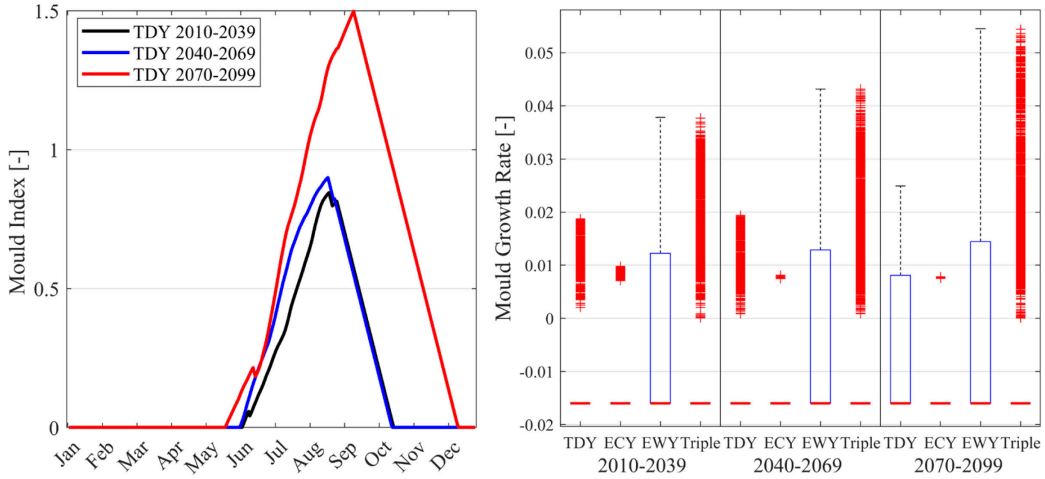

Figure 40: Mould index (on the left) and Mould growth rate (on the right) for interior side of insulation of retrofitted roof construction.

5.1.2 Project 2

Located in the periphery of the Danish capital city of Copenhagen, the second case study presents a large building complex. How the building performance changes under climatic conditions of the future is shown and discussed in the following section. In order to validate the script and model, the stead-state energy frame calculation for the initial building by the engineering consultancy was compared with the results of the BPS with the historical weather file of Copenhagen. The deviation of the energy use for heating in the initial building between the steady-state calculation and the simulation was 19 %. However, the energy use calculation results received included the auxiliary energy used for pumps and fans as well as energy use for domestic hot water.

5.1.2.1 Thermal Comfort

The diagram in Figure 41 represents the thermal discomfort according to EN 15 251 category II for the building average and six representative zones. The representative zones are located on the South-West in the middle of the building and in the South-Western corner. Selected zones were chosen as representatives due to their sizes being adequate as living room zones.

For the initial building it is seen, that discomfort in the TDY and EWY periods reaches building averages of 17 % and 8 % respectively. The evolution over time shows, that annual time of discomfort is decreasing, which is due to the operative temperatures in the winter not falling under the threshold. However, it can be observed, that overheating hours and thermal discomfort is gradually increasing in summer. Thermal discomfort reaches the highest values for the ECY time-periods. The building average is around 30 %, with single zones peaking at over 40 % discomfort. The annual balance shows, that most discomfort is during winter months, due to the operative temperatures falling slightly beneath the threshold of 20 °C. The values for ECY and EWY, however, are just an indicator, that thermal discomfort will be likely during extreme weather scenarios. The South-West zones have WWR of 40 %, which leads to discomfort due to cool radiation from windows in the wintertime. Passive measures, such as shading and increase of the clothing levels can be effective and increase of thermostat setpoints can also help to mitigate the local discomfort. In the retrofitted building, the zones showed discomfort during wintertime over long timeframes, during the near-term time-periods, which were minimised in TDY and EWY scenarios towards the end of the century. The discomfort due to heat-stress increased over the periods, yet, TDY and EWY show gradually falling trends, due to the decrease of cold-stress in winter periods. Overheating hours could be seen as increasing by 5 % to 20 % from the near-term to long-term EWY scenarios. To mitigate overheating hours, the implementation of passive measures such as an exterior shading system should be further investigated. Due to the fact that façades are mainly oriented towards East and West, the integrated horizontal shading in form of design elements shows limited effectivity. The integration of an exterior vertical shading system would be a measure to mitigate both summer and winter discomfort.

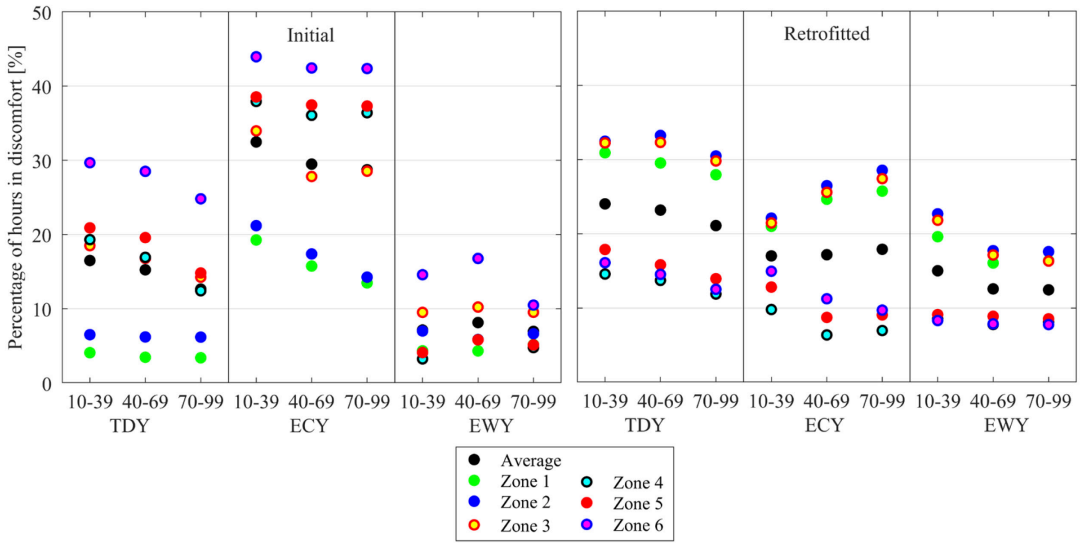

Figure 41: Percentage of time in discomfort: Building average, Zone 1: Typical Zone South-West Ground Floor, Zone 2: Typical Zone South-West Middle Floor, Zone 3: Typical Zone South-West Top Floor, Zone 4: Typical Zone South-West Corner Ground Floor, Zone 5: Typical Zone South-West Corner Middle Floor, Zone 6: Typical Zone South-West Corner Top Floor

5.1.2.2 Energy Use

Thermal bridges were evenly distributed over the U-value of the following constructions for initial and retrofitted building, as seen in Table 27 and Table 28. Significant impacts on the thermal conductivity of the thermal envelope of the building were represented by the junction between the external walls and intermediate floors in both initial and retrofit constructions.

Table 27: Overall U-values including thermal bridges of initial building

Construction	Heat loss projection	U-value $\left[\frac{W}{m^2 K}\right]$	$\Delta U_{thermal\_bridges}$ $\left[\frac{W}{m^2 K}\right]$	Overall U-value $\left[\frac{W}{m^2 K}\right]$
Exterior façade wall	'Ideal'	0.3671		
	'Plan section'	0.4078	0.0407	
	'Wall-intermediate floor junction'	0.4943	0.1272	
				0.5350
Exterior gable wall	'Ideal'	0.3298		
	'Wall-intermediate floor junction'	0.3321	0.0023	
				0.3321
Roof construction	'Ideal'	0.2198		
	'Section'	0.2328	0.0130	
				0.2328
Ground-Basement intermediate floor	'Ideal'	0.5111		
	'Section'	0.5432	0.0321	
				0.5432

Table 28: Overall U-values including thermal bridges of retrofitted building.

Construction	Heat loss projection	U-value $\left[\frac{W}{m^2 K}\right]$	$\Delta U_{thermal\_bridges}$ $\left[\frac{W}{m^2 K}\right]$	Overall U-value $\left[\frac{W}{m^2 K}\right]$
Exterior façade wall	'Ideal'	0.1103		
	Δ 'Plan section'	0.1224	0.0121	
	Δ 'Wall-intermediate floor junction'	0.1359	0.0256	
				0.1480
Exterior gable wall	'Ideal'	0.1103		
	'Plan section'	0.1448	0.0345	
	'Wall-intermediate floor junction'	0.1208	0.0105	
				0.1553
Roof construction	Construction without penetrations	0.1129		
				0.1129
Ground-Basement intermediate floor	'Ideal'	0.1664		
	'Section'	0.1696	0.0032	
				0.1696

The cumulative heating energy demand for the 15-storey building is shown in Figure 42. The TMY weather files for Copenhagen, used for validation, showed 20 % and 30 % higher heating energy demands as the TDY files for 2010-2039 for the initial and retrofitted buildings respectively. ECY scenarios represent the highest annual heating energy demand per square meter of heated floor area, TDY scenarios resulted in a 45 % to 60 % lower values. EWY scenarios showed 0.8 to 2.5 times lower values than the ones for TDY scenarios.

The parametric analysis of cumulative heating energy demands for the initial construction shows gradually falling heating energy demands for all scenarios from the near-term to long-term periods. Similar evolutions can be seen in the statistical analysis, presented in Figure 43 which shows gradually lower point in time heating loads. The Triple data sets show gradually falling building heating loads, which indicates, that less cold periods can be expected towards the end of the century.

Paradigms shown for the cumulative heating energy demand as well as the hourly building heating energy demand predict similar behaviour for the retrofitted case as already discussed for the initial stage. Heating demands during the TDY scenarios are object to a downward trend from the near-term period towards the end of the century. Between the near-term to medium-term TDY periods, a decrease of about 15 % of the heating energy demand can be seen. From mid-term to long-term, the difference is more than 17 %, resulting in a heating energy demand of about 6.3 kWh/m² in the TDY scenario in the period closest to the end of the century. As extremes are underrepresented in the TDY scenarios, the statistical analysis in Figure 42 and therein the boxplots for Triple, represent the accumulation of events with high hourly heating demands. It can be observed, that all figures for Triple show a mean that is equal to zero, which illustrates that no heating is needed for 50 % or more of time during a year. Towards the end of the century, a downward trend for the third quartile is seen, represented by the upper boundary of the boxplot. This indicates less intensive and continuous cold-periods and a raise of the average temperature, which is represented in the entire climate set. Outliers towards the upper end represent the probability of single events within the extremes. It can be seen that the number of events in the extreme spectrum is constant throughout the periods, however the peaks are decreasing. Values in Triple are more representative than in single scenarios, as the TDY scenarios underrepresents the extremes, but the ECY and EWY scenarios are constant extremes composing into annually extreme hot or cold scenarios. The falling frequency of high heating peak loads, represented by the upper whisker of the Triple data sets show, that less and less long-lasting heating periods as well as cold periods occur in future climate.

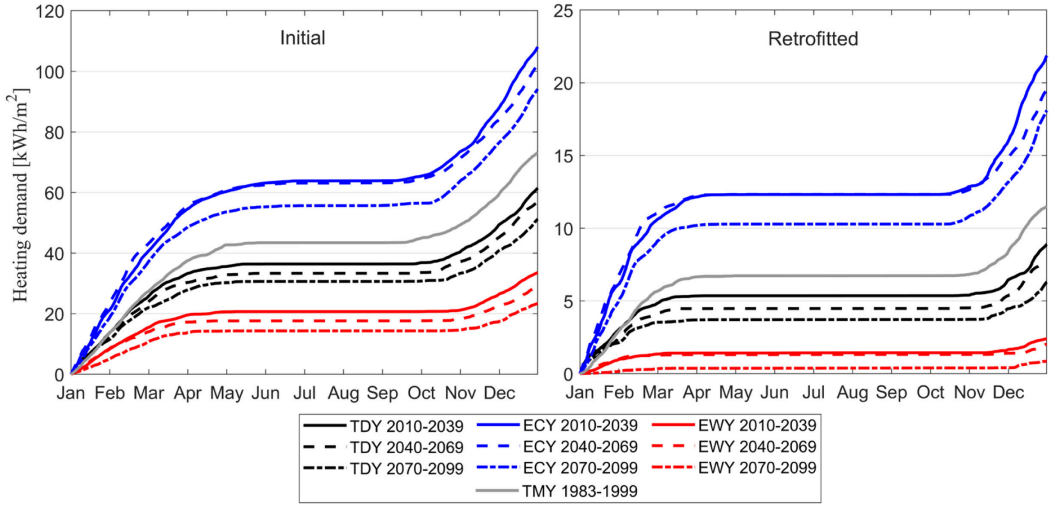

Figure 42: Cumulative heating demand. Initial building on the left, retrofitted building on the right.

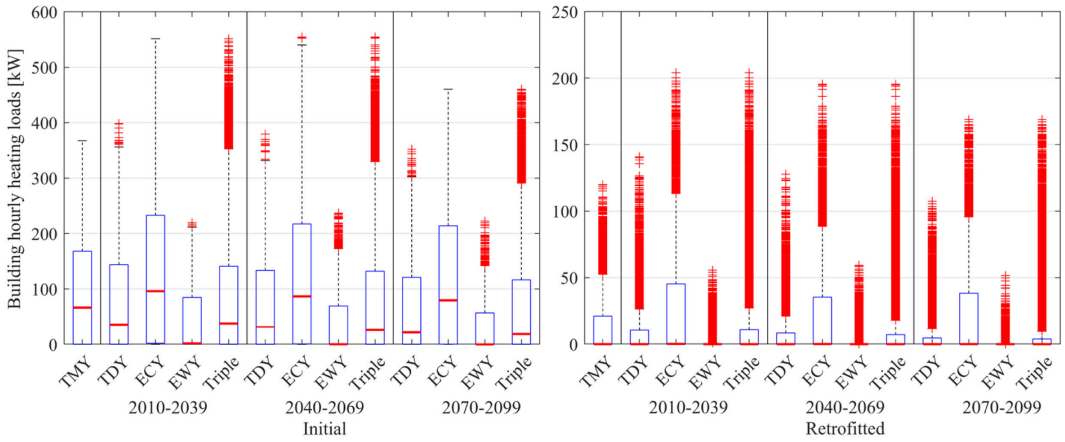

Figure 43: Statistical analysis of hourly building heating energy demands. Scale for initial on the left and retrofitted on the right adjusted for better visibility.

Heating peak loads on a zone and a building level are represented in Figure 44. Similar to the heating energy demand, it can be observed, that the level of zone heating peak loads drops towards the end of the century. For both initial as well as retrofitted building, the medium-term period of the EWY scenarios shows higher values than the near-term as well as long-term period, which can be explained by a long-lasting cold period represented in this file. Generally, the heating peak loads during the TDY periods were decreased drastically by over 50 % from the initial to the retrofitted stage. The retrofitted building represents zones with no actual heating demand, which can be explained by interior zones with adjacency to conditioned zones on all six sides of the room. Even zones located towards the exterior of the building show no need for heating systems during all three EWY periods. Not to underestimate extremes, systems should be designed in order to being able to provide enough heating power during long-lasting cold periods.

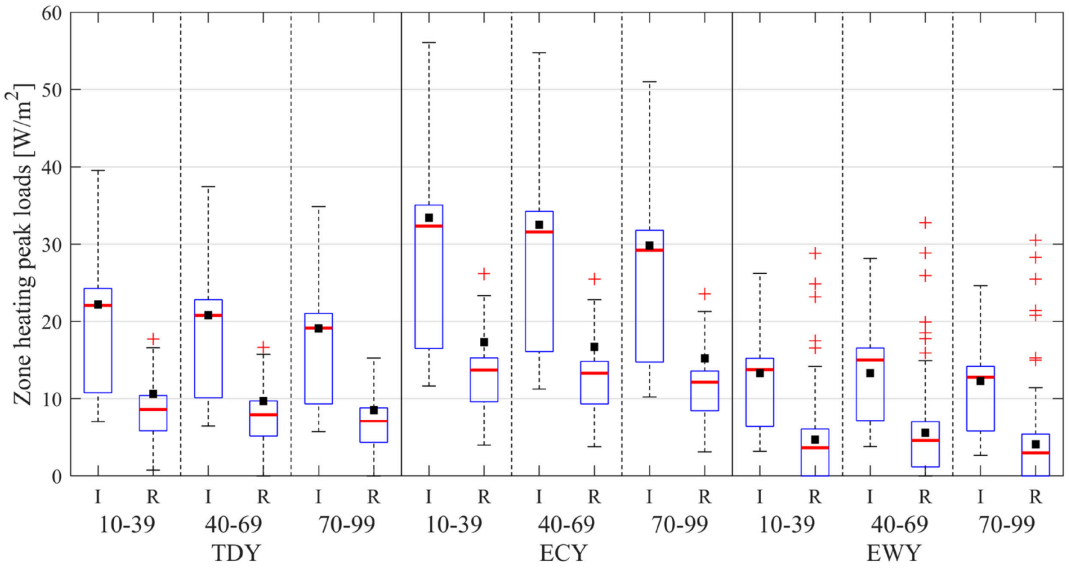

Figure 44: Zone heating peak loads represented through boxplots, building peak load shown as a black square.

5.1.2.3 Moisture Safety

Hygrothermal simulations for façades were carried out with North-East orientation, as it was proven that North-East orientation performed worse than the most wind-driven rain exposed South-West orientation. Gables were simulated with South-East rotation, as it performed worse than the other gable wall facing North-West. Driving rain coefficients in WUFI were set to a tall building with height exceeding 20 meters.

The exterior side of insulation of the initial façade shown on the left side of Figure 18 displays nearly three fourths of dataset values with larger RH than 75 %, as seen in Section 10.2.2. Mould index for this monitor position shows visually noticeable mould growth with coverage varying between 10 % and 100 % depending on a specific month of the year (see the left side of Figure 45). Assessment of mould growth rate visualized on the right side of Figure 45 indicated favourable mould growth conditions within all three time periods in all future climate scenarios. Lowest occasions of mould growth events are represented by ECY, what might be connected to generally lower and more predominant temperatures in winter periods where mould spores die. As it is highly unlikely for ECY scenario to take place in a continuous time-period, mould growth will remain positive in the future as presented by a Triple data sets. Furthermore, on-site investigations have reported moisture damages in the initial construction, what validates the assessment results. This construction is thus evaluated to be moisture unsafe as it includes wooden studs that are very sensitive to mould.

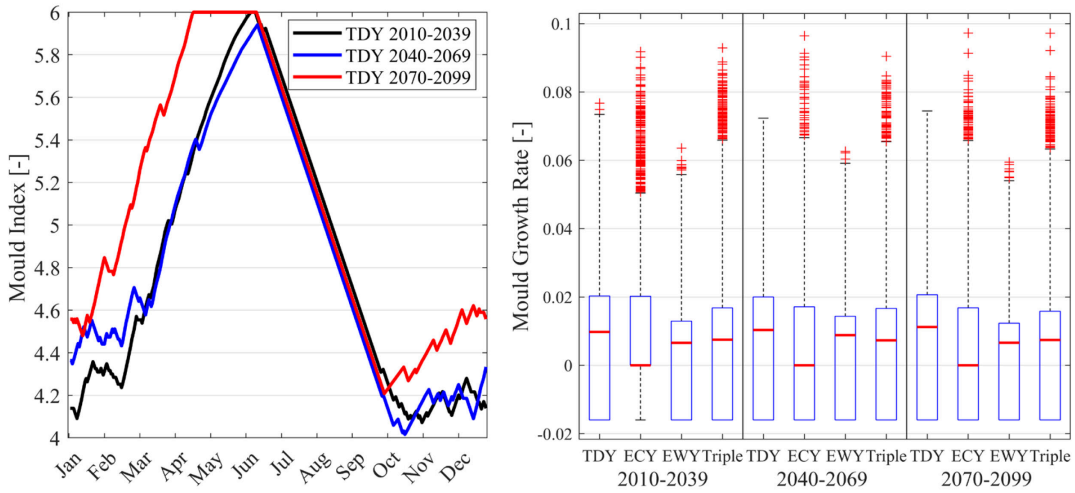

Figure 45: Mould index (on the left) and Mould growth rate (on the right) for exterior side of insulation of initial façade wall.

Initial gable construction shown on the left side of Figure 19 displays RH levels above 75% (see Section 10.2.2) in the exterior side of light weight concrete marked with monitor one, and exterior side of insulation marked with monitor two. Both of these positions have revealed mould index integers of six, corresponding to 100 % of visually detected coverage, as illustrated on the left side of Figure 46 and Figure 47. Favourable conditions for mould growth are indicated by positive mould growth displayed on the right side of Figure 46 and Figure 47, that is increasing throughout all three time periods integrated within Triple boxplots. This visualises an increasing moisture issues in long-term perspective that needs to be addressed. As already discussed in 5.1.1.3, for the initial wall construction composing of sandwich elements the mould growth in concrete-based products are highly unlikely. Furthermore, EPS insulation is a closed cell material, which is very good at resisting moisture and mould growth [133]. Nevertheless, load-carrying structures of a tall building like this must remain stable throughout the years without losing its integrity and being affected by wind driven rain. Gable walls were already renovated in the past, by mounting two new wall-ties for each concrete tile, which could indicate corrosion of initial wall ties caused by wind driven rain and high RH. Constantly increasing water content assessed for a 10-year period within exterior concrete tiles and light weight concrete indicates unsustainable design in future climate perspectives.

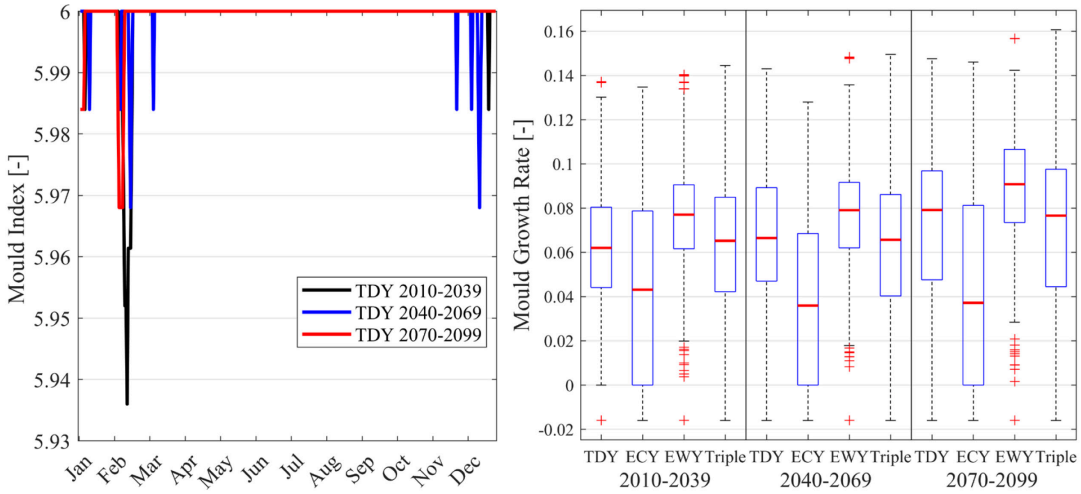

Figure 46: Mould index (on the left) and Mould growth rate (on the right) for exterior side of light weight concrete of initial gable wall.

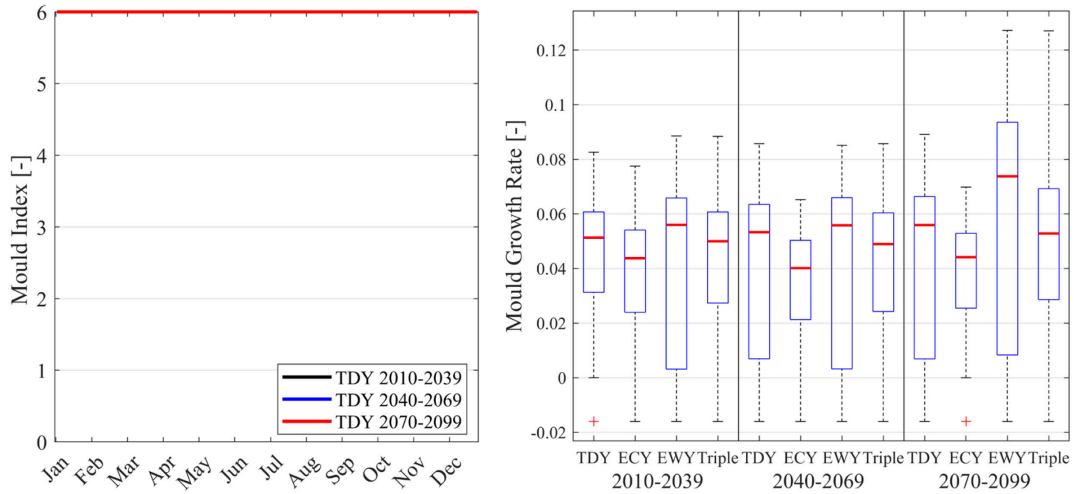

Figure 47: Mould index (on the left) and Mould growth rate (on the right) for exterior side of insulation of initial gable wall.

Relative humidity exceeding 75 % was proven to exist in monitor position 1, representing exterior side of exterior insulation of the retrofitted wall construction as displayed in Figure 18. This monitor was therefore studied further. Relative humidity for supplementary monitor positions described in section 10.2.2 was considered to be too low for posing mould growth risk. The performed mould index investigation, seen on the left side of Figure 48, for exterior side of exterior insulation has indicated a possibility for mould growth between late spring and summer months, corresponding to some growth detection only with microscopy. Assessment of mould growth rate for exterior side of exterior insulation, as seen from triple boxplots for different time periods presented on the right side of Figure 48, indicates that favourable conditions for mould growth (mould growth rate positive) only show outlier values, whereas the highest fraction of time mould growth rate is negative which relates to conditions in which mould spores die. Hence, the few occasions with a positive mould growth rate do not result in favourable mould growth conditions as they are being followed

by longer periods with negative mould growth rate. The following observations are coherent with mould index results. The construction is therefore evaluated to be safe under the studied future climate scenarios.

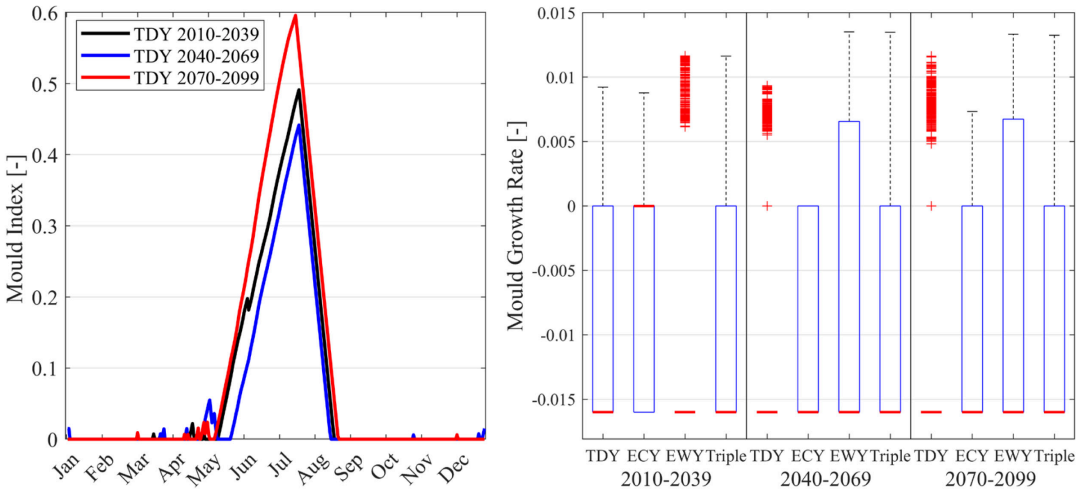

Figure 48: Mould index (on the left) and Mould growth rate (on the right) for exterior side of exterior insulation of retrofitted façade.

The exterior side of insulation marked as monitor one in the retrofitted gable construction shown on the right side of Figure 19, displays nearly four fourths of values with RH above 75 % as seen in Section 10.2.2. Performed mould index, seen on the left side of Figure 49 has indicated a slight possibility for mould growth, corresponding to some growth detection only with microscopy. Further assessment of the mould growth rate and mould index, represented in Figure 49, indicates unfavourable conditions for mould growth for the largest share of values within the periods and scenarios studied, whereas positive events do not last long enough for mould spores to survive as they are being followed by longer periods with negative mould growth rate. The whole retrofitted gable wall is therefore estimated to be mould safe under the individual future climate predictions, as well as Triple data sets.

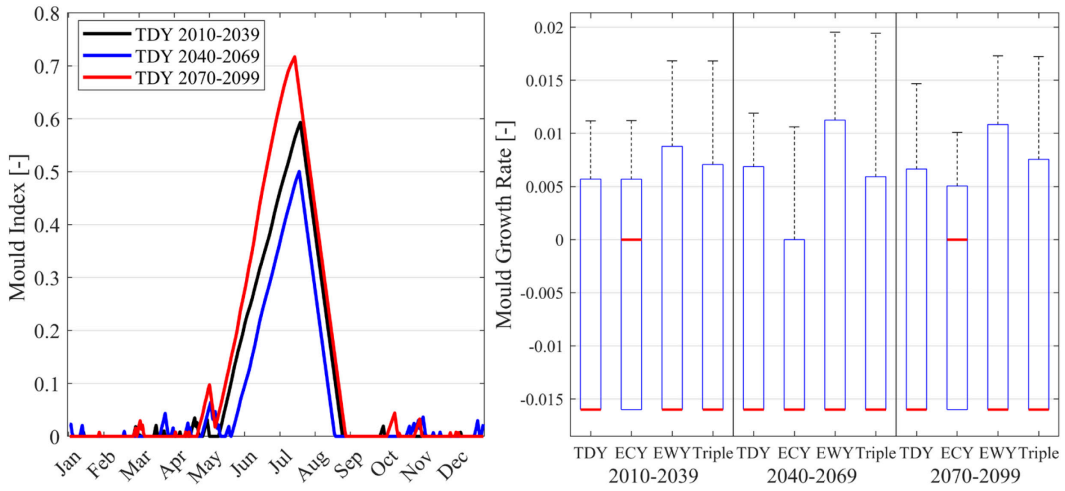

Figure 49: Mould index (on the left) and Mould growth rate (on the right) for exterior side of insulation of retrofitted gable wall.

More than three fourths of all values throughout the datasets have a higher RH than 75 % within wooden profiled boards (monitor one) and exterior side of insulation (monitor two), as displayed in section 10.2.2 and initial roof assembly shown in Figure 20.
Mould indexes for both layers indicate some mould growth ranging between none to some growth visible only with microscopy, as seen on the left side of Figure 50 and Figure 51. Assessment of mould growth rate, displayed on the right side of Figure 50 and Figure 51, revealed that the construction might be more vulnerable for mould growth in some future climate scenarios than the others. The roof construction can be evaluated as moisture safe for the TDY periods, as the occasions with positive mould growth are statistically lower than the conditions in which mould spores die. The same paradigm can be seen in the EWY future predictions. Worse performance with high statistical likelihood of mould growth is given during the middle-term ECY periods. As ECY and EWY scenarios are unlikely to happen in a full-year scale, Triple data sets, combining extremes and non-extreme conditions are a more realistic representation of future climate. The analysis of the Triple data shows, that during near-term and long-term periods the majority of events predicts negative mould growth conditions. In the medium-term period, however, the statistical representation of positive mould growth and negative mould growth is equal, which indicates that growth of mould spores cannot necessarily be avoided by sequences with anti-growth conditions.

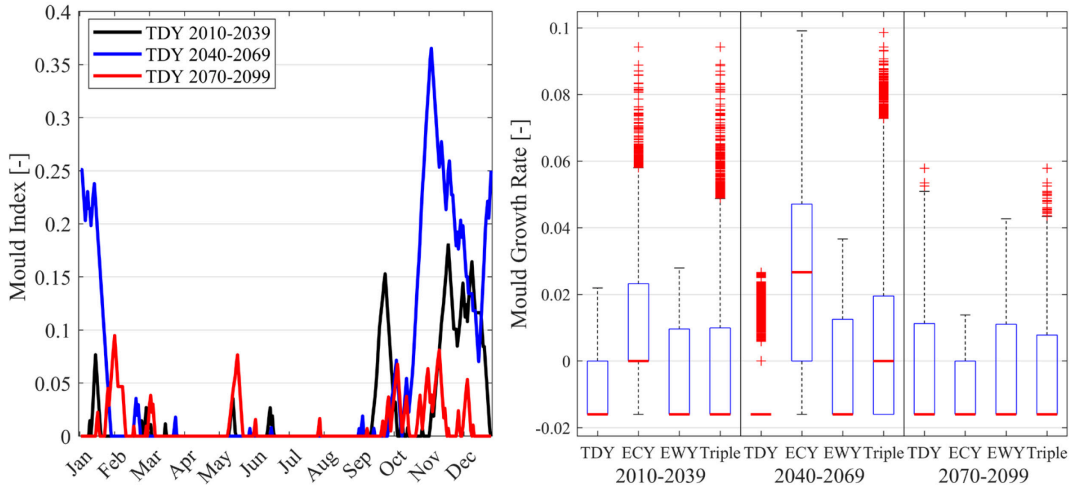

Figure 50: Mould index for wooden profiled boards of initial roof construction.

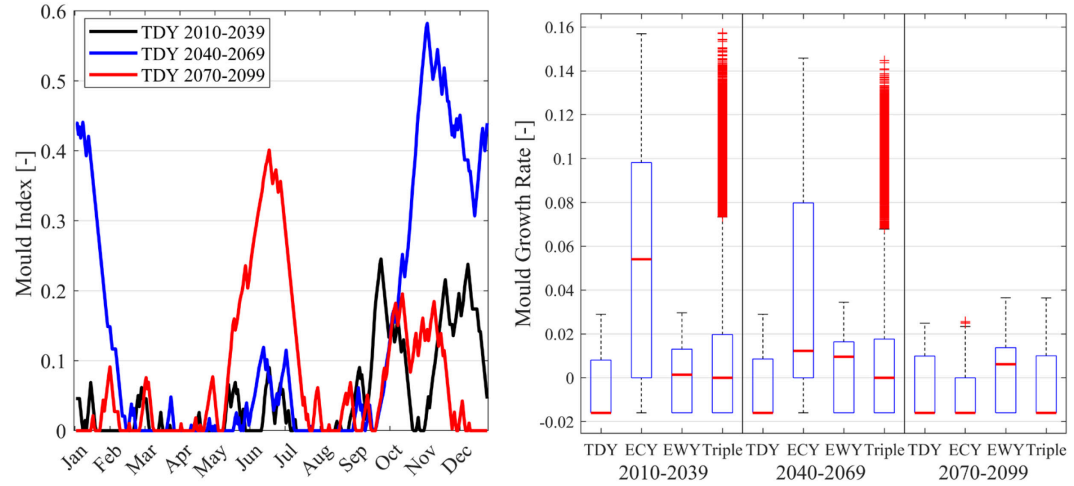

Figure 51: Mould index for exterior side of insulation of initial roof construction.

5.2 Germany

The analysis of the two projects located in Stuttgart, is presented in the following. The building owner of both projects followed different concepts for the individual buildings, where the first project was designed to a low energy standard, better than the standard for new buildings at the time, the second project was the retrofit and renovation of a historic building.

5.2.1 Project 3

The impact of climate change on a commonly carried out building retrofit was assessed for the case study in the following. The results of BPS and Hygrothermal simulations are shown and discussed below. With the aid of the calculation of the thermal performance for the building carried out by a building physician office, the validation of the BPS script and model were carried out with the TMY weather file for Stuttgart. The simulated heating energy demand was 30 % under the results of the steady-state calculation. Reasoning for the large discrepancies can be found in the climate data used in steady-state calculation and simulation. As the input parameters in the BPS were set likewise as in the calculation, the simulation results were found as adequate.

5.2.1.1 Thermal Comfort

The diagram in Figure 52 shows the percentage of time that the building is in discomfort. In the initial stage, before the retrofit was carried out, the thermal discomfort maxed out at about 30 % for the typical zone on the top floor in the EWY scenario in the period closest to the end of the century. The building average is in all TDY periods far below 10 % discomfort. This can be reduced to a few factors, of which the high infiltration rate in the initial case is the most important one. High infiltration losses and bad thermal properties of the building envelope result in a high space heating demand, but neither overheating, nor cold can be sensed. The initial building also has low WWR, which result in less discomfort due to cold window surfaces, even in the ECY periods, only minimal discomfort can be sensed. The top floor zones show worse thermal comfort than the ground and intermediate floor zones.

Since no mechanical ventilation was considered for the building, and the building envelope was tightened up by installing airtightness layers, the infiltration losses in the retrofitted case were minimised compared to the initial case. Even schedules for window ventilation to use night flush ventilation and to cool down the air in the space are not effective enough to prevent high numbers of overheating hours throughout TDY, ECY and EWY time periods. In all scenarios, the medium-term time period from 2040-2069 shows the highest discomfort values. High discomfort in the retrofitted case is due to the increase in glazing area in the retrofit. Especially on the southern façade and attic zones facing south, the discomfort reaches values of over 70 % of time in the TDY periods, which corresponds to both, high overheating hours and high winter thermal comfort. Overheating and summer thermal comfort can be diminished by correct user behaviour, by opening windows and enabling the shading. The general trends with the window ventilation and shading system already in place, however, show that thermal discomfort will be an issue in future climate. The lack of a controlled ventilation system, as well as an active or passive cooling system will result in extensive discomfort due to overheating. Time periods with extreme warm conditions will

lead to constant discomfort, mitigation of the such is seen not effective by the passive systems in use.

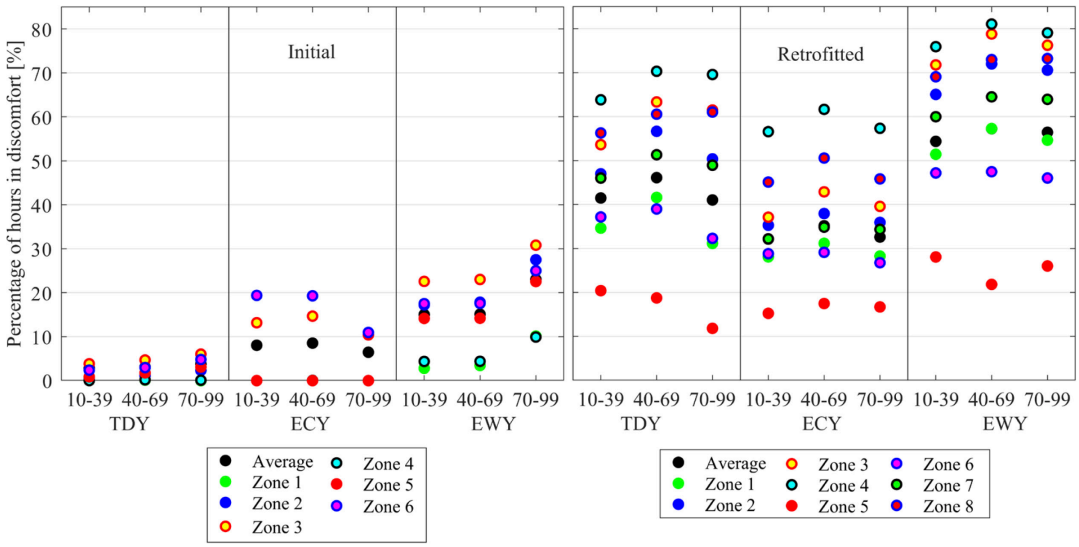

Figure 52: Percentage of time in discomfort: Building average, Initial: Zone 1:Typical Zone South Ground Floor, Zone 2: Typical Zone South Middle Floor, Zone 3: Typical Zone South Top Floor, Zone 4: Typical Zone North Ground Floor, Zone 5: Typical Zone North Middle Floor, Zone 6: Typical Zone North Top Floor; Retrofit: Zone 1: Typical Zone South Ground Floor, Zone 2: Typical Zone South Middle Floor, Zone 3: Typical Zone South Top Floor, Zone 4:Typical Zone South Attic, Zone 5: Typical Zone North Ground Floor, Zone 6: Typical Zone North Middle Floor, Zone 7: Typical Zone North Top Floor, Zone 8: Typical Zone North Attic

5.2.1.2 Energy Use

The construction types employed in this project showed penetrations inducing thermal bridges only due to the intermediate floor junctions, as well as in the retrofitted roof construction. U-values for ideal and thermally bridged constructions can be observed in Table 29 and Table 30.

Table 29: Overall U-values including thermal bridges of initial building.

Construction	Heat loss projection	U-value $\left[\frac{W}{m^2 K}\right]$	$\Delta U_{thermal\_bridges}$ $\left[\frac{W}{m^2 K}\right]$	Overall U-value $\left[\frac{W}{m^2 K}\right]$
Exterior façade wall	'Ideal'	1.8947		
	'Wall-intermediate floor junction'	1.9193	0.0246	**1.9193**
Roof construction	Construction without penetrations	4.0503		**4.0503**
Ground-Basement intermediate floor	Construction without penetrations	1.1149		**1.1149**

Table 30: Overall U-values including thermal bridges of retrofitted building.

Construction	Heat loss projection	U-value $\left[\frac{W}{m^2 K}\right]$	$\Delta U_{thermal\_bridges}$ $\left[\frac{W}{m^2 K}\right]$	Overall U-value $\left[\frac{W}{m^2 K}\right]$
Exterior façade wall	'Ideal'	0.1799		
	'Wall-intermediate floor junction'	0.1802	0.0003	
				0.1802
Roof construction	'Ideal'	0.1174		
	'Section'	0.1313	0.0139	
				0.1313
Ground-Basement intermediate floor	Construction without penetrations	0.1499		**0.1499**

Heating demand normalized per square meter cumulated over annual periods for the different weather scenarios and periods is presented in Figure 53. The validation of the model was undertaken with the TMY file for Stuttgart, composing representative months of historical weather between 1982 to 1992. The initial building shows annual heating energy demands of up to 80 kWh/m² in the TDY 2010-2039 scenario. The heating demand intensity is about 1.5 times the one as predicted in the first TDY period. The results of the retrofitted construction show a fourfold heating demand for the TMY file used for validation of the building model to the TDY 2010-2039 period. The retrofitted case shows even higher heating energy demand than for the ECY 2010-2039 period. Low heating energy demand can partially be explained with the climate file analysis in 3.3.1. The diagram shows, that especially winter periods are milder and have no long remaining cold periods that would lead to high heating energy demands. The effectivity of the retrofit measures to mitigate heating energy demands can be observed in Figure 53, which shows that the heating season lasts from mid-November to the end of February with low demands in March. In the initial case, the heating season lasts from mid-October to the end of April. Effects of the highly insulative building envelope, however, show in the indoor thermal comfort, as described in 5.2.1.1, by high percentages of discomfort due to overheating. Similar long-lasting heating periods are predicted by the TMY weather data.

Figure 54 illustrates the statistical frequencies of hourly heating loads for the entire building. The TMY file of Stuttgart used for validation of the model, represents similarly to the cumulative heating demand higher heating loads for the building than TDY and Triple data sets. It can be seen, that the retrofitted building has no heating need for more than 50 % of the year, as the mean values for TDY and Triple are zero. By comparing the Triple data sets between the periods, a decrease from 2 kW to close to 0 kW for the retrofitted building can be observed. This shows, that towards the end of the century heating periods are getting shorter and less frequent. Outliers represent single hourly values with heating demands of up to 30 kWh in the extreme cold scenarios. The heating periods for the initial building are lasting longer than half the years which shows with means above 0 for both TDY and Triple data sets over all periods. However, upper whisker ranges for the Triple data sets decrease from period to period which can support the observations for the retrofitted building, that cold periods are less frequent and of shorter nature.

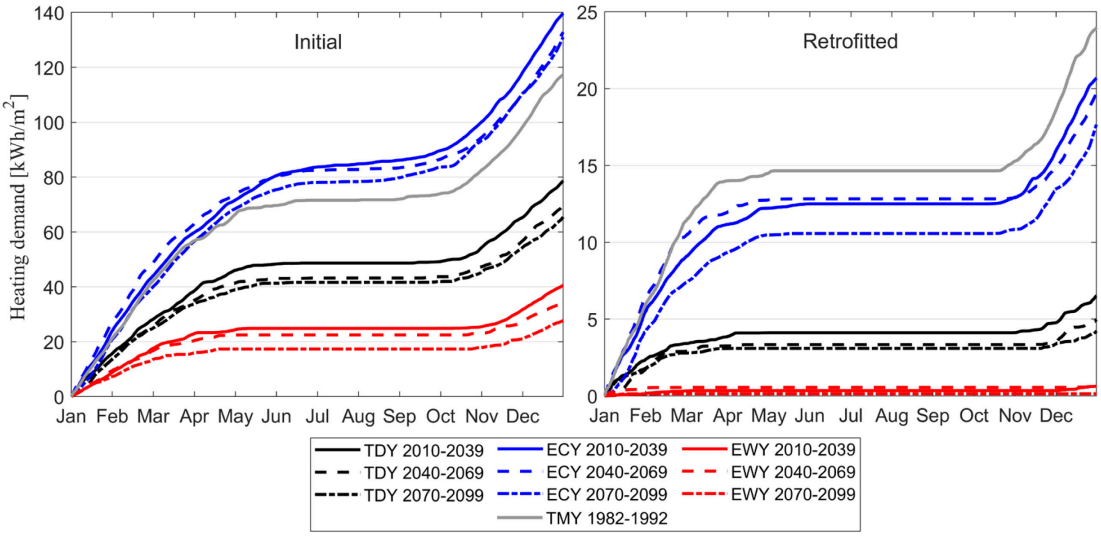

Figure 53: Cumulative heating demand. Initial building on the left, retrofitted building on the right. Scale is adjusted for better visibility.

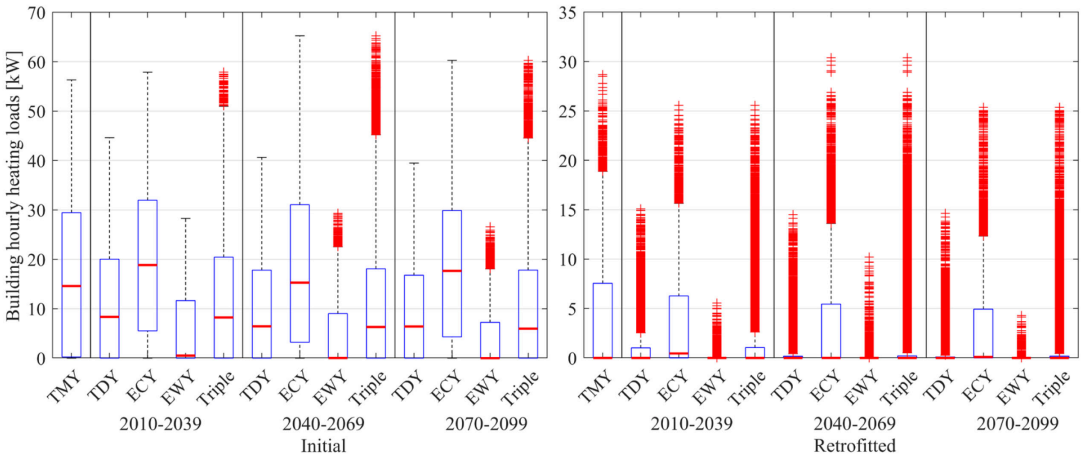

Figure 54: Statistical analysis of hourly building heating energy demands. Scale for initial on the left and retrofitted on the right adjusted for better visibility.

In Figure 55, the zone heating peak loads, as well as the building average heating peak loads are shown. It can be observed, that throughout all scenarios, the heating peak loads were diminished by about 50 % from the initial to the retrofitted building stage. In both building stages, the TDY zone and average heating peak loads are reduced from the near-term period to the long-term period, whereas the ECY and EWY medium-term period shows upward outlier results compared to the other periods. As the heating energy demand decreases from period to period, as seen in Figure 53, a reasonable explanation is a long-lasting cold period in the ECY and EWY 2040-2069 weather files. The heating peak loads in the TDY periods decrease gradually from the first to the last period, by in total about 1 W/m². The step from near-term to medium-term is, however, far bigger than from medium-term to the long-term period. The heating system, as well as the zone terminal devices should be capable to deliver loads as high as in extreme events, in order to be able to cover for extreme cold periods, which can result in 15-20 % increased peak heating loads.

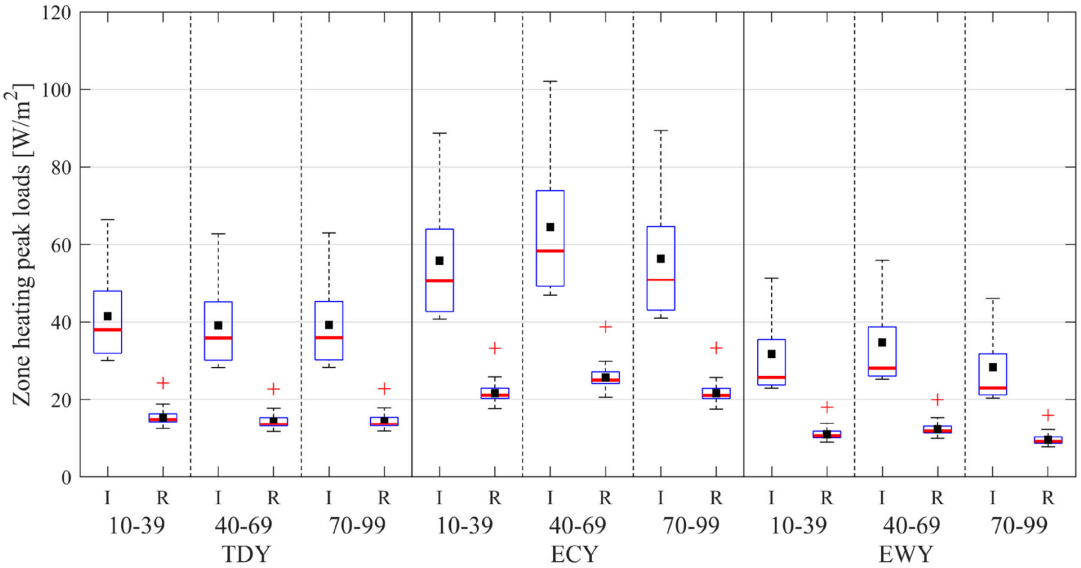

Figure 55: Zone heating peak loads represented through boxplots, building peak load shown as a black square.

5.2.1.3 Moisture Safety

Hygrothermal simulations for wall constructions were carried out with the most wind-driven rain exposed South-West orientation, as it was proven that it performed worse than the least solar radiation receiving North orientation. Driving rain coefficients in WUFI were set to a tall building with a height between 10 and 20 meters representing the highest exposure of exterior walls in this project.

The initial wall construction shown on the left side of Figure 23 displays RH levels above 75 % for the exterior side of pumice aggregate concrete blocks along with the interior surface, seen in Section 10.2.3. A stable mould index with an integer of six is kept within both monitors throughout a period between 2010-2099 in TDY climate scenario, corresponding to visually detected coverage up to 100 %. Positive values in the assessment of mould growth rate, displayed in Figure 56 and Figure 57 confirm favourable conditions for mould growth. Triple data sets for both monitors show least mould growth during short-term and utmost mould growth during long-term periods, what indicates increasing moisture issues in the future climate. Even though cement based materials like pumice concrete blocks are considered to resist mould growth well [131], interconnected air-filled voids within the block makes it a perfect hygroscopic material with the ability to attract and store water molecules that results in increasing total water content for the assessed 10-year period [134]. A combination of high RH levels and increasing water content indicates failing construction in future climate, which would require a closer investigation.

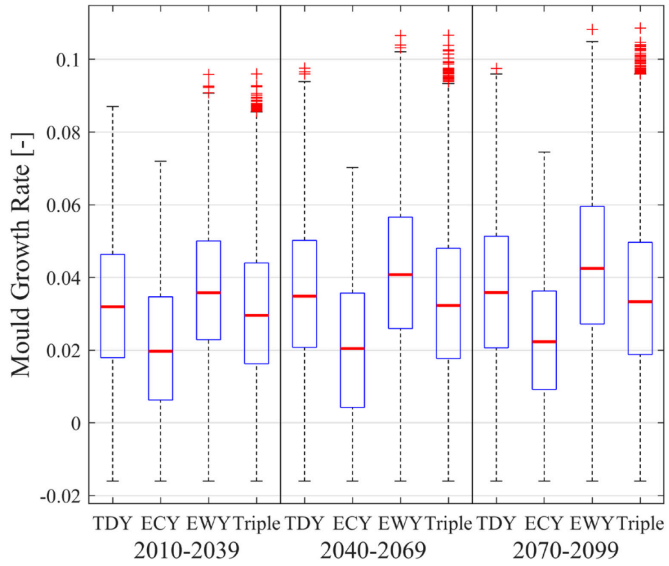

Figure 56: Mould growth rate for exterior side of concrete blocks of initial wall construction.

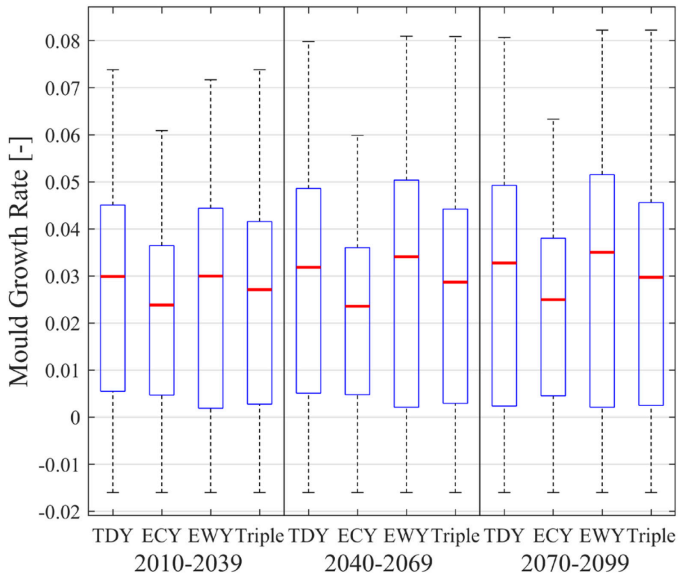

Figure 57: Mould growth rate for interior surface of initial wall construction.

Retrofitted wall construction shown on the right side of Figure 23 displays RH levels above 75 %, as seen in Section 10.2.3, for exterior side of insulation, interior side of EPS insulation and exterior side of pumice aggregate concrete blocks. Mould index indicated no mould growth for the two inner layers, however the exterior side of EPS insulation, seen on the left side of Figure 58, showed visually detected coverage up to 100 %. Mould growth rate presented on the right side of Figure 58 displayed positive values indicating favourable conditions for mould growth. The same trends of increasing mould growth rate are noticed in the Triple data sets during future climate scenarios, as in the initial wall construction. However, this time external render system along with EPS insulation is facing the outside conditions. As EPS is a closed cell foam which is very good at resisting moisture absorption and mould growth [133], the construction is considered safe, due to absence of mould

sensitive materials such as untreated wood or other organic substances containing carbon atoms. In addition, the retrofitted façade was treated with fungicides and algaecides to prevent growth of fungi and algae on the exterior surface, that furthermore decreases the risk of mould growth.

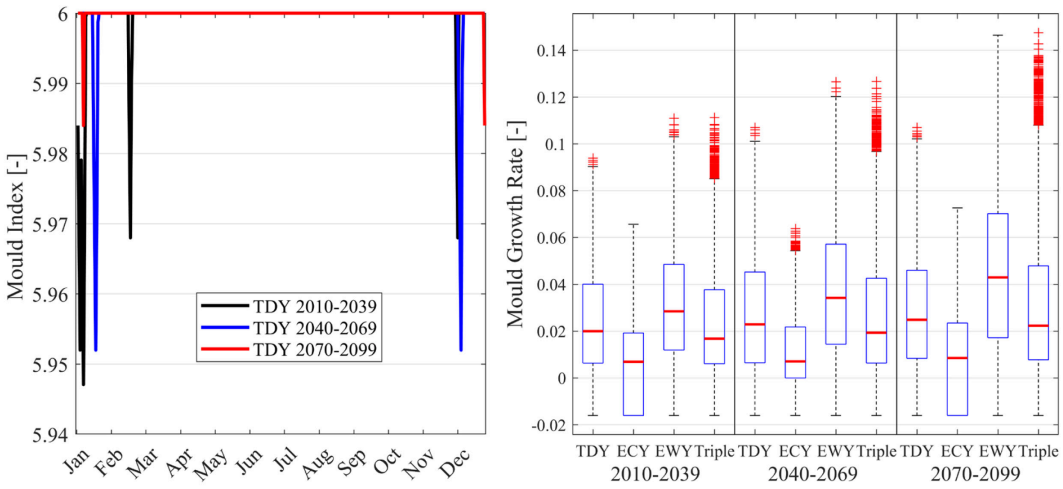

Figure 58: Mould index (on the left) and Mould growth rate (on the right) for exterior side of insulation of retrofitted wall construction.

The retrofitted roof construction shown on the right side of Figure 24 displays three monitors with high RH levels, as seen in Section 10.2.3. Monitor two and three referring to interior side of wood fibre insulation and exterior side of mineral wool insulation showed no mould growth in the mould index assessment. Exterior side of wood fibre insulation indicated possible mould growth events within some of TDY and ECY future climate scenarios, as seen in Figure 59. Triple data sets however, indicates unfavourable mould growth conditions in all three time periods, that suggest a mould safe construction. Coherent results were observed in mould index plots.

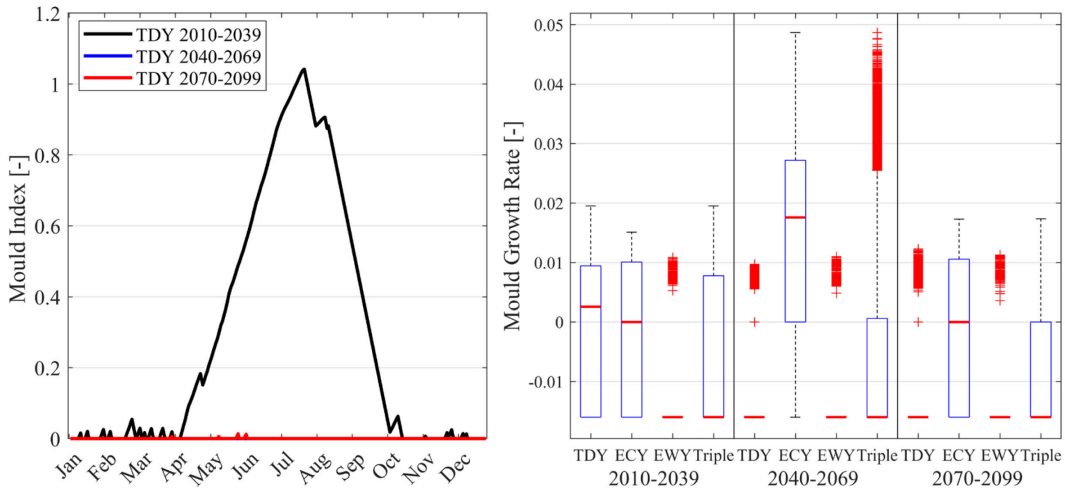

Figure 59: Mould index for exterior side of wood fibre insulation of retrofitted roof construction.

5.2.2 Project 4

The performance of a building retrofit that respected the historical value of the building in its surrounding under future climate conditions is shown and discussed in what follows. To validate the building model and simulation script used in BPS, the conditions of the thermal insulation certificate were compared with simulation results of the building with the TMY weather file for Stuttgart, based on historical weather measurements. The differences between the simulated heating energy demand and the steady-state calculation was 8 %.

5.2.2.1 Thermal Comfort

The plot of percentage of time in discomfort for the initial and retrofitted building stage in Figure 60 shows the values for building average and 6 typical zones facing North and South. The building average shows low values of discomfort throughout the periods for TDY and ECY in both initial and retrofitted building stages. The high infiltration rate through the free ventilation concept results in low overheating hours in TDY and ECY scenarios. Small glazing ratios also cause low overheating and prevent too low mean radiant temperatures in winter months by low cold radiation from window surfaces. In the EWY periods, overheating hours occur over long time periods, which is seen as the cause of discomfort values of up to 40 %. Even though, that overheating and thermal discomfort values are low, the gradually increasing discomfort, seen for the TDY periods, indicate summer discomfort to become an issue towards the end of the century. During these times, large infiltration, window-opening and shading shows no effectivity, which entails the need for passive or active cooling measures to be applied.

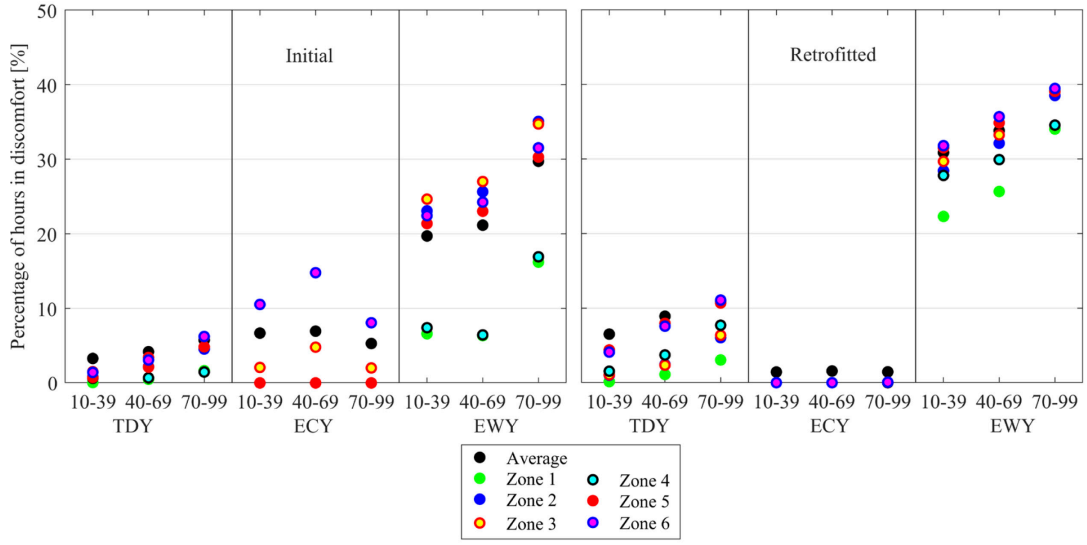

Figure 60: Percentage of time in discomfort: Building average, Zone 1: Typical Zone South Ground Floor, Zone 2: Typical Zone South Middle Floor, Zone 3: Typical Zone South Top Floor, Zone 4: Typical Zone North Ground Floor, Zone 5: Typical Zone North Middle Floor, Zone 6: Typical Zone North Top Floor

5.2.2.2 Energy Use

The thermally bridged structures for initial and retrofitted constructions of the thermal envelope are as displayed in Table 31 and Table 32 respectively. It can be seen, that thermal bridges through wooden beams have positive effect on the overall thermal conductivity of ground floor and top floor ceiling constructions of both initial and retrofitted projects. This is due to the better thermal conductivity properties of the wooden beams compared to the filling material slag. The exterior façade construction is impacted by the wall to intermediate floor construction, which was not insulated with the interior insulation boards.

Table 31: Overall U-values including thermal bridges of initial building.

Construction	Heat loss projection	U-value $\left[\frac{W}{m^2 K}\right]$	$\Delta U_{thermal\_bridges}$ $\left[\frac{W}{m^2 K}\right]$	Overall U-value $\left[\frac{W}{m^2 K}\right]$
Exterior façade wall	Construction without penetrations	1.4647		**1.4647**
Roof construction	'Ideal' 'Section'	1.6663 1.5872	 -0.0758*	**1.5872**
Ground-Basement intermediate floor	'Ideal' 'Section'	1.6663 1.5872	 -0.0758*	**1.5872**

* Negative values represent lower thermal conductivity of wooden beams in respect to higher thermal conductivity of slag filling in between these beams.

Table 32: Overall U-values including thermal bridges of retrofitted building.

Construction	Heat loss projection	U-value $\left[\frac{W}{m^2 K}\right]$	$\Delta U_{thermal\_bridges}$ $\left[\frac{W}{m^2 K}\right]$	Overall U-value $\left[\frac{W}{m^2 K}\right]$
Exterior façade wall	'Ideal' 'Wall-intermediate floor junction'	0.3845	 0.098	**0.4825**
Roof construction	'Ideal' 'Section'	0.2834	 -0.027*	**0.2807**
Ground-Basement intermediate floor	'Ideal' 'Section'	0.2649	 -0.026*	**0.2623**

* Negative values represent lower thermal conductivity of wooden beams in respect to higher thermal conductivity of slag filling in between these beams.

The cumulative heating demand in Figure 61 shows the building energy demand over a one-year period. Displayed are 10 heating energy demand patterns for both the building in its initial stage and the building after the retrofit was performed. The TMY weather data for Stuttgart, which was used to validate the simulation model, shows discrepancies to the TDY 2010-2039 in both building stages. For the initial building, the TMY file predicts annual heating energy demand of over 1.5 times the value obtained for the TDY 2010-2039 scenario. Within the retrofit, the TMY heating demand is just over 40 % higher as the TDY 2010-2039 file. Opposed to the other case studies, thermal conductivity as well as airtightness of the thermal envelope have been decreased far less compared to the initial building stage. This behaviour reflects in the heating energy demand, which was decreased by close to 50 %, and thus complies with regulations. However, the decrease is not as drastic as it can be seen in the other cases. EWY periods show about half the annual heating energy demand, whereas ECY show about double the annual heating energy demand towards the respective TDY periods. The heating seasons for the project remaining the same range from mid-October to end-April in the retrofitted building as well as in the initial building stage.

The statistical analysis, displayed in Figure 62, shows similar differences between the TMY file used for validation and the near-term period of the TDY scenario. The frequency of high heating demands, as well as the mean, and upper whisker are far lower in the first TDY period than in the TMY results, this shows for both initial and retrofitted building stage. Further, it can be observed, that the upper whisker range for Triple data sets is gradually falling for initial and retrofit. However, the outliers in the medium-term period are higher, which is due to the high peaks in the ECY scenario. This indicates, that the medium-term period composes an extremely cold period. Whereas the annual heating energy demand could be decreased by about 50 % in the retrofit, the building highest hourly heating load was decreased by just under 40 % compared to the initial building.

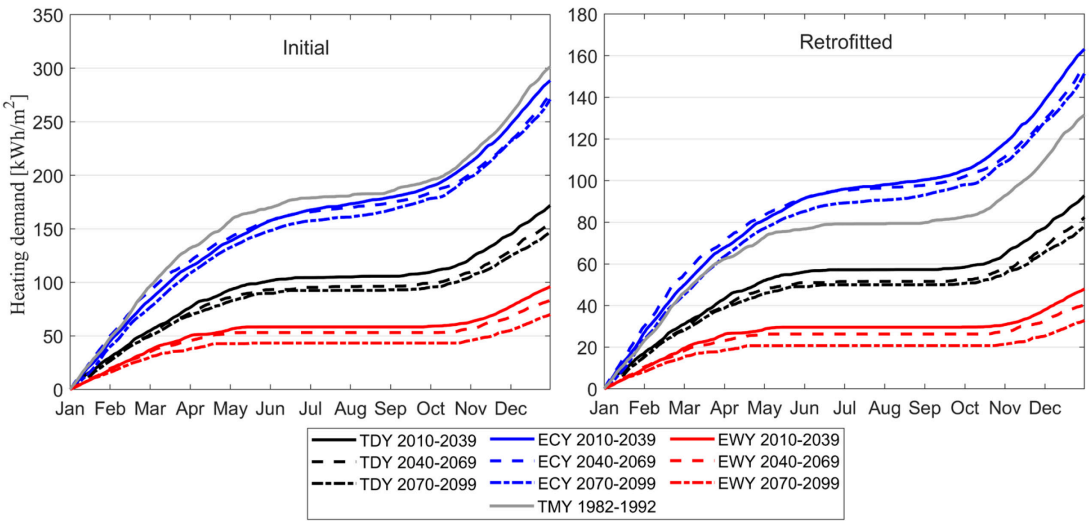

Figure 61: Cumulative heating demand. Initial building on the left, retrofitted building on the right. Scale is adjusted for better visibility.

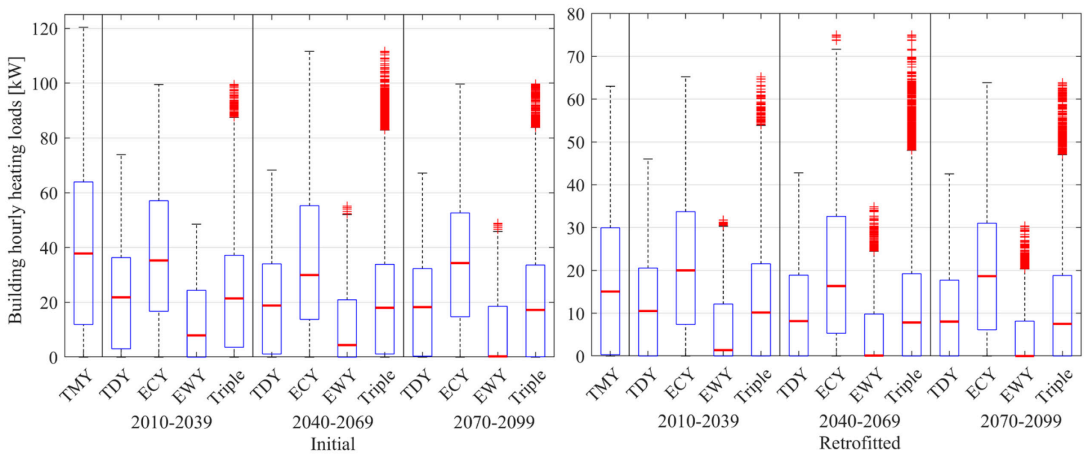

Figure 62: Statistical analysis of hourly building heating energy demands. Scale for initial on the left and retrofitted on the right adjusted for better visibility.

Figure 63 represents the zone heating peak loads as well as the building average heating peak loads normalized by the heated floor area. For initial and retrofitted building stages under the nine employed future climate scenarios. It can be seen, that both the individual zones as well as the building average heating peak loads in Watts per square meter of heated floor area were decreased by about one third by the measures taken in the building retrofit compared to the initial building. As already observed in project 3, described under 5.2.1.2, the TDY periods represent mostly stable heating peak loads, but in the ECY and EWY scenarios the medium-term period yields higher heating peak loads than the near-term as well as long-term.

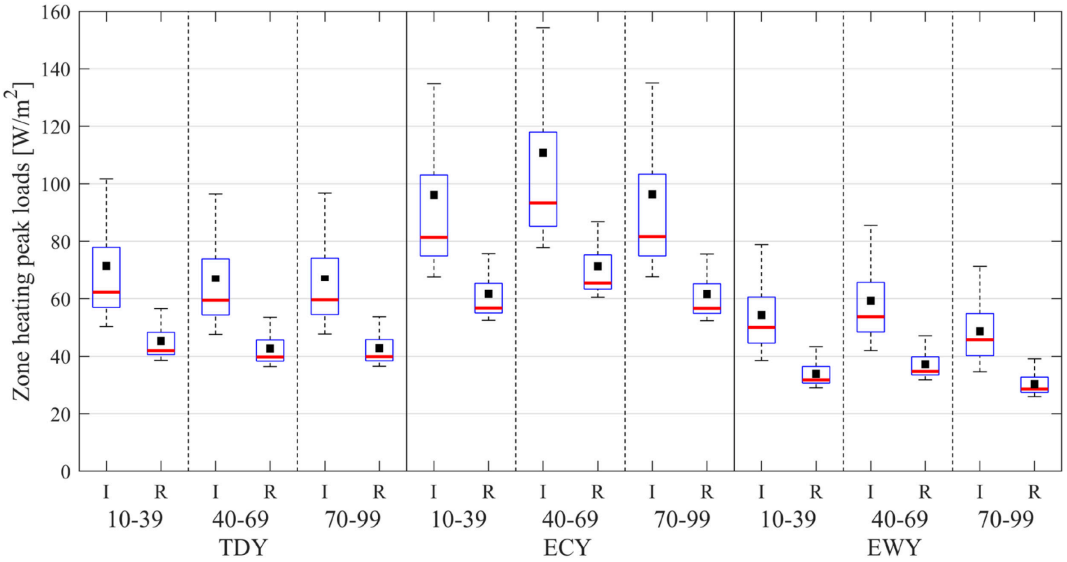

Figure 63: Zone heating peak loads represented through boxplots, building peak load shown as a black square.

5.2.2.3 Moisture Safety

Hygrothermal simulations for wall constructions were carried out with the most wind-driven rain exposed West orientation, as it was proven that it performed worse than the least solar radiation receiving North orientation. Driving rain coefficients in WUFI were set to a tall building with a height between 10 and 20 meters representing the highest part of the wall constructions.

Monitor one representing the interior side of the brick wall in the initial wall construction, shown on the left side of Figure 27, displayed RH values above 75 %, as shown in Section 10.2.4. Mould index for this surface showed a stable integer of six, that corresponds to visually detected mould with full surface coverage. The positive Mould growth rates, visualised in Figure 64, indicate favourable conditions for mould growth within organic materials. The median in triple data sets are gradually increasing in all three investigated time-periods. However, the upper whisker of the short-term period is higher than the whiskers of medium-term and long-term periods, that is partially a result of more occasions with favourable mould growth conditions in the short-term EWY scenario. This effect chain might be caused by a very warm event lasting for a longer time. Masonry walls contain no nutrients and therefore do not support mould growth, unless walls are covered with dust, pollen, mud or other organic materials, that can be a result of poor maintenance as well as climatic conditions and location. The increasing total water content of the exterior wall in a ten-year assessment period indicates dew point conditions resulting in water molecule storage within brick masonry. With time it can result in cracking or spalling of the bricks due to freeze/thaw effect chain. Even though this construction is evaluated to be mould growth free, further investigation is necessary for freeze/thaw action.

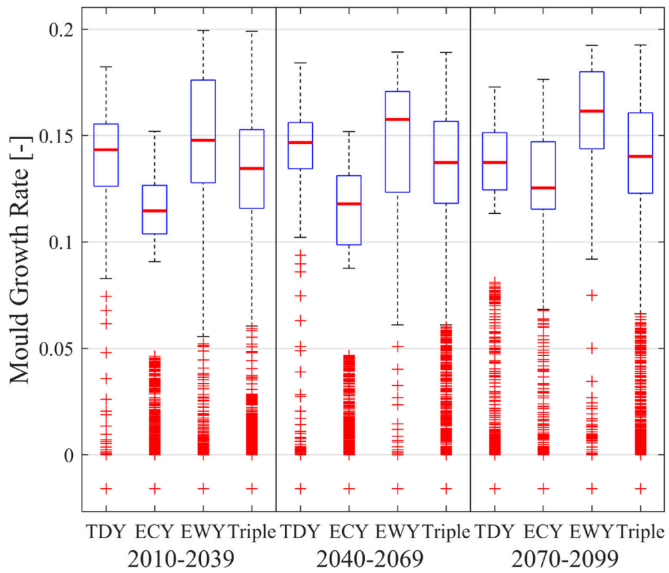

Figure 64: Mould growth rate for interior side of bricks of initial wall construction.

Three monitors, located on the right side of Figure 27, displayed RH values above 75 %, as shown in Section 10.2.4. The interior side of the brick wall maintained a stable mould index of six for the retrofitted construction, whereas mould index at the interior side of initial

mineral plaster layer increased from no growth to visible growth with fluctuations between 50 % and 100 % visually detected coverage, as seen on the left side of Figure 66. This behaviour can be explained by the addition of the interior insulation boards, that caused changes in temperature and RH which are more favourable for mould growth. The assessment of the mould index for the exterior side of insulation board indicated visible surface coverage of up to 100 % for TDY future climate scenarios between 2010 and 2069, as seen on the left side of Figure 67. Whereas the TDY long-term period displayed the least growth varying between moderate growth detected with microscopy to some visually detected growth. Similar, declining trends are noticed for the interior side of mineral plaster. The largest differences between TDY periods are noticed during summertime, what suggest that due to temperature increase in the future climate constructions might exhibit less mould growth during summer periods as a result of decrease in RH. This though, does not in any case signal an overall mould growth decrease, as the increased temperatures during winters will as well create more favourable growth conditions for other seasons of the year. The same observation, regarding the trends of the increasing median and varying upper extreme in a Triple data sets are made for all three investigated time-periods for interior side of bricks of retrofitted wall, as was concluded for the initial one. Examined mould growth rates visible in on the right side of Figure 66, Figure 67 and Figure 65 for the above described layers have indicated favourable conditions for mould growth in all three future climate scenarios within the combined triple data sets. However, as the whole construction does not include any organic materials, there are no nutrients to support mould growth. In addition, the design team chose perlite internal insulation boards, made of natural perlite and silicic acid, which does not support mould growth due to absence of organic materials. Additionally, this material was specifically developed to regulate moisture content in occupied spaces [130]. It was proven that the retrofitted wall construction is not exhibiting any moisture issues while performing, a comprehensive study over four years. As a result, the construction is evaluated to be mould growth safe. Nevertheless, supplementary freeze/thaw investigation for exterior brick façade is needed.

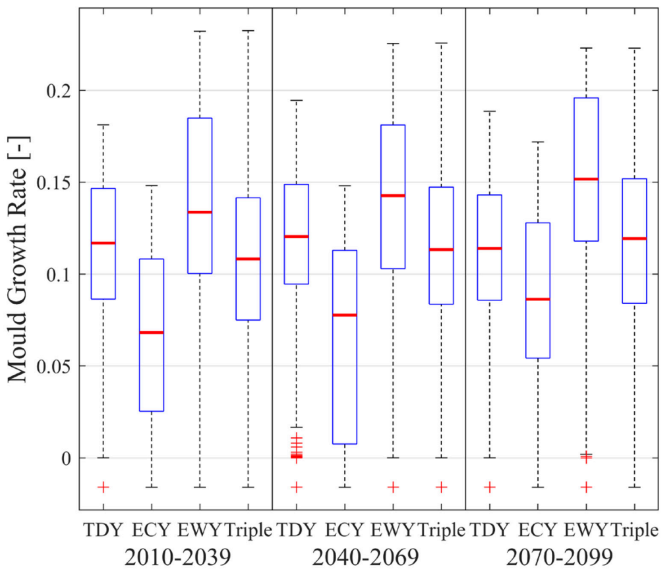

Figure 65: Mould growth rate for interior side of bricks of retrofitted wall construction.

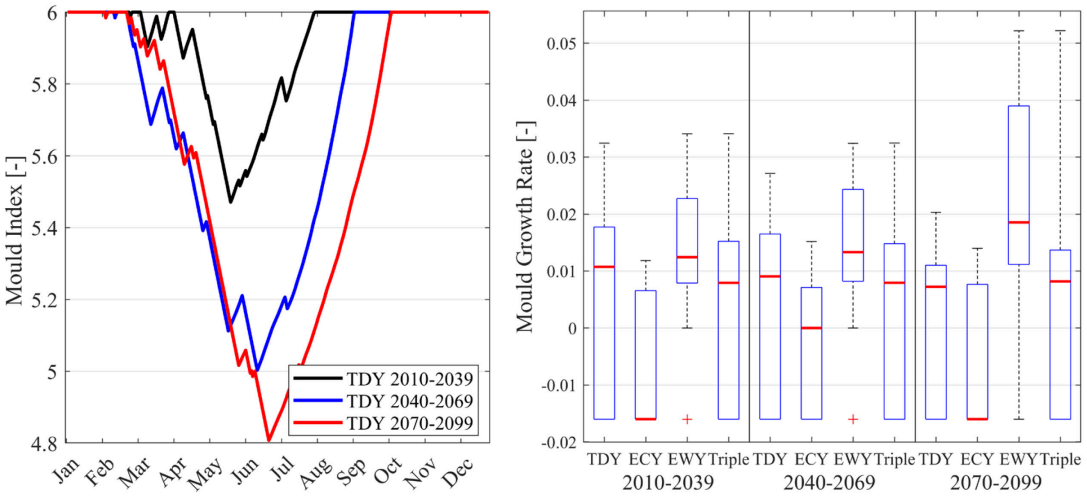

Figure 66: Mould index (on the left) and Mould growth rate (on the right) for interior side of mineral plaster of retrofitted wall construction.

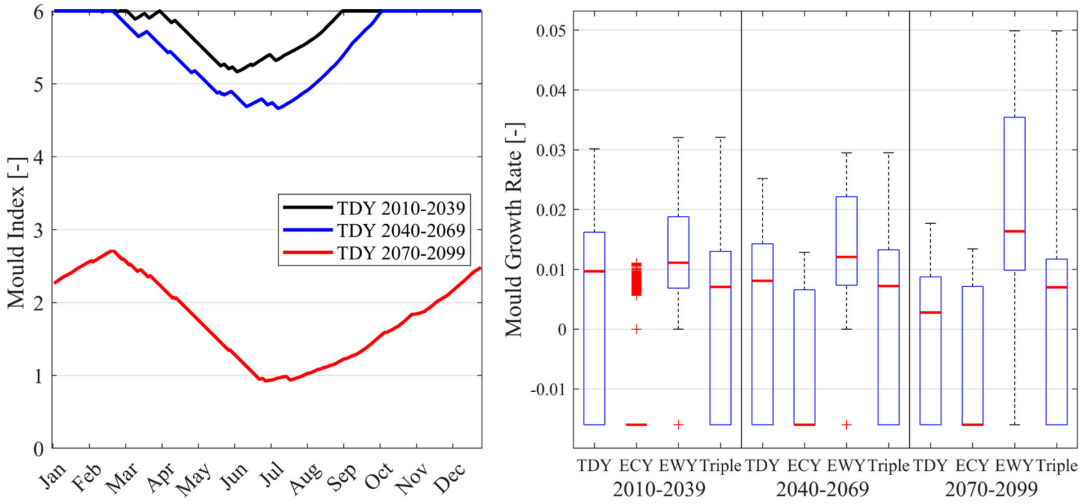

Figure 67: Mould index (on the left) and Mould growth rate (on the right) for exterior side of insulation board of retrofitted wall construction.

5.3 Common Results and Discussion

The comparison and discussion of the results of the individual case studies is composed hereafter. Building studies located in Denmark and Germany showed different behaviour in some factors, other aspects in turn show similarities between all cases. Some results discussed in the following represent threads which should result in a shift towards considering uncertainties of future climate in the industry.

All results discussed in the following are results from case studies which provide indicators for the performance in a broader perspective. A sensibility and uncertainty analysis were not carried out, therefore the retrieved results cannot be reviewed and extrapolated onto other cases in a quantitative manner. However, the results can be used as qualitative indicators and show scalability to a certain extend. The development of a method to analyse the performance of buildings under future climate scenarios is presented and can be employed for future studies. Building Performance Simulations (BPS) were organised, so simulations can be run seamlessly with parametrical change in climate scenarios and time steps. The iterative workflow allows also for data capturing in common file types that can be used for further analysis. As both BPS and hygrothermal simulations were only run with representative weather data over a timeframe of one year, the results retrieved are non-stochastically. Accuracy of the simulations is highly affected by user-defined settings such as the ventilation and infiltration rates as well as other specifications. Beyond that, user-behaviour such as window-opening, operation of shading systems, changes in the surrounding and other factors that are subject to human influence are not accounted for in the simulations. The weather files used are according to the methodology developed by Nik [10] which is under development, uncertainties of the weather files were not analysed in this study. In the present study, an applicable method of the weather files for BPS and hygrothermal simulations of retrofitting projects with the engines EnergyPlus and Wufi was presented. Further uncertainties are given in the utilised model for mould growth, validation of the VTT Viitanen [12] model were carried out throughout various studies and are not objective of this study. Simulations are carried out up to standards that represent the state-of-the-art procedures aiming to account for most certainties and uncertainties, used simplifications and assumptions can however be apart from actual performance.

5.3.1.1 Thermal Comfort

Over all four case studies, it was observed, that the retrofitted buildings show a higher portion of time in discomfort compared to the initial buildings within the TDY periods. The values for ECY decreased for the fourth project (5.2.2.1) from initial building towards retrofit, as the thermal envelope construction was improved, so the likeliness of discomfort in extreme winter-conditions was decreased. Large glazing ratios in the other projects, led to high discomfort in extreme cold scenarios. It was seen, that thermal discomfort in project 1 and 2 was affected by the large glazing areas in combination with the heating setpoint being 21 °C instead of 22 °C as in both German projects. Manually increasing the thermostat setpoint, physical activity to increase the metabolic rate and higher clothing levels are simple measures that occupants can carry out to mitigate discomfort during cold periods.

Thermal comfort is sensed differently by all human beings individually, thus people less sensitive to cold can feel comfortable, while others feel cold.

As extremes are not represented in the TDY files, ECY and EWY predictions should be considered to account for the such. Active or passive cooling system design according to the results in the EWY periods is advised in order to prevent for thermal comfort during weather extremes. All project simulations for thermal comfort were done using a schedule for window opening to diminish overheating and to account for user-behaviour. However, the German cases showed high thermal discomfort due to overheating in the EWY periods, increasing towards the end of the century, which means that the lack of balanced ventilation systems with heat recovery as well as the absence of active cooling systems will yield in thermal discomfort within extreme weather events. Even the fact that shading in form of shutters was present and scheduled to decrease solar heat gains and high glazing surface temperatures influencing the operative temperature, still resulted in overheating and thermal discomfort during hot summer months. For project 3 and 4 it can for the abovementioned reasons be concluded, that the measures employed in the energy-efficient retrofit have negative impacts on the summer thermal comfort as well as during warm weather extremes.

All four case studies indicated an increase in discomfort levels due to overheating from near-term over medium-term to long-term periods. The results obtained for the southern Germany cases show a higher impact of thermal discomfort towards the end of the century, than the Danish climate. This signals, that climate change and future climate have a negative effect on summer thermal comfort. With the raising frequency of weather extremes, thermal discomfort levels based on too hot conditions are getting more significant. The passive measures, such as night flush ventilation, exterior horizontal and vertical shading, as well as high ventilation rates through infiltration were proven to be effective to mitigate thermal discomfort. Active measures, such as balanced ventilation systems with heat recovery and low cooling capacity through air cooling showed no significant effects as the cooling capacity of the supplied air was minimal. Decreasing the supply air temperatures would yield in condensation risks and should therefore be avoided. The increase of supply air to maximise the cooling load, can be effective but has to be within the system boundaries. The implementation of active cooling systems was proven to be essential, when very airtight and highly insulated envelope constructions were realised.

5.3.1.2 Energy Use

All evaluated retrofitting measures are effective and decrease the heating energy demand. The first three case studies with highly insulated thermal envelopes showed higher reductions in energy use than the fourth project with worse conductivity of thermal building envelope elements such as wall, roof, ground floor and windows. The case studies in Denmark both show a highly decreased annual heating energy demand along with a decrease of heating peak loads. Project 3, situated in Germany, shows a very effective decrease of heating energy demand through the measures taken. This is due to a comprehensive retrofit with upgrade of the thermal envelope to a level better than required for newly constructed buildings along with a reduction of infiltration losses. Project 4 which is located in close proximity to project 3, followed a different paradigm, where the conservation of the brick-façade was prioritised over the decrease in heating energy. Yet, peak heating loads and the heating energy demand could both be decreased by one third and

one half respectively. Throughout all cases, a gradually decreasing heating energy demand can be observed for all scenarios (TDY, ECY and EWY) from the near-term periods to the long-term periods. Between 5 % and 25 % decrease from 30-year period to the next one can be seen. This indicates, that climate change has a significant positive effect on decreasing the heating energy demand.

As weather extremes, are likely to occur more often towards the end of the century, a resilient zone heating system design should be done, considering extreme cold scenarios. The likelihood of ECY or EWY scenarios happening in a full year is, however, extremely unlikely. This is due to the fact, that extreme cold and warm predictions composing the worst-case conditions over the 30-year periods which source in 13 different climate predictions with divergent extremes. Time fragments represented in these files, can occur in broad and fine frequencies. Quarterly, annually, each decade, or once a century extreme weather occasions can occur and are represented in the ECY and EWY files. Thus, heating system sizing has to be done to obviate for extreme cold climate occasions by the systems itself or by providing auxiliary systems that cover extreme climate periods. It is, however, key not to over dimension systems to save construction costs. Therefore, higher heating fluid flow rates or temperatures to cover for extreme scenarios should be possible from the system side. Higher fluid temperatures are limited to the system boundaries, which plays a major role in district heating systems. Those have fixed supply temperatures and require return temperatures within the margins specified by the provider. Auxiliary systems that rise the supply fluid temperature to supply more heat than in an optimal design can be a cost-efficient way to provide for extremes. However, employing auxiliary systems results usually in a decrease of system efficiency. When the number of extreme cold or hot events is minimal and occurs only occasionally, the sacrifice in low efficiency during that event is more reasonable, than over-dimensioning the systems in the first place and running on lower efficiency for the longer time periods with non-extreme behaviour.

5.3.1.3 Moisture Safety

During climate analyses in section 3.3.1, it was noticed that all three climate scenarios increase their yearly average temperatures with each term located in the further future. Thus, a significant difference was noticed in the increase of temperatures during winter seasons. Even though there is a very limited likelihood of ECY or EWY scenario occurring during the continuous year, the temperature during winter periods will continue increasing, as these are the predominant trends of all future weather climate files assessed for both Denmark and Germany. This climate change effect is crucial for hygrothermal assessment of constructions, as decay fungi, along with algae and lichen are fostering during temperatures in the rage between 0 °C and 45 °C, mould fungi between 0 °C and 50 °C, and blue-stain fungi between -5 °C and 45 °C. If temperatures during colder periods are not dropping and retaining long enough where mould spores die, it is highly likely that multiply mould growth outbreaks will be noticed on building materials located close to or exposed to the outside. Two general observations for late spring, summer and early autumn were made for mould index in the future climate scenarios. Constructions tended to either display gradually increasing or decreasing trends throughout three investigated time-periods. Specific upwards or downwards change was caused by increasing temperatures due to global warming, where construction layer in question was either drying out or moisture of the neighbouring layer located closer to the outside was moved inwards while resulting in higher moisture for

affected layer. The further the monitor for moisture assessment is located from the exterior climatic conditions, the more complex mould growth assessment becomes in regard to the future climate. In properly designed thermal building envelopes RH tends to increase close to the outside conditions, what exhibits a largest mould growth probability. In order to sustain mould growth in the construction layers mould spores, its food, appropriate temperature and high RH must be kept. The first three requirements are often found in thermal building envelopes and cannot be avoided, especially when taking into account the global temperature increase nowadays and in the future. However, by employing hygrothermal simulations and a proper set of future climate models, RH can and should be minimized at all costs in order to create a truly moisture safe construction that could withstand future climate change.

Common results presented below represent studied trends of extreme weather scenarios. However, it must be noted, that there is extremely small likelihood of extreme weather scenarios (ECY or EWY) to occur continuously over the whole year. Studied initial and retrofitted wall constructions for all four projects have displayed similar tendencies, where EWY resulted in highest mould growth risk and ECY in the lowest mould growth risk. Few exceptions were noticed in the time period between 2010 and 2039 for retrofitted façade and gable wall for Project 1 and Project 2, where ECY climate scenario indicated more favourable conditions for mould growth than EWY, that creates a hypothesis of possible correlation to the presence of ventilated air gap and outside air temperatures. Hygrothermal assessment results of investigated roof constructions with ventilated air gaps for Project 1, Project 2 and Project 3 indicated that ECY future climate scenario will result in higher mould growth risk compared to EWY scenario for plywood and profiled wooden boards used as an underlayer for bituminous roofing paper and exterior side of insulation. Only a newly retrofitted flat roof construction in Project 1 displayed higher risks in EWY in comparison to ECY. Performance of the specific construction appears to vary in respect to future climate scenarios as well as design chosen and therefore, requires in-depth investigation of individual construction in early design stages. Mould growth rate increased with each period further in the future and in some constructions period between 2040 and 2066 appeared to be most favourable for mould growth risk, what might be caused by a single extreme event in the dataset. No clear correlations were found between mould growth and future climate scenarios in three time periods in respect to a single influencing factor. Mould growth was found to be influenced by combination of aspects including driving rain direction, fraction of normal rain, solar radiation, outside air temperature, rotation of the building component, presence or absence of ventilated air gap, material properties and similar.

Some correlations were noticed between presence or absence of ventilated air gap and worse performing rotations. External wall constructions with ventilated air gap performed worse for rotations with least solar radiation, whereas constructions without ventilated airgap performed worse for most wind-driven exposed rotation. In addition, significant increase in RH values was noticed for higher building heights for external wall of tall structures without ventilated gap compared to ones with ventilated air gap. Generally, it was observed that exterior and interior insulation systems without ventilation gap were chosen for two projects in Stuttgart that displayed higher RH values than in retrofitted building facades and gables with ventilation gap chosen for two Danish projects. Exterior plaster and EPS insulation system is a common exterior wall construction, however construction with ventilation gap is assessed to be more suitable to withstand climate change without accumulation of additional

moisture. Furthermore, it must be noted that in order to design a durable construction with ventilated gap inorganic materials must be chosen for exterior cladding as well as distance laths in the ventilated air cavity itself along with a well-designed and executed flashing system that applies for all building constructions. Exterior side of the outermost material layer performed worst in terms of highest RH levels and mould growth risk in all studied cases. Behaviour like this might be explained by most favourable events for mould growth within the whole construction. Even though retrofitted cases included reasonably larger amounts of insulation that was necessary measure for improving thermal comfort and decreasing energy consumption, mould growth risk was decreased significantly, due to improved construction design regarding moisture safety and inorganic material choices. As hygrothermal assessments were performed for the worse rotation in regard to wind-driven rain and the least solar radiation receiving rotation, failing constructions should perform better facing the opposite direction. Lastly, occupant behaviour plays an important role in moisture accumulation in everyday situations and air vapour transfer in construction materials. Tenants must be properly informed about adequate ventilation, differences in vapour permeable and impermeable wall pains, along with consequences of penetrating damp proof membranes by simple nails and similar.

6 Conclusions

If retrofitting measures that are currently applied in practice are resilient to climate change was the main research question of the present work. Moreover, it was examined, what impact the measures and future climate have on the heating energy demand of buildings. How the heating system design is affected by weather extremes and how zone and building systems should be dimensioned was examined. Implications of future climate as well as weather extremes on indoor thermal comfort were assessed additionally. The performance of thermal envelope constructions exposed to outdoor climate undertook a study to show if moisture related issues occur in future climate. In order to address the objectives of the study, four cases located in Denmark and Germany were considered. Thermal comfort, energy use and moisture safety were assessed with numerical modelling by means of building performance simulations. Weather files, containing climate predictions until the end of the 21st century according to the methodology developed by Nik [10], were used in the study. Nik´s approach is to synthesize multiple future climate predictions in 30-year periods, for each period, data sets composing of a typical downscaled year (TDY), an extreme cold year (ECY) and an extreme warm year (EWY) were produced. The methodology employed in this study shows, how the impact assessment of climate change can be implemented in the early design stages of a retrofit project. This is a contribution to the UN Sustainable Development Goal number 13 (Climate Change) [2], which calls for actions to adopt to climate change.

The four case studies carried out in this study, showed, that all the retrofit measures were proven to be effective in order to decrease the space heating energy demand. Also, the sizing of thermal devices to provide space heating were diminished in all cases by improving the conductivity and airtightness properties of the thermal envelope. The effect of climate changed showed towards the end of the century, as heating energy demands were decreasing over all cases. Additionally, peak loads on the zone scale were decreased. More significantly was the decrease in loads for the building system, which indicates that long-lasting cold periods and average winter temperatures gradually decline towards the end of the century. For the German climatic conditions, extreme warm weather conditions yield in thermal discomfort during summertime. Even the use of window ventilation and shutters as shading devices are not effective enough to prevent overheating in extreme warm periods. The future climate scenarios predict an increase in summer thermal discomfort towards the end of the century. Less airtight construction and less drastic thermal insulation measures were proven to result in less thermal discomfort due to less heat being trapped. This, however, yielded in a high heating energy demand and thermal discomfort during extreme warm summer periods could not be prevented. Large window areas with a low heating setpoint, were a cause for thermal discomfort due to too cold operative temperatures. Occupant behaviour, such as movement for high metabolic rates, adequate clothing and higher thermostat setpoints in occupied zones are effective measures to counteract on thermal discomfort due to cold. Projects with large glazing areas, especially towards South, East and West orientations, showed that the biggest portion of space discomfort was due to too high operative temperatures. The two Danish projects were both designed with overhangs, providing shading, but those passive measures were proven to be not effective enough to prevent thermal discomfort in extreme and non-extreme scenarios, even the active ventilation systems providing a certain cooling capacity did not show enough effectivity to decrease summer discomfort. Therefore, the installation of active cooling systems will be

inevitable to maintain pleasant indoor thermal comfort conditions under future climate. The design of active systems like heating, cooling and ventilation systems but also passive design decisions, such as window area, material choice, shading and airtightness has crucial effect to the performance of building retrofits under climate change. System design and the design of passive measures must be done by taking extreme weather scenarios into account. Failure in doing so was proven to have enormous negative effects on thermal comfort. Designing heating systems and terminal devices according to non-extreme weather conditions leads to under-dimensioning of those.

As a result of climate change, global temperatures are predicted to gradually increase in the years to come. Since mould spores foster at specific temperatures, it is very important to consider uncertainties of the future climate. Performing a hygrothermal analysis of constructions designed to withstand future climate change must incorporate extreme events that are predicted to take place more frequently along with becoming more intense. The extreme cold and hot events are, however, highly unlikely to occur in a continuous sequence during the whole year. The study revealed that increasing temperatures in the future will create gradually intensifying positive mould growth events for the years to come. As winters will become warmer, the death of mould spores will not be as frequent.
A total of four requirements, including appropriate temperatures, availability of mould spores and mould food as well as favourable RH must occur for mould growth to take place. Setting temperatures in habitable places so mould dies, does not represent a solution for indoor spaces as most common organisms can grow between -5 °C and 60 °C. Mould spores are present in the outdoor environment and cannot be avoided. Mould food in building constructions, however, can be minimised by using materials without or very limited amounts of organic substances. Mould sensitive materials like untreated wood, sometimes cannot be avoided, in which case a moisture safety assessment must be performed. Additionally, in order to maintain mould growth free façades, exterior surfaces can be treated with fungicides, algaecides and maintained regularly by cleaning. Relative humidity is the only factor that fosters mould growth, which can be decreased during the design stage of thermal envelope constructions. It is crucial to make an appropriate material choice and arrange construction layers adequately.

Observations of similarities and differences for studied buildings before and after renovations, show the necessity of assessing moisture related issues under future climate for the building stock. Initial construction designs showed a majority of positive mould growth events representing failing construction design in future climate. All retrofitting measures demonstrated less vulnerabilities towards mould growth, as they indicated only some to none mould index integers visible only with microscopy. Constructions with ventilated air gaps presented less favourable conditions for mould growth compared to constructions without. Uncertainties in future climate stresses the importance of a proper hygrothermal assessment for constructions designed to maintain their structural stability, as well as to remain moisture safe in a long-term perspective.

7 Further Research

Economic and environmental advantages and disadvantages of the improved retrofitting measures as well as total life-cycle assessment of the retrofitted versus initial buildings should be studied. It is important to understand whether life cycle costs of energy retrofitting measures are feasible over a lifetime of the building compared to total energy savings in heating consumption, while taking into consideration climate change and decline in heating energy demand in possible future scenarios. The effectivity of passive and active measures to mitigate thermal discomfort, has to be further investigated. Adoptability and scalability of the used method to buildings of other functions as well as buildings in other climate zones should be further explored.

8 Summary

Buildings within the European Union are a major contributor to primary energy use and carbon emissions. As there are many existing buildings that were constructed before building regulations restricted transmission losses and primary energy use of new built environment, the building stock is using multiple times the energy of the constructions recently built. Therefore, retrofitting measures to mitigate energy use of existing buildings are widely carried out and supported through legislation. Within the member-states of the European Union, incentives in the form of subsidies or low-interest loans are in place to motivate building owners to pursue retrofitting projects. Climate change and its effects on buildings are often neglected in the design of building retrofits, which leads to high uncertainties of how buildings perform in the next decades.

This study provides a workflow for the assessment of building retrofits under future climate scenarios. As a large share of energy is consumed in dwellings, this type of buildings was investigated. More specifically, a case study of four objects located in Denmark and Germany was carried out. A total of 13 future climate predictions from several institutes with different intensities were synthesized into representative weather files. To account for future climate until the end of the 21st century, three 30-year periods ranging from 2010-2039, 2040-2069 to 2070-2099 were characterised in separate weather files. Climate data sets representing the extreme conditions such as coldest and warmest occasions over the 30-year periods were used as extreme cold year (ECY) and extreme warm year (EWY) files. Those were additionally to the typical downscaled years (TDY), representing the most common conditions. Hence, sets of nine weather files for the locations Aarhus, Copenhagen and Munich were used. Building performance simulations with EnergyPlus and hygrothermal simulations with WUFI were carried out in order to assess indoor thermal comfort, energy use and moisture safety. Performing simulations for the non-retrofitted initial buildings as well as the retrofitted buildings resulted in a total of about 300 simulations. The assessment of indoor thermal comfort was according to the adaptive comfort model (EN 15 251 comfort band category II), analysing if the operative indoor temperature is laying within a comfort band of 6 °C width. The building heating energy demand was compared over the different weather scenarios and time periods, further a statistical analysis of the hourly building heating loads is given. To assess the zone heating device design, zone heating peak loads were compared. Moisture safety was evaluated by means of temperature and relative humidity measurements, as well as mould index and mould growth rate according to the Viitanen VTT model.

The results of the case study showed, that thermal discomfort due to overheating is gradually increasing towards the end of the century. The heating energy demand was effectively lowered in all cases from the initial to the retrofitted building. Over the assessed 30-year periods, a downward trend in heating energy demand was seen, resulting in lower energy use for heating by getting closer to the end of the century. Similar paradigms showed for the building heating peak loads that decreased and lower frequency of high heating peaks were obtained for the future periods. The analysis of moisture safety showed that moisture related issues in future climate scenarios are getting more likely, as temperatures becoming more favourable for mould growth due to global warming.

In order to design building retrofits resilient to future climate uncertainties, this study showed that a thorough assessment has to be carried out. Moreover, constructions have to be designed with great care to withstand higher temperatures and more frequent weather extremes. The study showed, that passive measures to mitigate overheating and summer discomfort are not sufficient during summer and extreme warm events. System design according to TDY scenarios showed an underestimation of cold weather extremes. Therefore, accounting for cold extremes should be considered when dimensioning building and zone systems.

9 References

[1] The United Nations, “About the Sustainable Development Goals,” *United Nations Sustainable Development*. [Online]. Available: https://www.un.org/sustainabledevelopment/sustainable-development-goals/. [Accessed: 13-May-2019].

[2] The United Nations, “Climate Change,” *United Nations Sustainable Development*. [Online]. Available: https://www.un.org/sustainabledevelopment/climate-change-2/. [Accessed: 13-May-2019].

[3] N. Mossin, S. Stilling, T. Chevalier Bøjstrup, V. Grupe Larsen, M. Lotz, and A. Blegvad, *AN ARCHITECTURE GUIDE to the UN 17 Sustainable Development Goals*, 1st ed. Copenhagen: Institute of Architecture and Technology, KADK, 2018.

[4] European Commission, “Energy performance of buildings,” *Energy - European Commission*, 31-Jul-2014. [Online]. Available: https://ec.europa.eu/energy/en/topics/energy-efficiency/energy-performance-of-buildings. [Accessed: 03-Jun-2019].

[5] “Share of European population by country living in flats 2015 | Statistic,” *Statista*. [Online]. Available: https://www.statista.com/statistics/503282/share-of-population-living-in-flats-europe-eu/. [Accessed: 17-May-2019].

[6] The United Nations, “Cities - United Nations Sustainable Development Action 2015,” *United Nations Sustainable Development*. [Online]. Available: https://www.un.org/sustainabledevelopment/cities/. [Accessed: 13-May-2019].

[7] S. Kunkel, E. Kontonasiou, A. Arcipowska, F. Mariottini, and B. Atanasiu, *Indoor air quality, thermal comfort and daylight. Analysis of residential buildings regulations in eight EU member states*. 2015.

[8] S. Kubba, “Chapter 7 - Indoor Environmental Quality,” in *LEED Practices, Certification, and Accreditation Handbook*, S. Kubba, Ed. Boston: Butterworth-Heinemann, 2010, pp. 211–269.

[9] The United Nations, “Health,” *United Nations Sustainable Development*. [Online]. Available: https://www.un.org/sustainabledevelopment/health/. [Accessed: 13-May-2019].

[10] V. M. Nik, “Making energy simulation easier for future climate – Synthesizing typical and extreme weather data sets out of regional climate models (RCMs),” *Appl. Energy*, vol. 177, pp. 204–226, Sep. 2016.

[11] M. Kottek, J. Grieser, C. Beck, B. Rudolf, and F. Rubel, “World Map of the Köppen-Geiger climate classification updated,” *Meteorol. Z.*, vol. 15, no. 3, pp. 259–263, Jul. 2006.

[12] A. Hukka and H. A. Viitanen, “A mathematical model of mould growth on wooden material,” *Wood Sci. Technol.*, vol. 33, no. 6, pp. 475–485, Dec. 1999.

[13] *Climate Change*. Elsevier, 2009.

[14] “Climate change evidence: How do we know?,” *Climate Change: Vital Signs of the Planet*. [Online]. Available: https://climate.nasa.gov/evidence. [Accessed: 04-Feb-2019].

[15] “Data.GISS: GISS Surface Temperature Analysis: Global Maps.” [Online]. Available: https://data.giss.nasa.gov/gistemp/maps/. [Accessed: 04-Feb-2019].

[16] J. Hansen, R. Ruedy, M. Sato, and K. Lo, “GLOBAL SURFACE TEMPERATURE CHANGE,” *Rev. Geophys.*, vol. 48, no. 4, Dec. 2010.

[17] S. VijayaVenkataRaman, S. Iniyan, and R. Goic, "A review of climate change, mitigation and adaptation," *Renew. Sustain. Energy Rev.*, vol. 16, no. 1, pp. 878–897, Jan. 2012.
[18] J. Zalasiewicz and M. Williams, "Chapter 6 - A Geological History of Climate Change," in *Climate Change*, T. M. Letcher, Ed. Amsterdam: Elsevier, 2009, pp. 127–142.
[19] D. J. Wuebbles *et al.*, "Executive summary. Climate Science Special Report: Fourth National Climate Assessment, Volume I," U.S. Global Change Research Program, 2017.
[20] R. P. Tuckett, "Chapter 1 - The Role of Atmospheric Gases in Global Warming," in *Climate Change*, T. M. Letcher, Ed. Amsterdam: Elsevier, 2009, pp. 3–19.
[21] "Clean energy for all Europeans," *Energy - European Commission*, 20-Oct-2017. [Online]. Available: https://ec.europa.eu/energy/en/topics/energy-strategy-and-energy-union/clean-energy-all-europeans. [Accessed: 23-Jan-2019].
[22] "Commission welcomes Council adoption of new rules on Renewable Energy, Energy Efficiency and Governance," *European Commission - European Commission*. [Online]. Available: https://ec.europa.eu/info/news/commission-welcomes-council-adoption-new-rules-renewable-energy-energy-efficiency-and-governance-2018-dec-04_en. [Accessed: 23-Jan-2019].
[23] "Energy Efficiency," *Energy - European Commission*, 22-Sep-2014. [Online]. Available: https://ec.europa.eu/energy/en/topics/energy-efficiency. [Accessed: 23-Jan-2019].
[24] E. Commission, "COMMUNICATION FROM THE COMMISSION TO THE EUROPEAN PARLIAMENT, THE COUNCIL, THE EUROPEAN ECONOMIC AND SOCIAL COMMITTEE AND THE COMMITTEE OF THE REGIONS." European Commission, 16-Feb-2016.
[25] "Heating and cooling," *Energy - European Commission*, 10-Jul-2015. [Online]. Available: https://ec.europa.eu/energy/en/topics/energy-efficiency/heating-and-cooling. [Accessed: 04-Feb-2019].
[26] *Directive 2012/27/EU of the European Parliament and of the Council of 25 October 2012 on energy efficiency, amending Directives 2009/125/EC and 2010/30/EU and repealing Directives 2004/8/EC and 2006/32/EC Text with EEA relevance*, vol. OJ L. 2012.
[27] "Assessment of the progress made by Member States towards the national energy efficiency targets for 2020 and towards the implementation of the Energy Efficiency Directive 2012/27/EU as required by Article 24 (3) of Energy Efficiency Directive 2012/27/EU - Part 1/2." European Commission, 18-Nov-2015.
[28] "Assessment of the progress made by Member States towards the national energy efficiency targets for 2020 and towards the implementation of the Energy Efficiency Directive 2012/27/EU as required by Article 24 (3) of Energy Efficiency Directive 2012/27/EU - Part 2/2." European Commission, 18-Nov-2015.
[29] "Clean energy for all Europeans," *Energy - European Commission*, 20-Oct-2017. [Online]. Available: https://ec.europa.eu/energy/en/topics/energy-strategy-and-energy-union/clean-energy-all-europeans. [Accessed: 06-Feb-2019].
[30] "European Commission - PRESS RELEASES - Press release - Commission welcomes European Parliament adoption of key files of the Clean Energy for All Europeans package." [Online]. Available: http://europa.eu/rapid/press-release_IP-18-6383_en.htm. [Accessed: 05-Feb-2019].

[31] "Energy Strategy and Energy Union," *Energy - European Commission*, 22-Sep-2014. [Online]. Available: https://ec.europa.eu/energy/en/topics/energy-strategy-and-energy-union. [Accessed: 05-Feb-2019].
[32] *Directive (EU) 2018/844 of the European Parliament and of the Council of 30 May 2018 amending Directive 2010/31/EU on the energy performance of buildings and Directive 2012/27/EU on energy efficiency (Text with EEA relevance)*, vol. OJ L. 2018.
[33] "New Energy Performance in Buildings Directive comes into force on 9 July 2018," *European Commission - European Commission*. [Online]. Available: https://ec.europa.eu/info/news/new-energy-performance-buildings-directive-comes-force-9-july-2018-2018-jun-19_en. [Accessed: 05-Feb-2019].
[34] "Buildings," *Energy - European Commission*, 31-Jul-2014. [Online]. Available: https://ec.europa.eu/energy/en/topics/energy-efficiency/buildings. [Accessed: 05-Feb-2019].
[35] C. Degreef, "The 'Clean energy for all Europeans'-Package: Key changes for renewab," *Stibbe*. [Online]. Available: https://www.stibbe.com/en/news/2018/december/the-clean-energy-for-all-europeanspackage-key-changes-for-renewables. [Accessed: 05-Feb-2019].
[36] *Directive (EU) 2018/2002 of the European Parliament and of the Council of 11 December 2018 amending Directive 2012/27/EU on energy efficiency (Text with EEA relevance.)*, vol. OJ L. 2018.
[37] *Directive (EU) 2018/2001 of the European Parliament and of the Council of 11 December 2018 on the promotion of the use of energy from renewable sources (Text with EEA relevance.)*, vol. OJ L. 2018.
[38] *Regulation (EU) 2018/1999 of the European Parliament and of the Council of 11 December 2018 on the Governance of the Energy Union and Climate Action, amending Regulations (EC) No 663/2009 and (EC) No 715/2009 of the European Parliament and of the Council, Directives 94/22/EC, 98/70/EC, 2009/31/EC, 2009/73/EC, 2010/31/EU, 2012/27/EU and 2013/30/EU of the European Parliament and of the Council, Council Directives 2009/119/EC and (EU) 2015/652 and repealing Regulation (EU) No 525/2013 of the European Parliament and of the Council (Text with EEA relevance.)*, vol. 328. 2018.
[39] United Nations, "Paris Agreement." United Nations, 12-Dec-2015.
[40] "Communication from the Commission — Guidelines on State aid for environmental protection and energy 2014-2020," p. 55.
[41] European Commission, "What is Horizon 2020?," *Horizon 2020 - European Commission*, 23-Oct-2013. [Online]. Available: https://ec.europa.eu/programmes/horizon2020/en/what-horizon-2020. [Accessed: 23-Jan-2019].
[42] "Enhancing the capacity of public authorities to plan and implement sustainable energy policies and measures | Programme | CORDIS | European Commission." [Online]. Available: https://cordis.europa.eu/programme/rcn/664701/en. [Accessed: 23-Jan-2019].
[43] "Nationaler Energieeffizienz-Aktionsplan (NEEAP) 2017 der Bundesrepublik Deutschland," p. 44.
[44] S. Birchall, I. Wallis, D. Churcher, S. Pezzutto, R. Fedrizzi, and E. Causse, "Survey on the energy needs and architectural features of the EU building stock," iNSPiRe, Dec. 2014.

[45] G. Erbach, "Understanding energy efficiency," *EPRS Eur. Parliam. Res. Serv.*, vol. PE 568.361, p. 10.
[46] K. Gram-Hanssen, "Existing buildings – Users, renovations and energy policy," *Renew. Energy*, vol. 61, pp. 136–140, Jan. 2014.
[47] A. Uihlein and P. Eder, "Policy options towards an energy efficient residential building stock in the EU-27," *Energy Build.*, vol. 42, no. 6, pp. 791–798, Jun. 2010.
[48] "IPCC, 2013: Climate Change 2013: The Physical Science Basis. Contribution of Working Group I to the Fifth Assessment Report of the Intergovernmental Panel on Climate Change [Stocker, T.F., D. Qin, G.-K. Plattner, M. Tignor, S.K. Allen, J. Boschung, A. Nauels, Y. Xia, V. Bex and P.M. Midgley (eds.)]. Cambridge University Press, Cambridge, United Kingdom and New York, NY, USA, 1535 pp."
[49] M. J. C. Crabbe, "Climate change, global warming and coral reefs: Modelling the effects of temperature," *Comput. Biol. Chem.*, vol. 32, no. 5, pp. 311–314, Oct. 2008.
[50] "United Nations Treaty Collection." [Online]. Available: https://treaties.un.org/pages/ViewDetails.aspx?src=TREATY&mtdsg_no=XXVII-7-d&chapter=27&clang=_en. [Accessed: 15-Feb-2019].
[51] D. Barriopedro, E. M. Fischer, J. Luterbacher, R. M. Trigo, and R. García-Herrera, "The hot summer of 2010: redrawing the temperature record map of Europe," *Science*, vol. 332, no. 6026, pp. 220–224, Apr. 2011.
[52] E. M. Fischer and C. Schär, "Consistent geographical patterns of changes in high-impact European heatwaves," *Nat. Geosci.*, vol. 3, no. 6, pp. 398–403, Jun. 2010.
[53] "Regional Climate Projections," *ResearchGate*. [Online]. Available: https://www.researchgate.net/publication/322237204_Regional_Climate_Projections. [Accessed: 15-Feb-2019].
[54] "Heatwave in northern Europe, summer 2018 – World Weather Attribution." [Online]. Available: https://www.worldweatherattribution.org/attribution-of-the-2018-heat-in-northern-europe/. [Accessed: 15-Feb-2019].
[55] "A hot, dry summer has led to drought in Europe in 2018 | NOAA Climate.gov." [Online]. Available: https://www.climate.gov/news-features/event-tracker/hot-dry-summer-has-led-drought-europe-2018. [Accessed: 15-Feb-2019].
[56] "Wind Driven Rain and Climate Change: A Simple Approach for the Impact Assessment and Uncertainty Analysis," *ResearchGate*. [Online]. Available: https://www.researchgate.net/publication/301684706_Wind_Driven_Rain_and_Climate_Change_A_Simple_Approach_for_the_Impact_Assessment_and_Uncertainty_Analysis. [Accessed: 15-Feb-2019].
[57] M. Herrera *et al.*, "A review of current and future weather data for building simulation," *Build. Serv. Eng. Res. Technol.*, vol. 38, no. 5, pp. 602–627, Sep. 2017.
[58] D. B. Crawley, L. K. Lawrie, B. Systems, and D. Consulting, "RETHINKING THE TMY: IS THE 'TYPICAL' METEOROLOGICAL YEAR BEST FOR BUILDING PERFORMANCE SIMULATION?," p. 8.
[59] V. M. Nik, S. O. Mundt-Petersen, A. S. Kalagasidis, and P. De Wilde, "Future moisture loads for building facades in Sweden: Climate change and wind-driven rain," *Build. Environ.*, vol. 93, pp. 362–375, Nov. 2015.
[60] P. O. of the E. Union, "European collaborative action 'Indoor air quality & its impact on man' : indoor air quality and the use of energy in buildings. Report No 17.," 16-Apr-1996. [Online]. Available: https://publications.europa.eu/en/publication-detail/-/publication/10bf2cfe-4cc3-41f1-a5f5-51b43eea1a16/language-en. [Accessed: 06-Feb-2019].

[61] N. E. Klepeis *et al.*, "The National Human Activity Pattern Survey (NHAPS): a resource for assessing exposure to environmental pollutants," *J. Expo. Sci. Environ. Epidemiol.*, vol. 11, no. 3, pp. 231–252, Jul. 2001.
[62] American Society of Heating, Refrigerating and Air-Conditioning Engineers, *ASHRAE Guideline 10P: Interactions Affecting the Achievement of Acceptable Indoor Environments*. ASHRAE, ATlanta, USA, 2010.
[63] Y. Al horr, M. Arif, M. Katafygiotou, A. Mazroei, A. Kaushik, and E. Elsarrag, "Impact of indoor environmental quality on occupant well-being and comfort: A review of the literature," *Int. J. Sustain. Built Environ.*, vol. 5, no. 1, pp. 1–11, Jun. 2016.
[64] NEPIS | US EPA, "Indoor Air Quality and Student Performance," Aug-2003. [Online]. Available: https://tinyurl.com/y4tq85na. [Accessed: 06-Feb-2019].
[65] D. Junhasavasdikul *et al.*, "Expiratory Flow Limitation During Mechanical Ventilation," *Chest*, vol. 154, no. 4, pp. 948–962, Oct. 2018.
[66] M. G. Apte, W. J. Fisk, and J. M. Daisey, "Associations Between Indoor CO2 Concentrations and Sick Building Syndrome Symptoms in U.S. Office Buildings: An Analysis of the 1994-1996 BASE Study Data," *Indoor Air*, vol. 10, no. 4, pp. 246–257, Dec. 2000.
[67] T. N. Quang, C. He, L. D. Knibbs, R. de Dear, and L. Morawska, "Co-optimisation of indoor environmental quality and energy consumption within urban office buildings," *Energy Build.*, vol. 85, pp. 225–234, Dec. 2014.
[68] "Improving indoor climates in retrofitted buildings." [Online]. Available: https://cordis.europa.eu/project/rcn/100571/brief/en. [Accessed: 23-Jan-2019].
[69] "vejledning-renoveringsstoetteordningen-medio-august-2018.pdf." [Online]. Available: https://www.lbf.dk/media/1554820/vejledning-renoveringsstoetteordningen-medio-august-2018.pdf. [Accessed: 08-Feb-2019].
[70] "Striking a balance between energy efficiency and indoor air quality." [Online]. Available: https://cordis.europa.eu/article/id/400004-indoor-air-quality/en. [Accessed: 23-Jan-2019].
[71] J. Lstiburek, T. Brennan, and N. Yost, "RR-0211: Mold—Causes, Health Effects and Clean-up," *Building Science Corporation*. [Online]. Available: https://buildingscience.com/documents/reports/rr-0211-mold-causes-health-effects-and-clean-up/view. [Accessed: 06-Feb-2019].
[72] N. F. Jensen, "Hygrothermal Analysis of Retrofitted Buildings in the Campus of Lund University," 2016.
[73] R. C. Shoemaker and D. E. House, "A time-series study of sick building syndrome: chronic, biotoxin-associated illness from exposure to water-damaged buildings," *Neurotoxicol. Teratol.*, vol. 27, no. 1, pp. 29–46, Jan. 2005.
[74] P. Johansson, T. Svensson, and A. Ekstrand-Tobin, "Validation of critical moisture conditions for mould growth on building materials," *Build. Environ.*, vol. 62, pp. 201–209, Apr. 2013.
[75] P. O. of the E. Union, "Good practice in energy efficiency : for a sustainable, safer and more competitive Europe.," 24-Apr-2017. [Online]. Available: https://publications.europa.eu/en/publication-detail/-/publication/54b16aac-2982-11e7-ab65-01aa75ed71a1/language-en/format-PDF. [Accessed: 05-Feb-2019].
[76] Robert McNeel and Associates, *Rhinoceros 3D*. USA: Robert McNeel & Associates.
[77] Algorithmic Modelling for Rhino, *Grasshopper*. 2014.
[78] M. Sadeghipour Roudsari and M. Pak, *Ladybug: a parametric environmental plugin for grasshopper to help designers create an environmentally-conscious design.* 2013.

[79] CORE Studio Thornton Tomasetti, *TT Toolbox*. USA: Thornton Tomasetti, 2017.
[80] neoarchaic, *Bumblebee*. 2016.
[81] National Renewable Energy Laboratory (NREL), *OpenStudio*. 2018.
[82] National Renewable Energy Laboratory (NREL), *EnergyPlus*. 2018.
[83] R. Andersen, V. Fabi, J. Toftum, S. P. Corgnati, and B. W. Olesen, "Window opening behaviour modelled from measurements in Danish dwellings," *Build. Environ.*, vol. 69, pp. 101–113, Nov. 2013.
[84] B. Berggren and M. Wall, "Calculation of thermal bridges in (Nordic) building envelopes – Risk of performance failure due to inconsistent use of methodology," *Energy Build.*, vol. 65, pp. 331–339, Oct. 2013.
[85] "THERM | Windows and Daylighting." [Online]. Available: https://windows.lbl.gov/software/therm. [Accessed: 14-Mar-2019].
[86] "HEAT2 – Heat transfer in two dimensions – Buildingphysics.com." .
[87] Fraunhofer IBP, *WUFI Pro*. 2017.
[88] Fraunhofer IBP, *WUFI Material Database Release: 6.2.1 2210.DB.26.0.82.0*. Holzkirchen, Germany, 2017.
[89] S. Mundt Petersen, *Moisture safety in wood frame walls : blind evaluation of the hygrothermal calculation tool WUFI 5.0 using field measurements and determination of factors affecting the moisture safety*. Byggnadsfysik LTH, Lunds Tekniska Högskola, 2013.
[90] S. Mundt Petersen, "Moisture Safety in Wood Frame Buildings - Blind evaluation of the hygrothermal calculation tool WUFI using field measurements and determination of factors affecting the moisture safety," thesis/doccomp, Lund University, 2015.
[91] S. Mundt Petersen and L.-E. Harderup, "Validation of a 1D transient heat and moisture calculation tool under real conditions," presented at the Thermal Performance of the Exterior Envelopes of Whole Buildings XII, 2013.
[92] J. Falk and K. Sandin, "Ventilated rainscreen cladding: Measurements of cavity air velocities, estimation of air change rates and evaluation of driving forces," *Build. Environ.*, vol. 59, pp. 164–176, Jan. 2013.
[93] S. M. Petersen and L.-E. Harderup, "Comparison of measured and calculated temperature and relative humidity with varied and constant air flow in the facade air gap," in *Proceedings of the 9th Nordic Symposium on Building Physics - NSB 2011*, 2011, pp. 147–154.
[94] The MathWorks, Inc., *MATLAB R2018b*. USA, 2018.
[95] H. Viitanen, M. Krus, T. Ojanen, V. Eitner, and D. Zirkelbach, "Mold Risk Classification Based on Comparative Evaluation of Two Established Growth Models," *Energy Procedia*, vol. 78, pp. 1425–1430, Nov. 2015.
[96] V. Nik, "Climate Simulation Of An Attic Using Future Weather Data Sets - Statistical Methods For Data Processing And Analysis," 2010.
[97] S. Wilcox and W. Marion, "Users Manual for TMY3 Data Sets," *Tech. Rep.*, p. 58, 2008.
[98] H. Lund, "The design reference year user's manual.," *Lyngby Therm. Insul. Lab. Tech. Univ. Den.*, Feb. 1995.
[99] T. Kershaw, M. Eames, and D. Coley, "Comparison of multi-year and reference year building simulations," *Build. Serv. Eng. Res. Technol.*, vol. 31, no. 4, pp. 357–369, Nov. 2010.
[100] "Sustainable buildings - Green growth and circular economy - Environment - European Commission." [Online]. Available: http://ec.europa.eu/environment/eussd/buildings.htm. [Accessed: 11-May-2019].

[101] V. M. Nik, "Hygrothermal Simulations of Buildings Concerning Uncertainties of the Future Climate," Chalmers University of Technology, 2012.
[102] V. M. Nik and A. Sasic Kalagasidis, "Impact study of the climate change on the energy performance of the building stock in Stockholm considering four climate uncertainties," *Build. Environ.*, vol. 60, pp. 291–304, Feb. 2013.
[103] V. M. Nik, "Application of typical and extreme weather data sets in the hygrothermal simulation of building components for future climate – A case study for a wooden frame wall," *Energy Build.*, vol. 154, pp. 30–45, Nov. 2017.
[104] A. Moazami, V. M. Nik, S. Carlucci, and S. Geving, "Impacts of future weather data typology on building energy performance – Investigating long-term patterns of climate change and extreme weather conditions," *Appl. Energy*, vol. 238, pp. 696–720, Mar. 2019.
[105] "Weather Data by Location | EnergyPlus." [Online]. Available: https://www.energyplus.net/weather-location/europe_wmo_region_6/DEU//DEU_Stuttgart.107380_IWEC. [Accessed: 13-May-2019].
[106] J. Engelmark, *Dansk byggeskik: etagebyggeriet gennem 150 år*, 2. udg. Herlev: Dansk Byggeskik.dk, 2014.
[107] "Bygningsreglement 1961 for Købstæderne og Landet," 01-Mar-1961. [Online]. Available: http://w2l.dk/file/502082/br_enogtres.pdf.
[108] P. O. of the E. Union, "CELEX1, Commission Regulation (EU) No 1253/2014 of 7 July 2014 implementing Directive 2009/125/EC of the European Parliament and of the Council with regard to ecodesign requirements for ventilation units Text with EEA relevance," 07-Jul-2014. [Online]. Available: https://publications.europa.eu/da/publication-detail/-/publication/a65efd48-747b-11e4-b593-01aa75ed71a1/language-en. [Accessed: 13-Feb-2019].
[109] "Bygningsreglement 2018 - BR18." [Online]. Available: http://bygningsreglementet.dk/Historisk/BR18_Version1/Tekniske-bestemmelser/11/BRV/Energiforbrug/Kap-1_7. [Accessed: 13-Feb-2019].
[110] "Tidligere Bygningsreglementer." [Online]. Available: https://historisk.bygningsreglementet.dk/tidligerebygreg/0/40. [Accessed: 13-Feb-2019].
[111] Danmark and Boligministeriet, *Bygningsreglement: udfærdiget i medfør af §5 i byggeloven af 26. juni 1975*. Kbh.: Boligministeriet : [Eksp. DBK, 1977.
[112] "Bygningsreglement 1995 - BR95," 01-Apr-1995. [Online]. Available: https://danskbyggeskik.dk/Publikationer/1397%20-%20BR%2095,%20det%20nye%20bygningsreglement.pdf.
[113] "Energi 2000 | Gyldendal - Den Store Danske." [Online]. Available: http://denstoredanske.dk/Samfund,_jura_og_politik/Økonomi/Energi-,_miljø-_og_forureningsøkonomi/Energi_2000. [Accessed: 13-Feb-2019].
[114] "En visionær dansk energipolitik 2025 - Transportministeriet." [Online]. Available: https://www.trm.dk/da/DA/Publikationer/2007/En visionaer dansk energipolitik. [Accessed: 13-Feb-2019].
[115] "En visionær dansk energipolitik." [Online]. Available: https://docplayer.dk/362099-En-visionaer-dansk-energipolitik.html. [Accessed: 13-Feb-2019].
[116] "Bygningsreglement 2008 - BR08." [Online]. Available: https://historisk.bygningsreglementet.dk/br07_02/0/42. [Accessed: 13-Feb-2019].
[117] "Bygningsreglement 2010 - BR10." [Online]. Available: https://historisk.bygningsreglementet.dk/br10_05/0/42. [Accessed: 13-Feb-2019].

[118] "Bygningsreglementet 2015 - BR15." [Online]. Available: https://historisk.bygningsreglementet.dk/br15_03/0/42. [Accessed: 13-Feb-2019].
[119] W. Eichhammer *et al.*, "Study on the Energy Savings Potentials in the EU Member States, Candidate Countries and EEA Countries - Wuppertal Institut für Klima, Umwelt, Energie." [Online]. Available: https://wupperinst.org/en/p/wi/p/s/pd/228/. [Accessed: 11-Feb-2019].
[120] J. Weiss, E. Dunkelberg, and T. Vogelpohl, "Improving policy instruments to better tap into homeowner refurbishment potential: Lessons learned from a case study in Germany," *Energy Policy*, vol. 44, pp. 406–415, May 2012.
[121] "EnEV 2014 Energieeinsparverordnung in Html-Format." [Online]. Available: http://www.enev-online.com/enev_2014_volltext/index.htm. [Accessed: 12-Feb-2019].
[122] Bundesministerium für Umwelt, Naturschutz und nukleare Sicherheit, "An Overview of German Climate Policy." [Online]. Available: https://www.bmu.de/en/topics/climate-energy/climate/national-climate-policy/. [Accessed: 11-Feb-2019].
[123] R. Galvin and M. Sunikka-Blank, "Economic viability in thermal retrofit policies: Learning from ten years of experience in Germany," *Energy Policy*, vol. 54, pp. 343–351, Mar. 2013.
[124] F. Meijer, L. Itard, and M. Sunikka-Blank, "Comparing European residential building stocks: performance, renovation and policy opportunities," *Build. Res. Inf.*, vol. 37, no. 5–6, pp. 533–551, Nov. 2009.
[125] R. Galvin, "Thermal upgrades of existing homes in Germany: The building code, subsidies, and economic efficiency," *Energy Build.*, vol. 42, no. 6, pp. 834–844, Jun. 2010.
[126] R. Galvin, "German Federal policy on thermal renovation of existing homes: A policy evaluation," *Sustain. Cities Soc.*, vol. 4, pp. 58–66, Oct. 2012.
[127] Institut für Wärme und Oeltechnik e.V. (IWO), "Energetische Gebäudesanierung in Deutschland," *FG Immobilienwirtschaft und Baubetriebswirtschaftslehre – Technische Universität Darmstadt*. [Online]. Available: https://www.real-estate.bwl.tu-darmstadt.de/praxistransfer/praxisorientierte_forschungsergebnisse/Energetische_Gebudesanierung_in_D.de.jsp. [Accessed: 12-Feb-2019].
[128] "Die Siedlung Ostheim | Ein einzigartiges Quartier in Stuttgart." [Online]. Available: https://www.die-siedlung-ostheim.de/. [Accessed: 10-May-2019].
[129] T. Salthammer, S. Mentese, and R. Marutzky, "Formaldehyde in the Indoor Environment," *Chem. Rev.*, vol. 110, no. 4, pp. 2536–2572, Apr. 2010.
[130] Sto Ltd, "Data Sheet - Sto-Perlite Internal Insulation," 08-May-2019. [Online]. Available: https://www.sto.com/webdocs/0000/SDB/N_00099-001_0001_EN_03_00.PDF. [Accessed: 08-May-2019].
[131] T. Ojanen, R. Peuhkuri, and H. Viitanen, "Classification of material sensitivity – New approach for mould growth modeling, in: Paper at the Ninth Nordic Symposium on Building Physics—NSB2011," *Ojanen Al*, p. 28, 2011.
[132] F. Fedorik, M. Malaska, R. Hannila, and A. Haapala, "Improving the thermal performance of concrete-sandwich envelopes in relation to the moisture behaviour of building structures in boreal conditions," *Energy Build.*, vol. 107, pp. 226–233, Nov. 2015.
[133] EPS Molders Association, "EPS Insulation Mold Resistance." EPS Industry Alliance, 2004.
[134] R. S Muralitharan and R. Vasudevan, "Basic Properties of Pumice Aggregate," *Int. J. Earth Sci. Eng.*, vol. 08, pp. 256–258, Sep. 2015.

10 Appendix

10.1 Validation of thermal bridge calculations

In order to validate the thermal bridge calculations in THERM, a similar workflow in HEAT2 was created. In the following paragraph, the results of the validation are shown by means of one example. The difference in overall U-value of the exterior wall between THERM and HEAT2 tools was estimated to be insignificant for both cases as presented further in this section.

A section of an exterior wall was modelled in a plan view using HEAT 2 in two variations; with and without wooden studs and distance battens as seen in Figure 68.

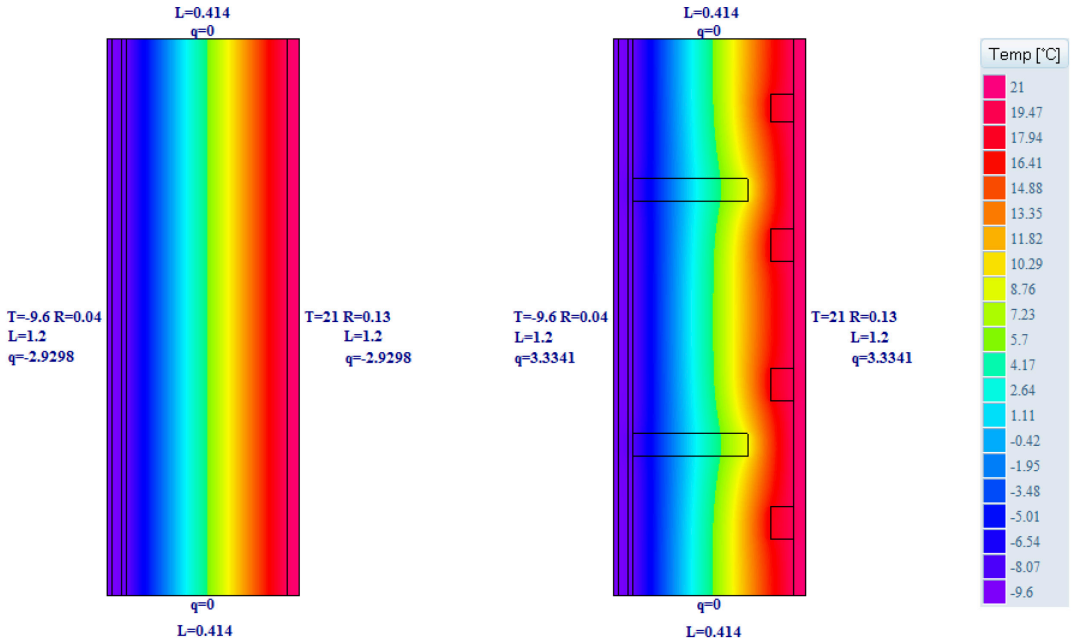

Figure 68: Retrofitted exterior wall seen from top (Project A). On the left: 'ideal' wall without penetrations. On the right: wall with executed wooden elements. Temperature distribution obtained in HEAT2.

The heat flux from the ideal wall was simulated to be 2.9298 W/m^2 in a steady state calculation executed in HEAT2. The temperature difference of 30.6 K between the inside and the outside was used, respectively the U-value of the ideal wall seen on the left side in Figure 68 was calculated to be 0.0957 W/m^2·K.

Heat flows received from the ideal wall and the one with wooden parts were used in Equation 1 to estimate the Ψ-value.

$$\Psi = \frac{(q_{\text{stud wall}} - q_{\text{ideal}}) \cdot L}{\Delta T} = \frac{\left(3.3341 \frac{W}{m^2} - 2.9298 \frac{W}{m^2}\right) \cdot 1.2\ m}{30.6\ K} = 0.0159 \frac{W}{m \cdot K} \quad (1)$$

The increase of U-value due to incorporation of wooden elements was integrated using Equation 2. It resulted in approximately 14 % increase in transmission losses in the exterior wall.

$$U_{new} = U_{ideal} + \frac{\Psi}{L} = 0.0957 \frac{W}{m^2 \cdot K} + \frac{0.0159 \frac{W}{m \cdot K}}{1.2\ m} = 0.1090 \frac{W}{m^2 \cdot K} \quad (2)$$

The process of executing an overall U-value simulation using THERM through Honeybee was started by modelling the 2D wall perimeter including precise layer thicknesses and their layout, as seen in Figure 69.

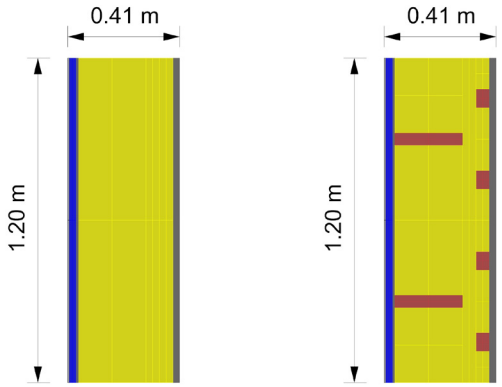

Figure 69: Retrofitted exterior wall modelled in Rhinoceros. On the left: 'ideal' wall without penetrations. On the right: wall with wooden studs.

Afterwards, materials used in the wall construction were written to EP library in accordance to the material specifications used for energy simulations. Afterwards, the same materials were referenced to the geometry and connected to a joint polygon, as seen in Figure 70.

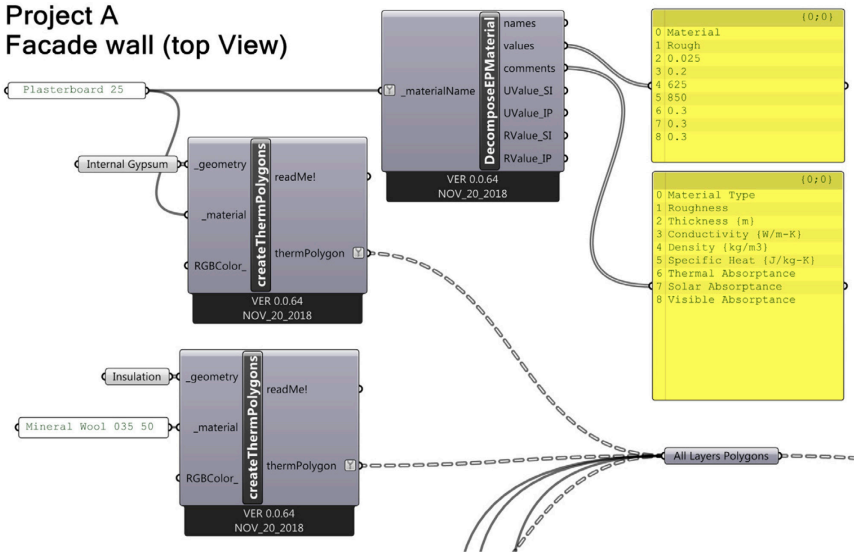

Figure 70: Surfaces to polygons

The polylines indicating boundary conditions were drawn in Rhinoceros and linked to grasshopper script as seen in Figure 71.

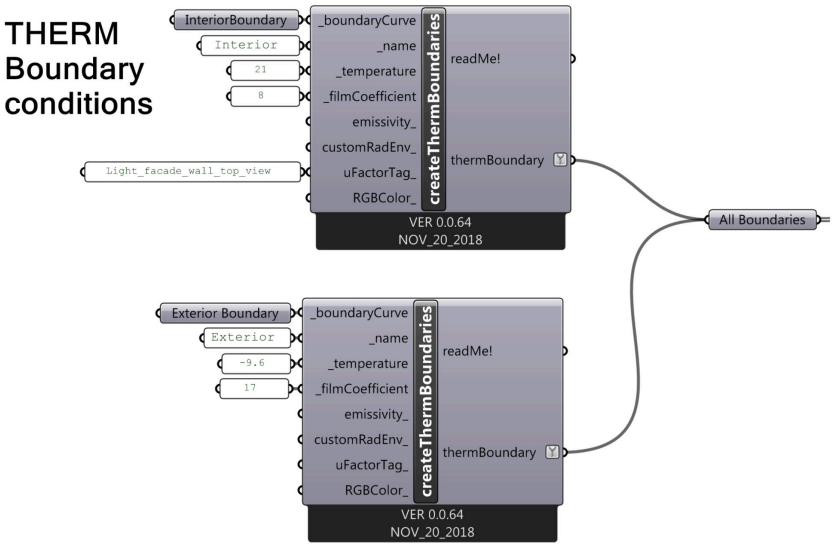

Figure 71: Interior and exterior boundaries

Out of surfaces and boundaries, a THERM file was written (Figure 72) and results of fluctuations in thermal heat loss were visualized as displayed in Figure 73.

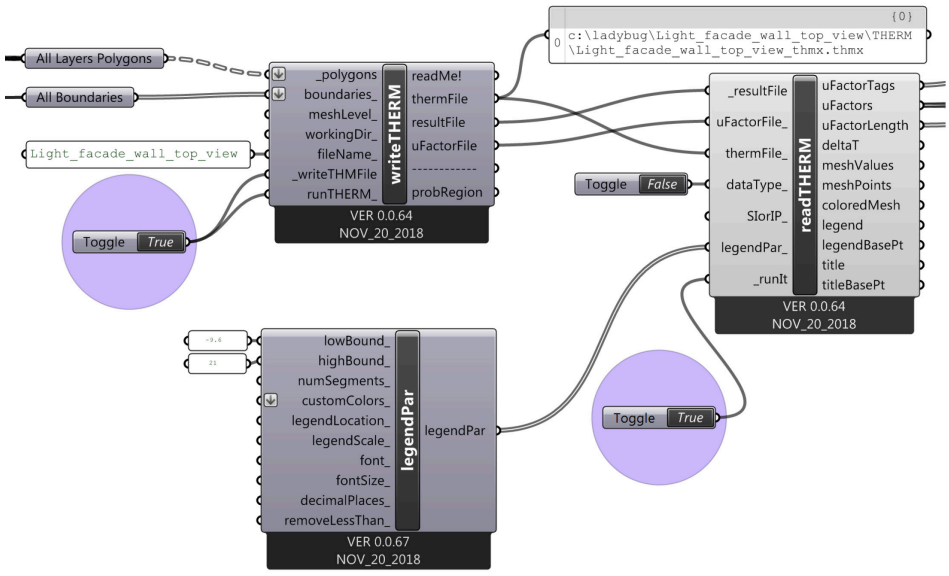

Figure 72: THERM simulation execution in Grasshopper script3

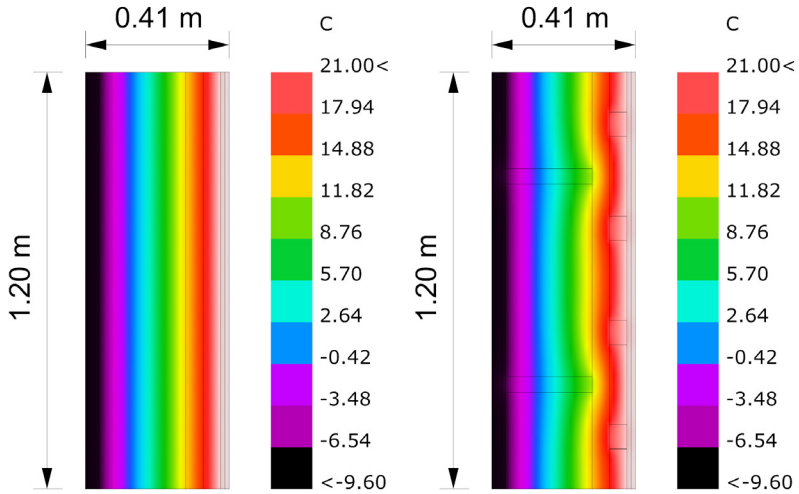

Figure 73: Heat flows through exterior wall. Visualisation created from Honeybee THERM results.

Simulation results executed with THERM were read and analysed carefully, as heat flux in 2D view should occur solely in one direction. In this example, heat flux occurred to the normal of the Y-axis, with an equivalent length of 1.2 m, obtained from the outputs visualised in Figure 74.

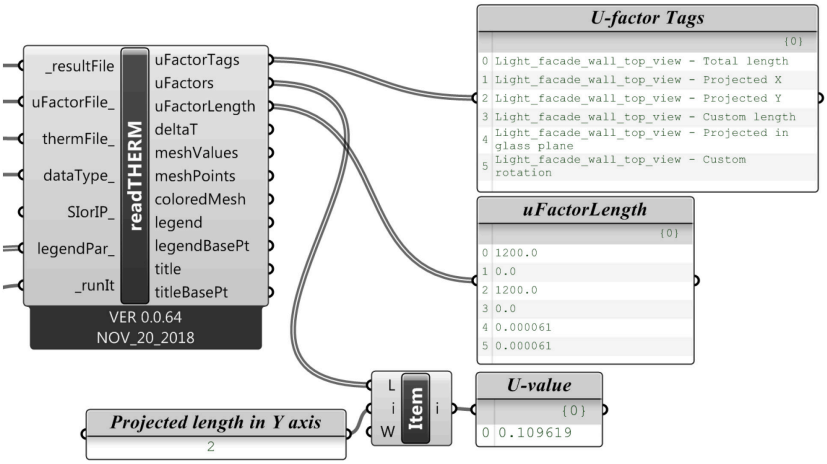

Figure 74: Heat flow projections and overall U-value result.

In addition to viewing results of the overall U-values on the Grasshopper canvas, the native THERM interface, seen in Figure 75, was used for error spotting and supplementary validation of the results.

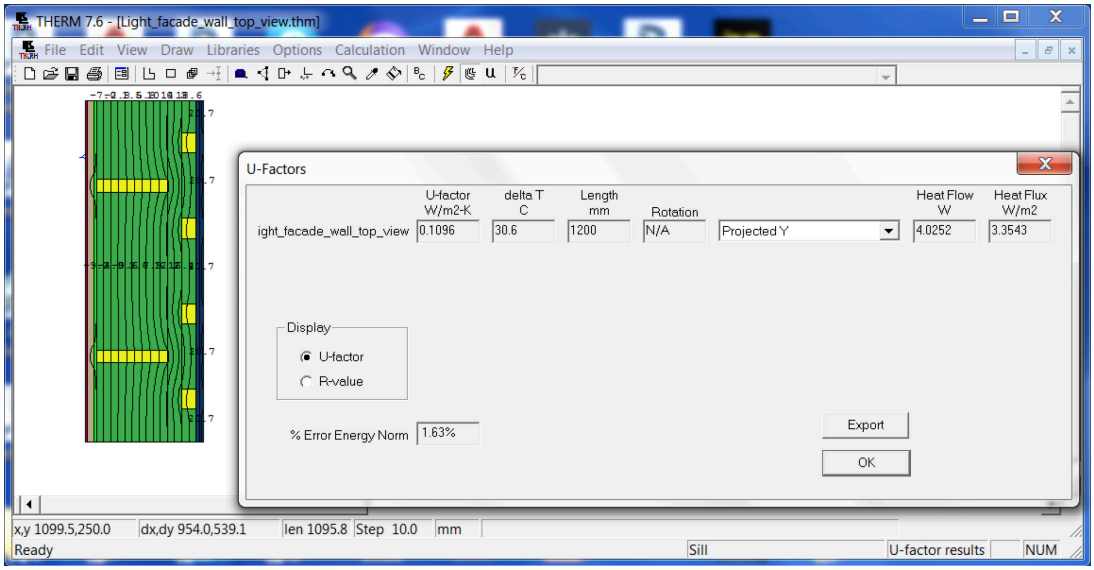

Figure 75: Overall U-value and heat flux of exterior wall with wooden elements in THERM interface.

Overall U-values obtained by THERM for ideal wall and with wooden studs can be seen in Table 33. The displayed results yield a difference of less than 1 % comparing the values from HEAT2 and THERM simulations. The results of the shown example have been proven by modelling, simulating and comparing the section view of the same wall construction, with and without wooden penetrations in the insulation layer, as well as the intermediate floor construction in HEAT2 and THERM through Honeybee.

Table 33: Overview of exterior wall simulation results.

Construction	Simulation tool	U-value $\left[\frac{W}{m^2 K}\right]$
Ideal wall	HEAT2	0.0957
	THERM	0.0966
Wall with wooden elements	HEAT2	0.1090
	THERM	0.1096

10.2 RH for multiple construction layers

10.2.1 Project 1

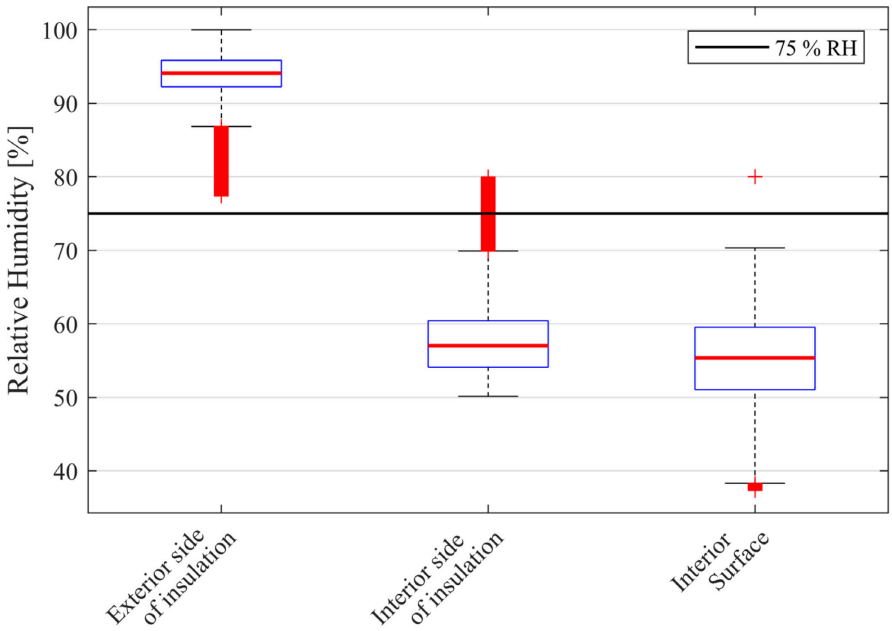

Figure 76: Boxplots for RH of assessed monitors within initial walls. Combined values between 2010-2039, 2040-2069, 2070-2099 time periods and TDY, ECY and EWY climate data sets.

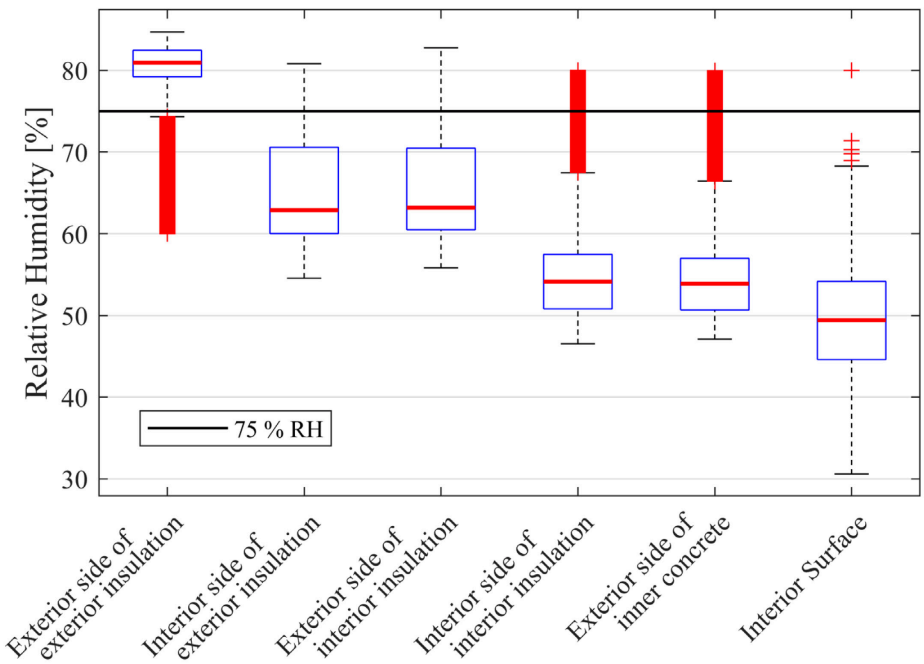

Figure 77: Boxplots for RH of assessed monitors within retrofitted gable. Combined values between 2010-2039, 2040-2069, 2070-2099 time periods and TDY, ECY and EWY climate data sets.

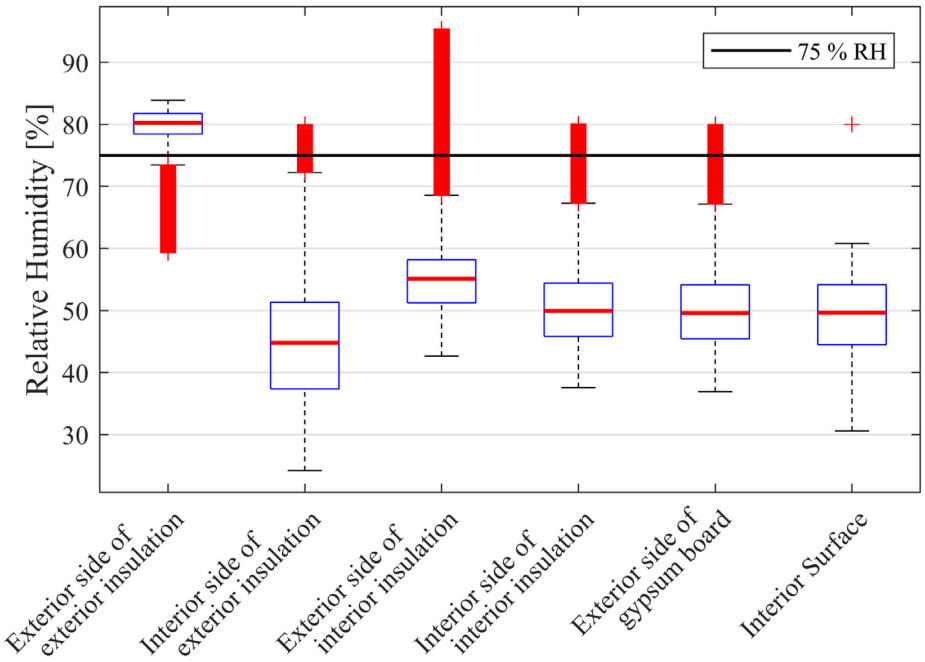

Figure 78: Boxplots for RH of assessed monitors within retrofitted façade. Combined values between 2010-2039, 2040-2069, 2070-2099 time periods and TDY, ECY and EWY climate data sets.

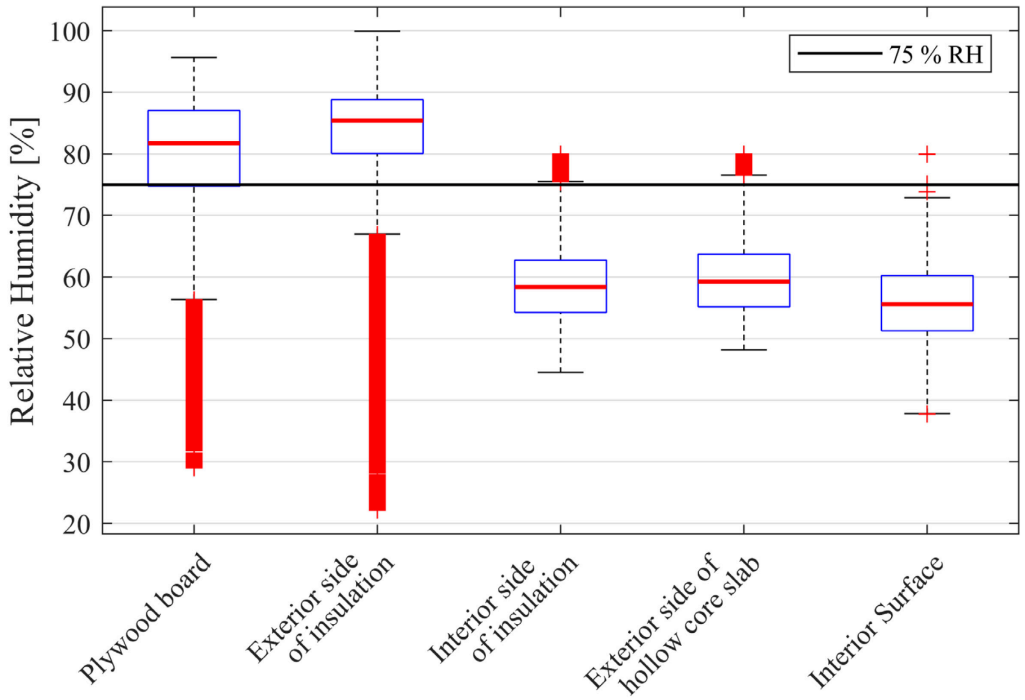

Figure 79: Boxplots for RH of assessed monitors within initial roof construction. Combined values between 2010-2039, 2040-2069, 2070-2099 time periods and TDY, ECY and EWY climate data sets.

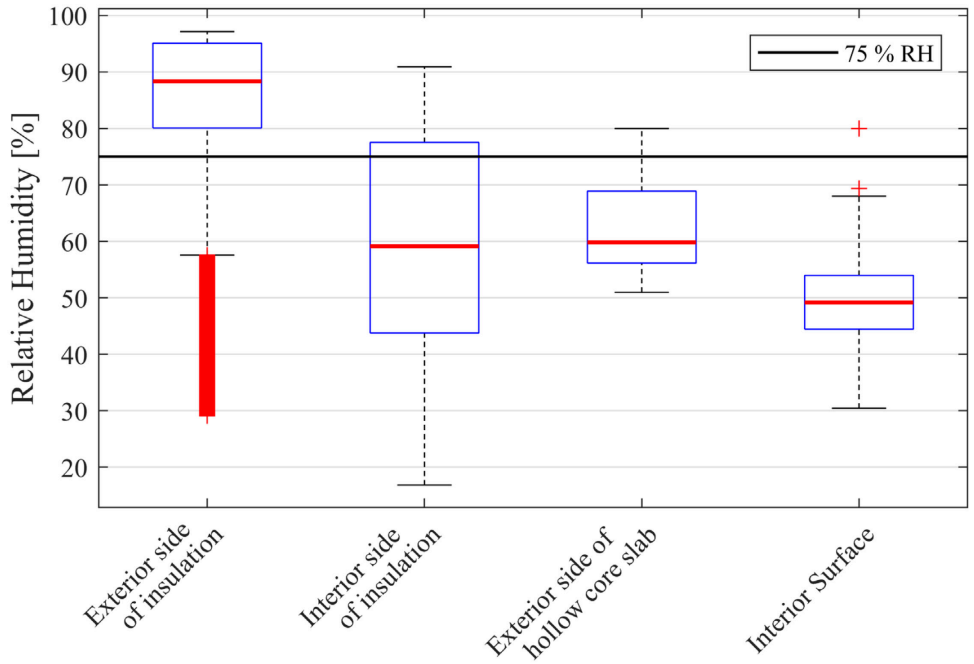

Figure 80: Boxplots for RH of assessed monitors within retrofitted roof construction. Combined values between 2010-2039, 2040-2069, 2070-2099 time periods and TDY, ECY and EWY climate data sets.

10.2.2 Project 2

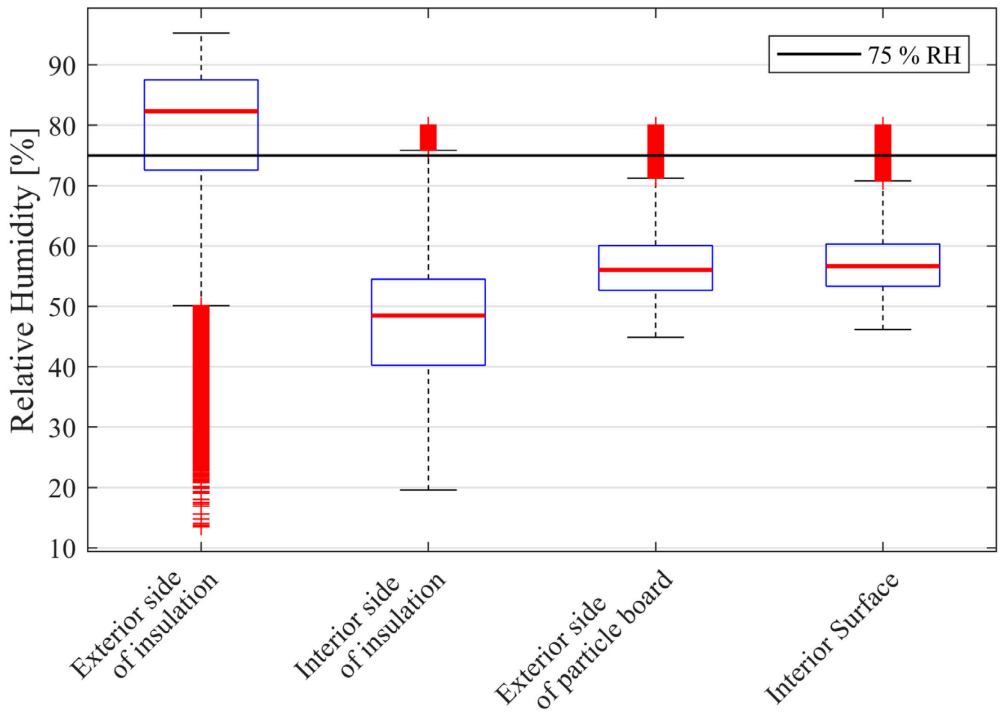

Figure 81: Boxplots for RH of assessed monitors within initial façade. Combined values between 2010-2039, 2040-2069, 2070-2099 time periods and TDY, ECY and EWY climate data sets.

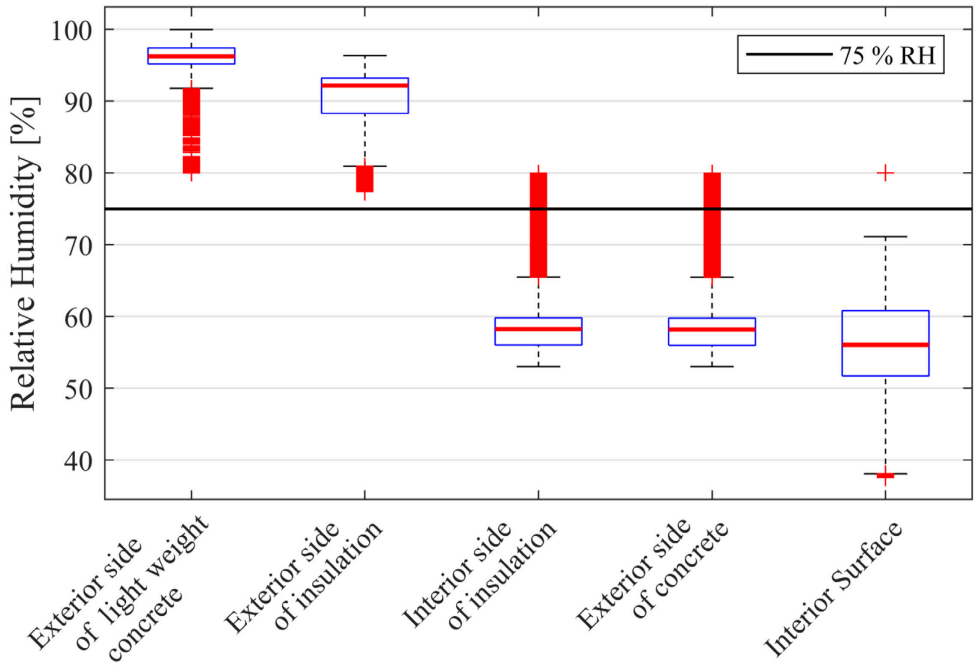

Figure 82: Boxplots for RH of assessed monitors within initial gable wall. Combined values between 2010-2039, 2040-2069, 2070-2099 time periods and TDY, ECY and EWY climate data sets.

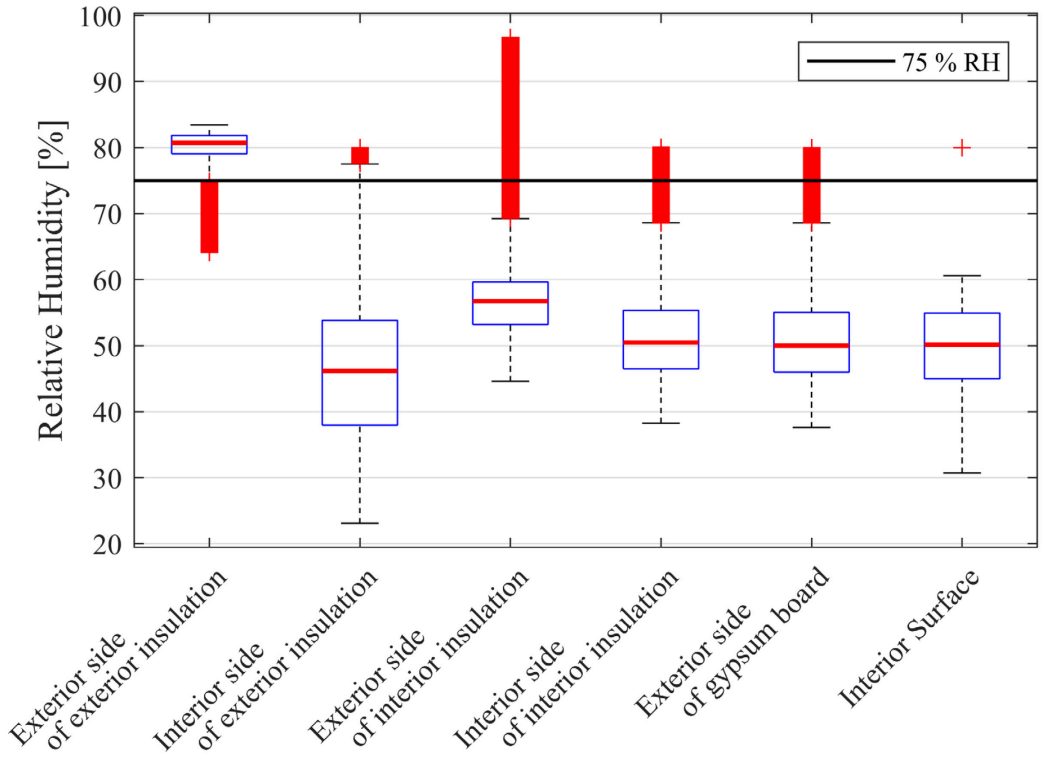

Figure 83: Boxplots for RH of assessed monitors within retrofitted façade. Combined values between 2010-2039, 2040-2069, 2070-2099 time periods and TDY, ECY and EWY climate data sets.

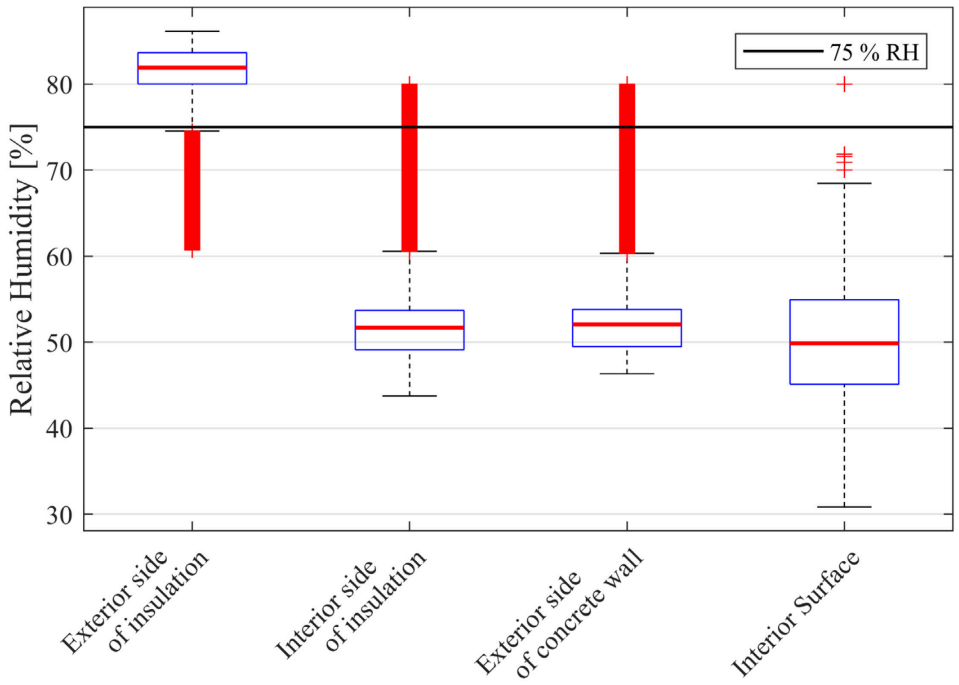

Figure 84: Boxplots for RH of assessed monitors within retrofitted gable walls. Combined values between 2010-2039, 2040-2069, 2070-2099 time periods and TDY, ECY and EWY climate data sets.

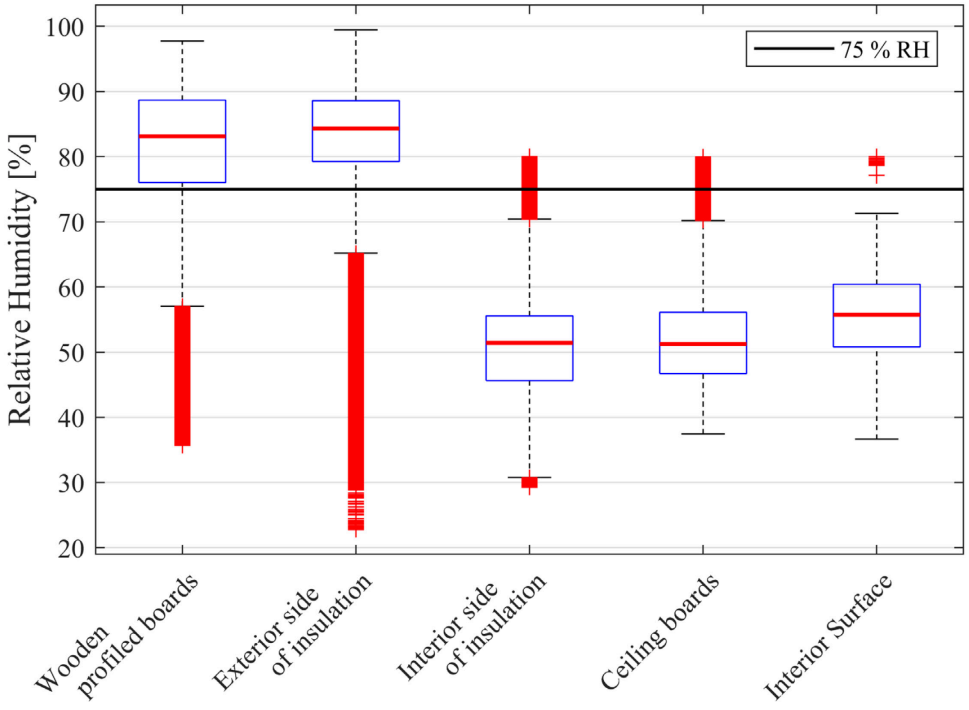

Figure 85: Boxplots for RH of assessed monitors within retrofitted roof. Combined values between 2010-2039, 2040-2069, 2070-2099 time periods and TDY, ECY and EWY climate data sets.

10.2.3 Project 3

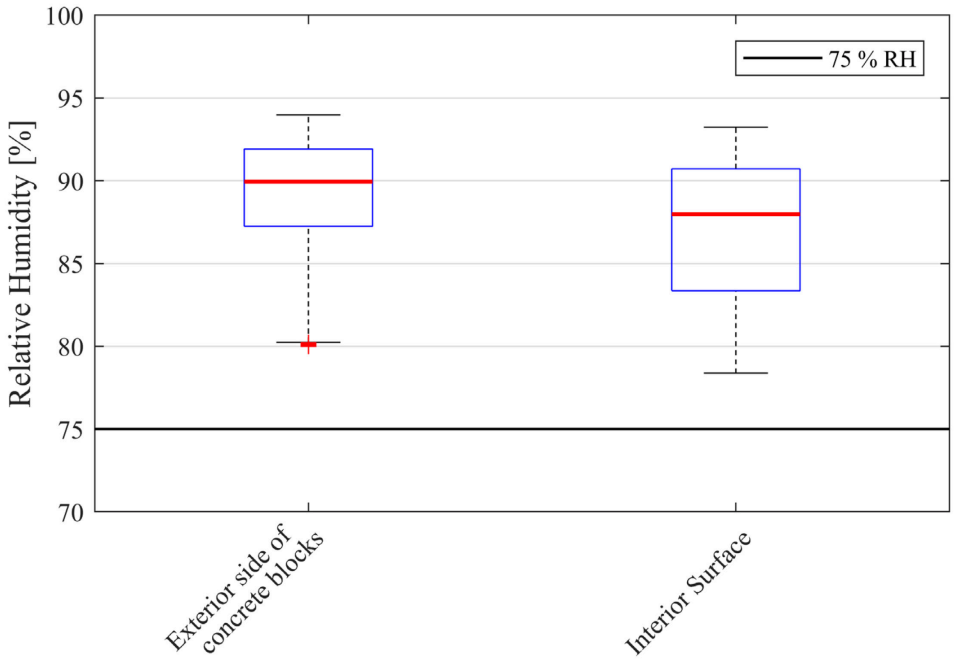

Figure 86: Boxplots for RH of assessed monitors within initial walls. Combined values between 2010-2039, 2040-2069, 2070-2099 time periods and TDY, ECY and EWY climate data sets.

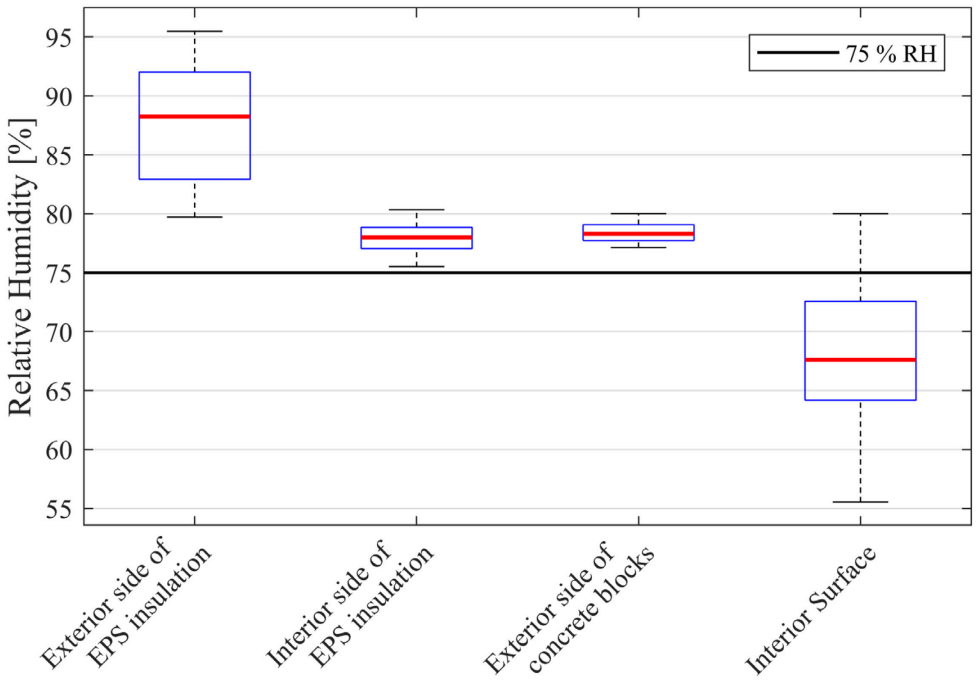

Figure 87: Boxplots for RH of assessed monitors within retrofitted wall. Combined values between 2010-2039, 2040-2069, 2070-2099 time periods and TDY, ECY and EWY climate data sets

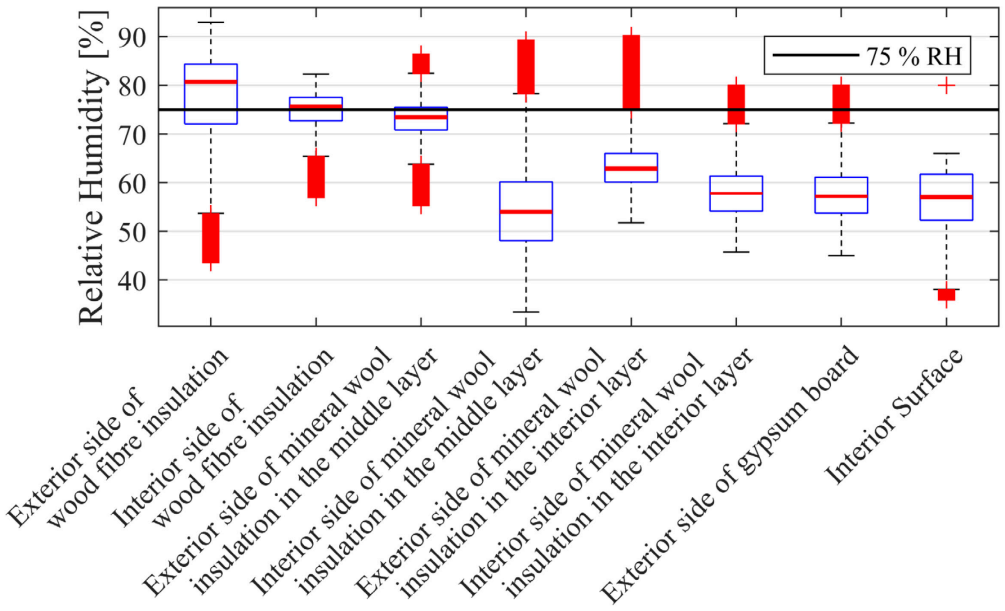

Figure 88: Boxplots for RH of assessed monitors within retrofitted roof. Combined values between 2010-2039, 2040-2069, 2070-2099 time periods and TDY, ECY and EWY climate data sets

10.2.4 Project 4

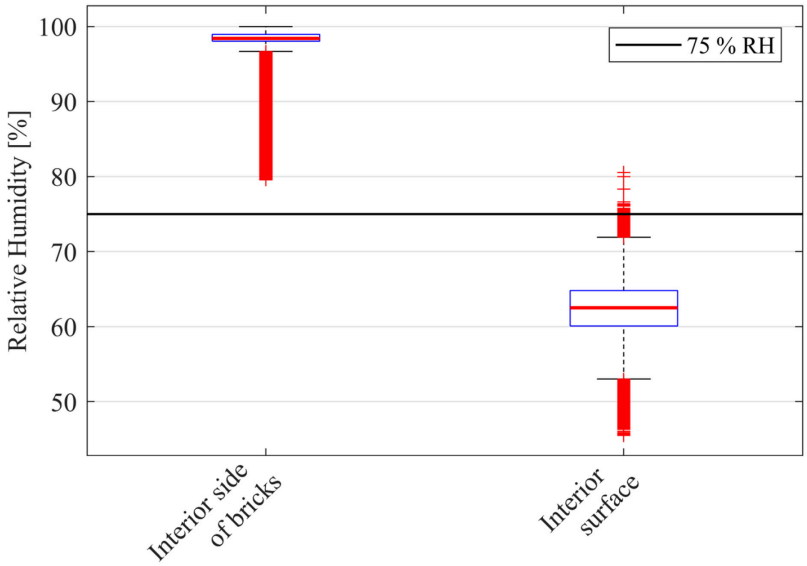

Figure 89: Boxplots for RH of assessed monitors within initial walls. Combined values between 2010-2039, 2040-2069, 2070-2099 time periods and TDY, ECY and EWY climate data sets.

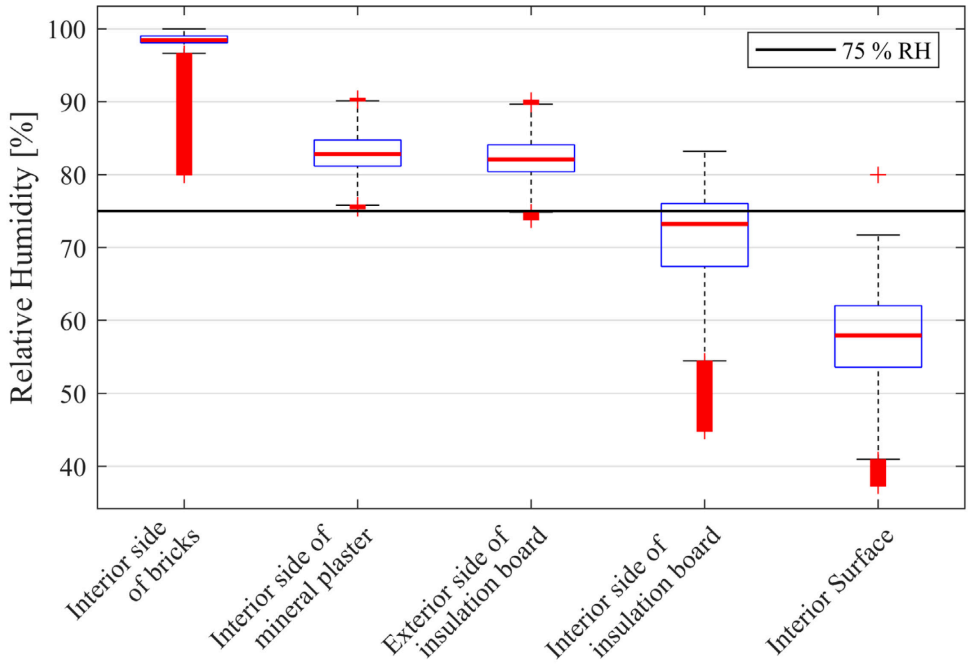

Figure 90: Boxplots for RH of assessed monitors within retrofitted walls. Combined values between 2010-2039, 2040-2069, 2070-2099 time periods and TDY, ECY and EWY climate data sets.

LUND UNIVERSITY

Dept of Architecture and Built Environment: Division of Energy and Building Design
Dept of Building and Environmental Technology: Divisions of Building Physics and Building Services